Stony Brook University

OFFICIAL COPY

The official electronic file of this thesis or dissertation is maintained by the University Libraries on behalf of The Graduate School at Stony Brook University.

© All Rights Reserved by Author.

Characterization of bacterial multi-component regulatory systems:

Nitric oxide, quorum sensing and "two-component" signaling

A Dissertation Presented

by

Takahiro Beachum Ueno

to

The Graduate School

in Partial Fulfillment of the

Requirements

for the Degree of

Doctor of Philosophy

in

Chemistry

Stony Brook University

May 2015

Stony Brook University

The Graduate School

Takahiro Beachum Ueno

We, the dissertation committee for the above candidate for the

Doctor of Philosophy degree, hereby recommend

acceptance of this dissertation.

Elizabeth M. Boon – Dissertation Advisor
Associate Professor, Department of Chemistry

Dale G. Drueckhammer – Chairperson of Defense
Professor, Department of Chemistry

Peter J. Tonge – Third Committee Member of Defense
Professor, Department of Chemistry

M. Raafat El-Maghrabi – Outside Committee Member of Defense
Associate Professor, Department of Physiology and Biophysics

This dissertation is accepted by the Graduate School

Charles Taber
Dean of the Graduate School

Abstract of the Dissertation

Characterization of bacterial multi-component regulatory systems:

Nitric oxide, quorum sensing and "two-component" signaling

by

Takahiro Beachum Ueno

Doctor of Philosophy

in

Chemistry

Stony Brook University

2015

Bacterial quorum sensing (QS) is an essential cell-to-cell communication system used by bacteria. Bacteria produce and detect small signaling molecules called autoinducers (AIs) to assess their surrounding bacterial population. Once the AI concentration reaches a threshold, the entire bacterial population undertakes a coordinated change in gene expression patterns. Thus, QS enables bacteria to orchestrate population-wide changes in behavior appropriate for different growth phases or environmental conditions. QS is widely spread among bacteria and regulates a wide array of biological functions that are critical for their survival. Controlled manipulation of QS may provide the means for the design of more selective antibiotics and improved bioproduction efficiency with engineered bacteria. Thus, understanding mechanisms of quorum sensing is of significant academic, medical and industrial interest. In this study, we report the identification and characterization of a nitric oxide (NO) responsive quorum sensing circuit in the marine pathogen *Vibrio parahaemolyticus*. We found that *V. parahaemolyticus* QS is regulated not only by AIs, but also by NO, through two-component signaling. *V. parahaemolyticus* detects NO through a nitric oxide/oxygen binding protein (H-NOX) and H-NOX regulates the activity of an H-NOX-associated histidine kinase (HahK). HahK ultimately modulates the activity of the QS master regulator, OpaR, through phosphoryl group transfer, and thus H-NOX/HahK participates in the *V. parahaemolyticus* QS circuit.

In this thesis, we also present the development of a medium-throughput filter-binding assay for histidine kinase phosphorylation. A major bacterial signaling pathway, two-component signaling, is based upon phosphorylation and phosphotransfer events by histidine kinases and

their partner proteins. In spite of its importance, understanding of two-component signaling is hindered by the lack of effective assay methods to quantify histidine kinase activity. To address this issue, we developed a carefully optimized filter-binding assay for kinase phosphorylation detection. We demonstrate the validity of the assay by monitoring phosphorylated histidine degradation under the proposed experimental conditions. Subsequently, we quantify kinase activities with respect to time, enzyme, and substrate concentrations, then determine their kinetic parameters.

To my family, friends and wife, Rebecca

Table of Contents

Dedication v

List of Figures ix

List of Tables xi

List of Abbreviations xii

Acknowledgments xiv

Chapter 1: Introduction 1

1.1 Two-component signaling 1

1.1.1 Simple two-component signaling 3

1.1.2 Hybrid two-component signaling 4

1.1.3 Variations of hybrid two-component signaling 5

1.1.4 One to many, many to one TCS 8

1.1.5 Auxiliary regulators 9

1.2 Nitric oxide and NO sensing protein H-NOX 10

1.2.1 Nitric oxide and soluble guanylate cyclase 11

1.2.2 NO sensing in bacteria 15

1.3 Bacterial quorum sensing 19

1.3.1 Types of autoinducers 19

1.3.2 Quorum sensing in gram positive bacteria 20

1.3.3 Quorum sensing in gram negative bacteria 21

1.3.4 Hybrid quorum sensing system in *Vibrio cholerae* 22

1.3.5 Hybrid quorum sensing system in *Vibrio harveyi* 23

1.3.6 Quorum sensing circuit in series 25

1.3.7 Inter-kingdom QS 26

1.3.8 Quorum quenching 26

1.3.9 NO responsive quorum sensing circuit in *V. harveyi* 27

1.4 Overview of research projects in this dissertation 28

Chapter 2: Development of filter paper based histidine kinase activity quantification method 29

2.1 Introduction 30

2.2 Materials and methods 30

2.2.1 Protein expression and purification 30
2.2.2 HK autophosphorylation 31
2.2.3 Phospho-His visualization 32
2.2.4 Phosho-His stability test 32
2.2.5 Filter binding assay 32
2.3 Results and Discussion 33
2.3.1 Phospho-His stability 34
2.3.2 Effect of time and enzyme concentration 37
2.3.3 Substrate kinetics 40
Chapter 3: Characterization of NO responsive QS circuit in *V. parahaemolyticus* 44
3.1 Introduction 45
3.2 Materials and methods 46
3.2.1 Bacterial strains and culture method 46
3.2.2 Molecular cloning and mutagenesis 46
3.2.3 Protein expression and purification 47
3.2.4 H-NOX complex preparation and electronic microscopy 47
3.2.5 NO dissociation rate 47
3.2.6 HK autophosphorylation assay 48
3.2.7 HK phosphatase activity assay 48
3.2.8 HK/LuxU phosphotransfer assay 48
3.2.9 HK autophosphorylation activity inhibition by H-NOX 49
3.2.10 Phosphotransfer profiling 49
3.2.11 Phosphotransfer specificity test 49
3.2.12 RNA extraction, cDNA synthesis and qPCR 49
3.3 Results and Discussion 50
3.3.1 *Vp* H-NOX is an NO-binding protein 50
3.3.2 *Vp* HqsK is an active hybrid kinase with kinase and phosphatase activities 55
3.3.3 *Vp* HqsK transfers phosphate to the quorum sensing phosphotransfer protein LuxU 57
3.3.4 LuxU is the cognate phosphotransfer protein for *Vp* HqsK 59
3.3.5 H-NOX suppresses *Vp* HqsK autophosphorylation upon NO binding 61
3.3.6 5 and 6-coordinate NO-bound H-NOX complexes both inhibit HqsK kinase activity 65
3.3.7 The effect of NO on the master quorum regulatory proteins OpaR and AphA 68
3.4 Perspectives 72

Chapter 4: Summary and future directions 73
References 76

List of Figures

Chapter 1: Introduction

Figure 1-1: Domain organization of simple TCS 4
Figure 1-2: Domain organization of hybrid TCS 5
Figure 1-3: Domain organization of TCS with double sensor kinase 6
Figure 1-4: Domain organization of KinA/Spo0F/Spo0B/Spo0A phosphorelay system 7
Figure 1-5: Domain organization of branched phosphotransfer networks 9
Figure 1-6: A schematic of eukaryotic NO signaling circuit 12
Figure 1-7: A schematic of sGC heterodimer domain organization 13
Figure 1-8: Gene orientation of selected H-NOX genes 16
Figure 1-9: Schematics of NO regulated DGC/PDE activities in *S. woodyi* 17
Figure 1-10: A schematic of NO/H-NOX mediated biofilm regulatory circuit in *S. oneidensis* 18
Figure 1-11: Structures of bacterial autoinducers 20
Figure 1-12: A schematic of canonical gram positive bacterial QS circuit 21
Figure 1-13: A schematic of canonical gram negative bacterial QS circuit in *V. fisheri* 22
Figure 1-14: A schematic of QS circuit in *V. cholerae* 23
Figure 1-15: A schematic of QS circuit in *V. harveyi* 24
Figure 1-16: A schematic of a tandem quorum sensing circuit in *P. aeruginosa* 25
Figure 1-17: A schematic of NO responsive QS circuit in *V. harveyi* 27

Chapter 2: Development of filter paper based histidine kinase activity quantification method

Figure 2-1: Stability of pHis on HKs 35
Figure 2-2: Quantified autoradiography band intensities from pHis stability tests 36
Figure 2-3: Time-dependent autophosphorylation of HKs 38
Figure 2-4: Enzyme concentration-dependent autophosphorylation of HKs 39
Figure 2-5: Substrate concentration-dependent autophosphorylation of HKs 41

Chapter 3: Characterization of NO responsive QS circuit in *V. parahaemolyticus*

Figure 3-1: Absorption spectra of *Vibrio parahaemolyticus* 51
Figure 3-2: Temperature dependent absorption spectra of *Vp* Fe^{II}-NO H-NOX 53
Figure 3-3: Absorption spectra during *Vp* H-NOX Fe^{II}-NO dissociation rate determination 54
Figure 3-4: *In vitro* autophosphorylation activity assay of *Vp* HqsK (D499A) 55
Figure 3-5: *In vitro* autophosphorylation activity assay of *Vp* HqsK (D499A) (Plot) 56
Figure 3-6: Phosphatase activity of *Vp* HK 57
Figure 3-7: *In vitro* phosphotransfer assay of *Vp* HqsK to LuxU 58
Figure 3-8: Phosphotransfer specificity test 59
Figure 3-9: Phosphotransfer profiling of *Vp* HqsK and three stand-alone *Vp* Hpt proteins 60
Figure 3-10: *V. parahaemolyticus* HK, Hpt phosphotransfer specificity test 61
Figure 3-11: *Vp* H-NOX inhibits kinase activity of HqsK 62
Figure 3-12: *Vp* H-NOX inhibits kinase activity of HqsK (Plot) 63
Figure 3-13: *Vp* HqsK autophosphorylation inhibition by various [NO·H-NOX] 64
Figure 3-14: *Vp* HqsK autophosphorylation inhibition by various [NO·H-NOX] (Plot) 65
Figure 3-15: *Vp* HqsK autophosphorylation inhibition by 5-, 6-coordinate NO·H-NOX 66
Figure 3-16: *Vp* HqsK autophosphorylation inhibition by 5-, 6-coordinate NO·H-NOX (Plot) 67
Figure 3-17: Growth curve of *V. parahaemolyticus* 69
Figure 3-18: *Vp* master quorum regulatory protein expression analysis by qPCR 70

List of Tables

Chapter 2: Development of filter paper based histidine kinase activity quantification method

Table 2-1: Summary of histidine kinase autophosphorylation kinetic parameters 42
Table 2-2: Bacterial strains, plasmids and primers used in the work..... 43

Chapter 3: Characterization of NO responsive QS circuit in *V. parahaemolyticus*

Table 3-1: Soret peaks and NO dissociation rates of various H-NOX proteins..... 52
Table 3-2: Bacterial strains, plasmids and primers used in the work..... 71

List of Abbreviations

AHL	Acyl homoserine lactone
AIS	Autoinducer synthase
AK	Autokinase domain
ATCC	American Type Culture Collection
ATP	Adenosine-5’-triphosphate
c-di-GMP	bis-(3’,5’)-cyclic dimeric guanosine monophosphate
cGMP	Guanosine-3’,5’-cyclic phosphate
DGC	Diguanylate Cyclase
DMSO	Dimethyl sulfoxide
DNA	Deoxyribonucleic acid
DPTA	Dipropylene triamine
EPS	Extracellular polysaccharide
Fe(II)	Ferrous
Fe(III)	Ferric
GTP	Guanosine-5’-triphosphate
HahK	H-NOX associated histidine kinase
HK	Histidine kinase
Hpt	Histidine containing phosphotransfer protein
HqsK	H-NOX associated quorum sensing kinase
H-NOX	Heme nitric oxide/oxygen binding protein

IKR	Internal kinase receiver domain
LB	Lysogeny broth
Lp	*Legionella pneumophila*
NB	Nutrient broth
NO	Nitric oxide
NOS	Nitric oxide synthase
OD	Optical density
OMFP	O-methylfluorescein phosphate
PDE	Phosphodiesterase
QS	Quorum sensing
RNA	Ribonucleic acid
RR	Response regulator
RRR	Response regulator receiver domain
SDS-PAGE	Sodium dodecyl sulphate polyacrylamide gel electrophoresis
SEM	Standard error of the mean
sGC	Soluble guanylate cyclase
So	*Shewanella oneidensis*
TCS	Two-component (regulatory) system
Tt	*Thermoanaerobacter tengcongensis*
Vh	*Vibrio harveyi*
Vp	*Vibrio parahaemolyticus*

Acknowledgments

I want to thank all the current and previous members of the Boon group, Natasha, Sandhya, Bernadette, Dhruv, Niu, Tanaya, Saj, Yueming, John K, Kate, Patryk, Fiona, Bez, Lisa and John F.

Dr. El-Maghrabi and Dr. Roger Johnson for their help with the development of filter-binding assay.

Group members of Carrico group, Drueckhammer group, Laughlin group, Raleigh group, Sampson group, Schärer group and Tonge group.

All the faculties and staff at the Chemistry department, Charmine, Deborah, Heidi, Katherine, Kim, Liz, Naz, Norma and Mike Teta.

Most of all, I want to thank my PI Dr. Elizabeth Boon for her guidance and support.

Chapter 1: Introduction

1.1 Two-component signaling

Detection of environmental stimuli and appropriate cellular adaptation are critical and fundamental functions for any organisms to survive. In bacteria this is predominantly done by the signaling system called "two-component signaling" (or two-component regulatory system, TCS)[1,2,3,4]. Two-component signaling consists of a sensory histidine kinase (HK) that detects an environmental stimulus and a response regulator (RR) that exerts an output response[5]. HKs transmit an external stimulus to RR by means of phosphoryl group transfer. The phosphotransfer from HK to RR may be done by a single step or through multiple steps, called phosphorelay[6]. Two-component regulatory systems are widely distributed among bacteria[7]. On average bacteria have 52 TCS proteins[8], but the number varies from bacterium to bacterium. For example, *Escherichia coli* has 30/32 (HKs/RRs), *Myxococcus xanthus* has 132/119 and *Mycoplasma genitalium* has no predicted TCS proteins[9].

All two-component systems have modular domain organizations[5,10]. A sensory HK has a sensory domain, a dimerization histidine phosphotransfer (DHp) domain and a catalytic ATP binding (CA) domain. The DHp domain is a four-helix complex formed by homodimerization of two HKs that contains a conserved His residue that is phosphorylated. The CA domain binds an ATP and catalyzes γ-phosphoryl group transfer to the DHp domain[11,12]. The DHp domain and CA domain together are called an autokinase domain (AK)[2]. The sensory domains of HKs are poorly conserved and for many TCS systems, their physiological signals are unknown[5]. Relatively few numbers of environmental stimuli are determined, but many of the identified signals are small molecules such as peptides[13], carboxylic acids[14], nitrates[15] and antibiotics[16] that directly bind the sensory domains. Sensory histidine kinases' affinities for these ligands vary, but are in the range of submicromolar to millimolar. Other environmental stimuli detected by HK include light[17], temperature[18] and osmotic pressure[19]. Some HKs lack sensing domains, so ligands are detected by a separate sensory protein that modulates the activity of HK as seen in a LuxP/Q sensory protein, HK pair in *Vibrio harveyi* quorum sensing system[20,21,22,23].

Signal detection by a HK sensing domain triggers HK homodimerization and autophosphorylation on its conserved His residue in DHp domain. It is believed that the universal mode of histidine kinase phosphorylation is by the trans mechanism, in which the CA domain from one HK monomer transfers a phosphate to another HK monomer's His in the DHp domain[24,25]. However, autophosphorylation via cis mechanisms (phosphate transfer from one

monomer CA to its own DHp domain) has been recently reported in *Thermotoga maritima* HK[26]. The phosphoryl group on DHp His is further transferred to a conserved Asp residue in the RR receiver domain. Many HKs are bifunctional proteins, they have both phosphotransferase and phosphohydrolase activities, that either transfer or remove phosphates from their cognate partner proteins[27,28,29]. There are a variety of responses upon ligand binding to HKs, either increasing or decreasing HK kinase activities in some whereas in others, the binding increases phosphatase activities[24].

Histidine kinase response regulators control a broad spectrum of biological functions including chemotaxis, osmoregulation, biofilm formation, sporulation and virulence[30,5,31]. A typical response regulator consists of an N-terminus response regulator receiver domain (RRR) that contains conserved phosphoryl group accepting Asp, and a C-terminus effector domain. Based on gene analysis, at least 10 different types of effector domains have been identified[32]. Approximately 66% of RRs are transcription factors. Other RRs are either stand alone RRR or RRR coupled with RNA binding or enzymatic domains. The most common effector domain followed by DNA binding domains are GGDEF/EAL domains, which are involved in the metabolism of bacterial second messenger signaling protein, c-di-GMP[32]. GGDEF domains are the characteristic domain seen in diguanylate cyclase (DGC), the function of which is to synthesize c-di-GMP[33]. EAL domains are seen in phosphodiesterase (PDE) that degrades c-di-GMP[34]. Cyclic-di-GMP is a widely used second messenger signaling molecule in bacteria, predicted to be present in 85% of all bacteria[35]. Although its mechanism is not yet well understood, it plays a critical role in the regulation of virulence[36], motility[37] and biofilm formations[38,39].

The majority of RRs are active only when they are phosphorylated[40,41] and the duration of an output response corresponds to the life time of the phosphorylated RR[42]. As mentioned earlier, some HKs have phosphatase activities to remove phosphates from their partner RRs. In addition, many RRs have autophosphatase activities which remove their own phosphates[43]. The autophosphatase activities of RRs vary from RR to RR with half-lives ranging from seconds to hours[24]. Kinase and phosphatase activities of a HK or a RR are not the only means to regulate a RR phosphorylation state. There are other proteins that modulate the RR phosphorylation state. This group of proteins, called TCS connectors (or auxiliary regulators), is one such example that modulates HK and RR activities to fine tune cellular responses[44,45]. TCS connectors are prevalent in bacteria and affect the TCS through various means including promotion or inhibition of autophosphorylation, phosphotransfer, dephosphorylation, altering RR's DNA binding ability or by inhibiting the recruitment of RNA polymerase[46,47,48,45]. The detail of auxiliary proteins will be discussed in section 1.1.5 of this thesis.

1.1.1 Simple two-component signaling

In its simplest form called orthodox (or simple) two-component regulatory system, TCS consists of a sensory histidine kinase and a cytoplasmic response regulator[49] (Figure 1-1). Typically, HKs are membrane bound homodimeric proteins[50,51], with each monomer comprised of N-terminus sensing domains, dimerization phosphotransfer domains and catalytic ATP binding domains[5,52,10]. Upon ligand binding to the sensing domain, HK catalyzes ATP/divalent cation dependent phosphorylation on the conserved histidine in its DHp domain[53]. The receiver domain of the partner RR then catalyzes the phosphoryl group transfer from HK to the conserved aspartic acid in the RR receiver domain[54,55]. The majority of the RRs are transcription factors that dimerize upon phosphorylation and bind to their target genes to modulate gene expressions[5]. Some RRs' effector domains are enzymatic domains as seen in a methyltransferase CheB[56] and a phosphodiesterase RegA[57]. Orthodox TCS is the most common TCS architecture in bacteria[24]. The duration of the cellular response triggered by a ligand binding corresponds to the duration of the RR phosphorylation[5]. To have a tight control on phosphorylated RR, many HKs have phosphatase activities as well as kinase activities[5]. In addition, some RRs have autophosphatase activities to for self-dephosphorylation[58].

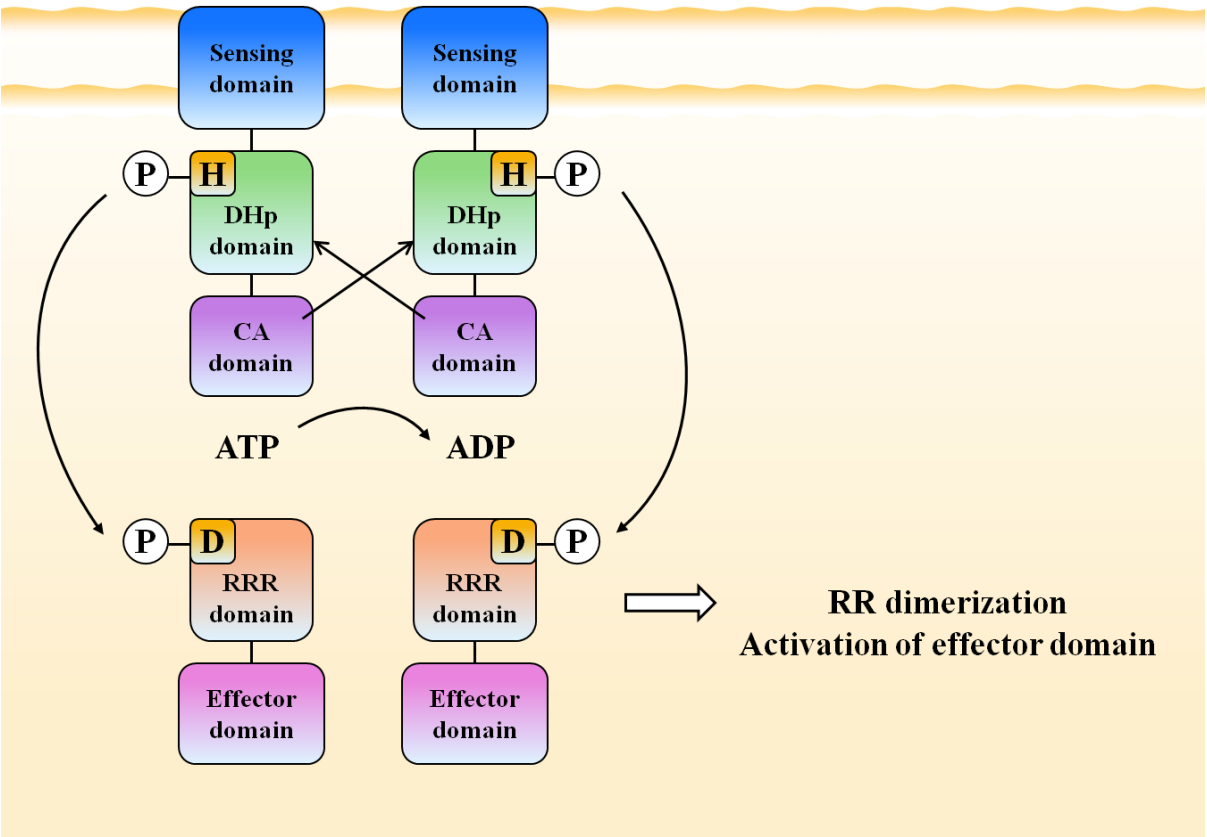

Figure 1-1. Domain organization of simple two-component system. Histidine kinase sensory domains detect a specific environmental stimulus. ATP bound to a catalytic ATP binding domain transfers γ-phosphoryl group to the DHp domain of another HK monomer. The phosphoryl group is then further transferred to the conserved Asp on the response regulator (RR), activating the RR effector domain. The HK autophosphorylation may occur by cis or trans mechanisms. The figure above depicts the trans autophosphorylation.

1.1.2 Hybrid two-component signaling

In another TCS, called hybrid two-component regulatory system (or phosphorelay), the phosphate is transferred from HK to RR through multiple His-Asp-His-Asp phosphotransfer steps. In this phosphorelay system, a HK (now called hybrid HK) contains a receiver domain (internal kinase receiver domain, IKR) and a histidine containing phosphotransfer domain (Hpt) in addition to DHp and CA domains[59]. Following autophosphorylation on DHp His, the phosphate is transferred to IKR Asp, Hpt His and then finally to RR Asp[6]. Both of IKR and Hpt domains are devoid of autokinase activities but are capable of transferring phosphate toward or away from RR[60,61]. The phosphorylation of RR activates its effector domain and elicits an adaptive response. Hpt domains are often found within hybrid kinases, but may exist as a separate stand-alone protein[1]. This multi-step phosphotransfer provides the TCS system

additional channels for signal input and regulations[62]. Phosphorelay architecture is most common in eukaryotes but also seen in bacteria[30,1,63].

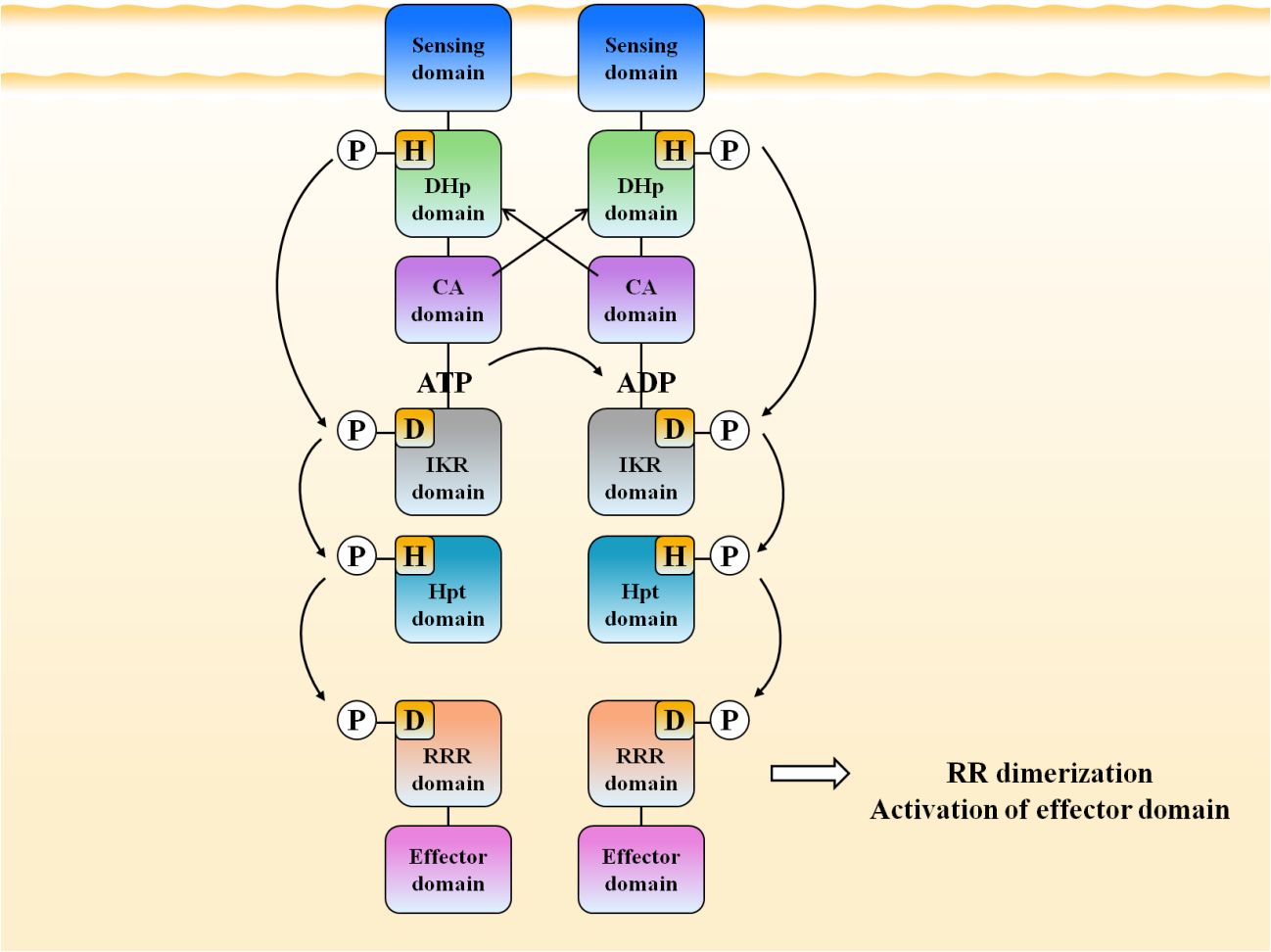

Figure 1-2. Domain organization of hybrid two-component regulatory system. Hybrid HK has IKR and HPt domains in addition to DHp and CA domains. The input signal is transduced from HK to RR through His-Asp-His-Asp phosphorelay. Phosphorylation sites are denoted as H (His) or D (Asp).

1.1.3 Variations of hybrid two-component signaling

Aside from archetypical hybrid TCS, shown above, a couple of different variations of hybrid TCS have been reported. One is a phosphorelay system with double sensor kinases, in which HK has two sensory domains and two autokinase domains (Figure 1-3). In *Pseudomonas putida*, one of the most well studied organisms with double sensor kinase, the N-terminus autokinase domain's activity is regulated by ligand (toluene, stryene, o-Xylene) binding to the

adjacent N-terminus sensing domain[64,65,66,67]. The ligand for C-terminus sensing domain hasn't been identified and whether or not these C-terminus autokinase domain activities are regulated by their adjacent sensing domains is not known. All of the identified double sensor kinases to date are involved in hydrocarbon degradations as seen in *Pseudomonas putida* TodS (toluene degradation)[65], *Pseudomonas fluorescence* StyS (styrene degradation)[66], *Thauera aromatica* TutC (toluene degradation)[68] and *Pseudomonas mendocina* TmoS (toluene degradation)[67]. Thus, there may be a correlation between this domain arrangement and its hydrocarbon degradation function.

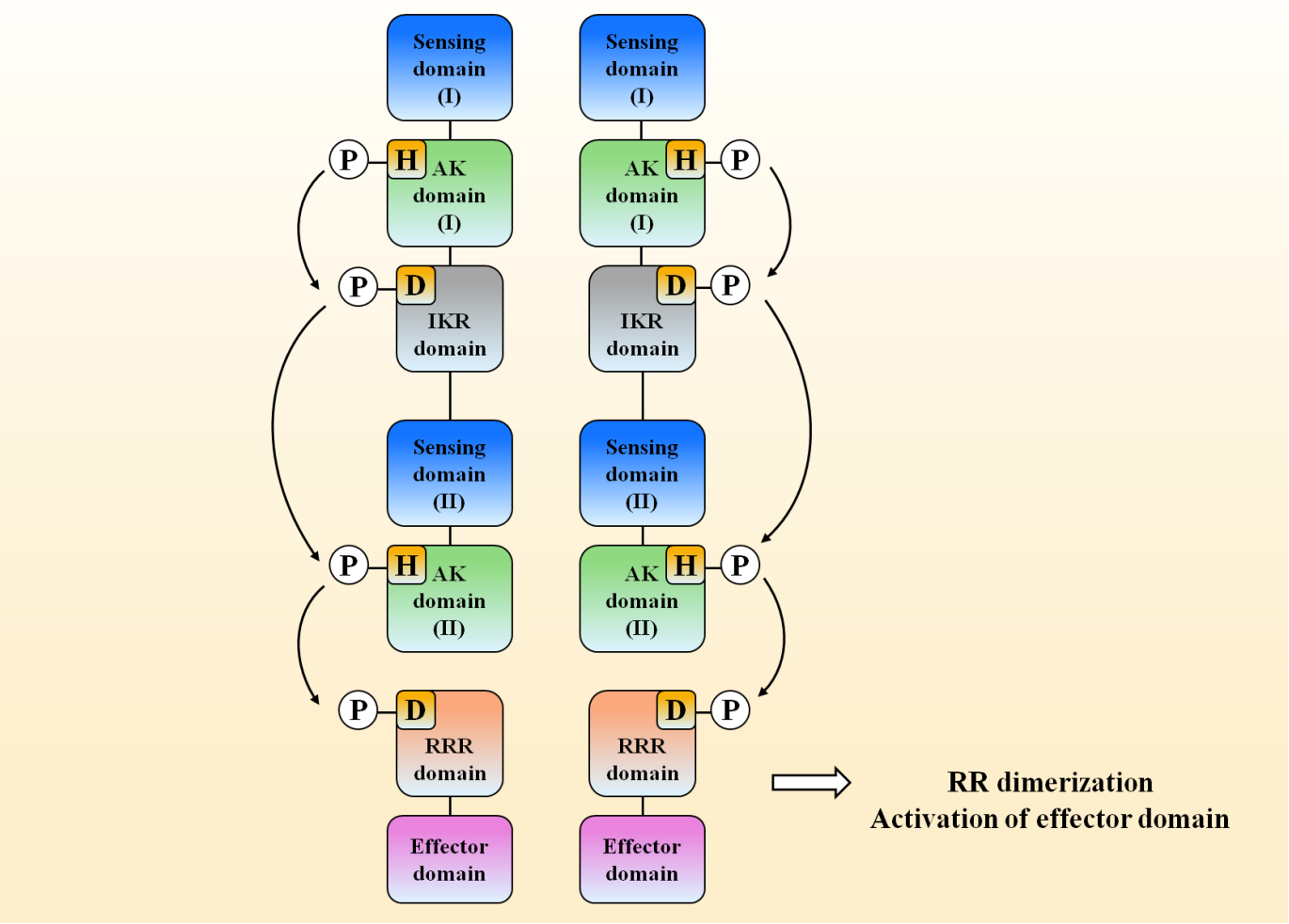

Figure 1-3. Domain organization of TCS with double sensor kinase. The sensory HK has two each of sensory domains and autokinase domains. The activity of an N-terminus AK domain is regulated by ligand binding to the neighboring N-terminus sensory domain. Neither the relationship between a C-terminus sensory domain and its neighboring autokinase domain nor C-terminus sensory domain's ligand have been identified.

Another hybrid TCS derivative is the KinA/Spo0F/Spo0B/Spo0A system in *Bacillus subtilis*. This phosphorelay circuit consists of a sensory HK KinA that has three sensory domains, phosphotransfer protein Spo0F, Spo0B and a RR Spo0A[69]. It is thought the activity of KinA is fine-tuned by the integration of multiple external signals detected by corresponding three sensory domains, however none of these ligands have been identified yet.

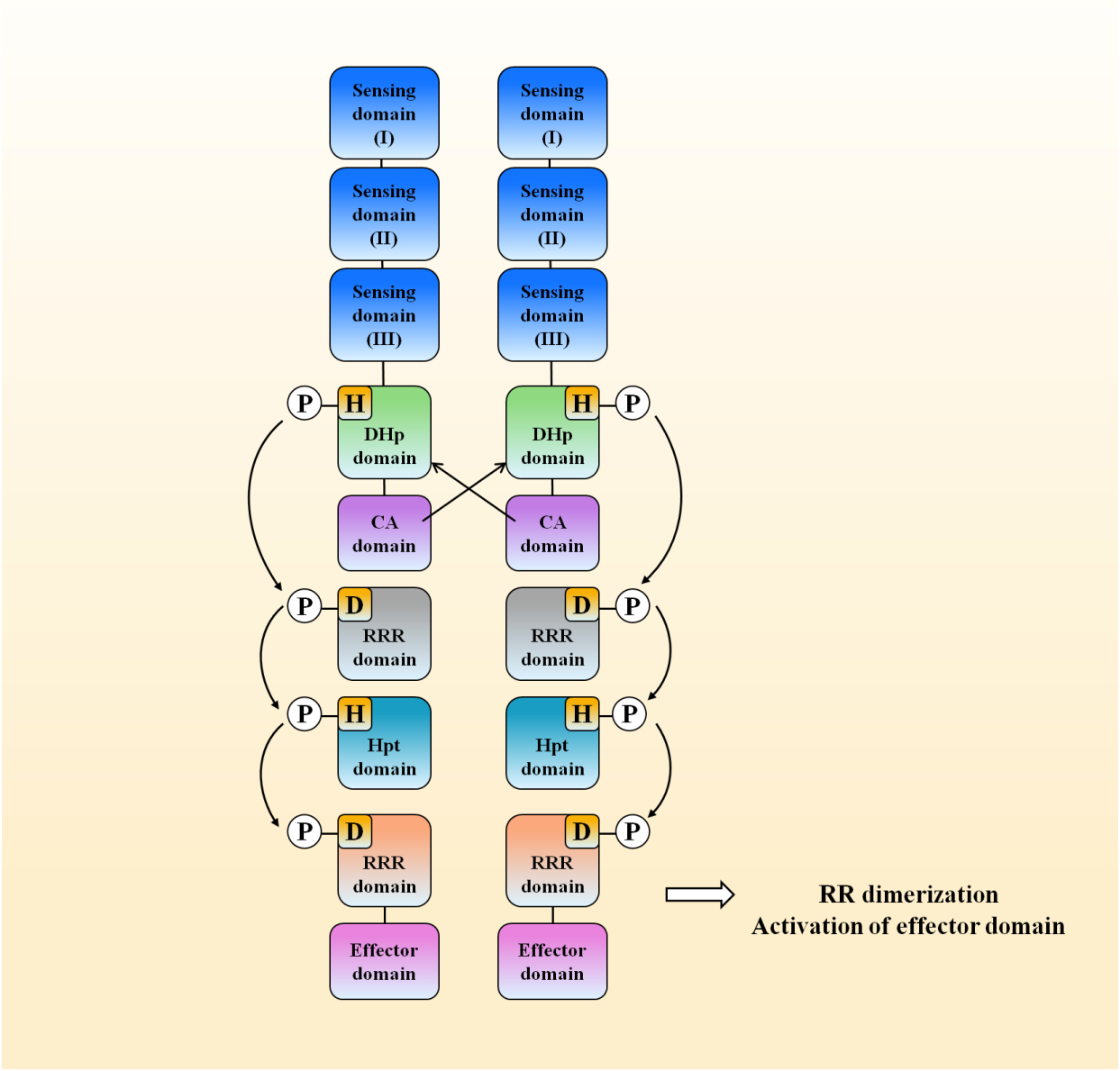

Figure 1-4. Domain organization of a KinA/Spo0F/Spo0B/Spo0A phosphorelay system in *Bacillus subtilis*. Hybrid HK KinA contains three sensing domains. KinA's activity is thought to be regulated by three different sensory domains and their ligands, however these input signals are unidentified. Phosphate is transferred from HK to RR through stand alone RRR and an Hpt protein.

1.1.4 One to many, many to one TCS

All of the above TCSs involved single HK and RR. However, there are TCSs that have a branched phosphotransfer network. In one branched network, called "one to many TCS"[70], a single sensory HK transfers phosphate to multiple RRs. The most well studied example of one to many TCS is the *E. coli* CheA/CheY/CheB system. CheA is a chemoattractant sensory HK that transfers phosphate to two RRs, CheY (master chemotaxis regulator) and CheB (methylesterase)[71]. Another type of branched phosphorelay network is "many to one TCS"[70]. In this phosphorelay network, multiple HKs transfer phosphate to a single RR as seen in *Vibrio harveyi* QS circuit and the *Bacillus subtilis* KinA/Spo0F/Spo0B/Spo0A phosphorelay system. The *Vibrio harveyi* QS circuit utilizes three sensory HKs to transfer phosphate toward/away from a single RR LuxO[72]. In a *B. sublitilis* phosphorelay circuit, RR Spo0A receives phosphates from two HKs, KinA and KinB through phosphotransfer proteins[73]. Based on genome sequence, many bacteria have a large disparity between the number of HK and RR[74], suggesting these one to many, many to one TCS are widely spread.

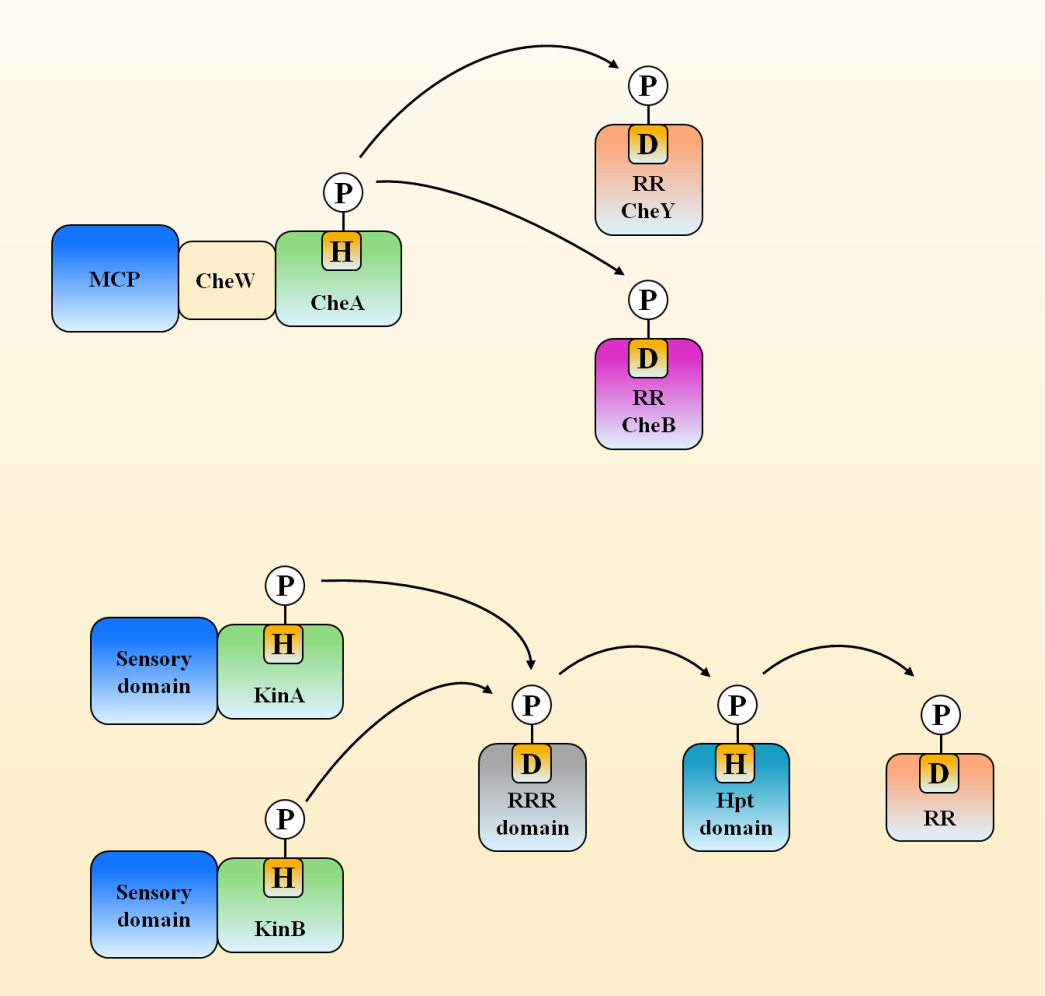

Figure 1-5. Domain organizations of branched phosphotransfer networks. (A) One to many TCS network of an *E. coli* CheA/CheY/CheB system. Sensory HK transfers phosphate to two RR proteins CheB and CheY. (B) Many to one TCS circuit of *Bacillus subtilis* KinA/Spo0F/Spo0B/Spo0A phosphorelay system. Sensory HKs KinA and KinB transfer phosphates to a common RR SpoA through a multi-step phosphotransfer.

1.1.5 Auxiliary regulators

In recent years, a group of proteins have been discovered to play important roles in TCSs. These proteins, called auxiliary regulators (a.k.a. accessory proteins or TCS connectors) modulate TCS signaling circuits through various means. These auxiliary proteins are most commonly synthesized in response to an external stimulus that is different from what's detected by HKs[75]. Sensory proteins are one type of auxiliary protein. These sensory accessory proteins detect environmental stimuli and modulate the activities of their partner HKs. Examples of this

type of protein are *Salmonella enterica* RcsF[76], *Bacillus subtilis* BceAB[77], methyl accepting chemotaxis proteins[78] and *Vibrio harveyi* LuxP proteins[20]. Another group of auxiliary proteins take part in TCS by controlling the phosphate flow at various points of the TCS circuit. In *Sinorhizobium meliloti*, a small accessory protein FixT inhibits HK FixL's autophosphorylation activity via an unknown mechanism[79]. *E. coli* CpxP inhibits the target HK autophosphorylation by binding the kinase's sensory domain under non-stress conditions[80]. *E. coli* SixA removes phosphate specifically from hybrid HK ArcB Hpt domains[81]. In a *Basillus subtilis* phosphorelay system, two auxiliary proteins KipI and Sda bind the HK KinA's DHp domain to cause conformational change to prevent its autophosphorylation[46,82].

There are other methods by which accessory proteins modulate TCS signaling. Some of the known modes of action are: scaffolds to assemble a TCS circuit[83,84], activation of HK expression[85], inhibition of RR dephosphorylation[86], inhibition of RR's DNA binding[87,88] or inhibition of other accessory proteins from degrading TCS proteins[89,90]. Auxiliary proteins provide TCSs to fine-tune cellular response to the mixed environmental stimuli. The comparison between the two types of circuits shows a TCS connector mediated pathway allows amplified signal output, or smaller/larger transcriptional activation/deactivation delays relative to a directly regulated circuit[91]. These properties of TCS connector mediated circuits may provide a number of benefits to bacteria. For example, a RR PmrA stimulates modification of a membrane in response to toxic materials. Delay of RR PmrA dephosphorylation by an accessory protein PmrD provides expression persistence and may be beneficial in a fluctuating environment[91]. An accelerated RR dephosphorylation by accessory proteins allows the cell to quickly respond to environmental changes without producing new proteins[75]. In addition, TCS connectors can integrate multiple environmental cues and coordinate the proper time to execute gene expressions. For example, the auxiliary protein Sda causes delay in the initiation of sporulation in case of DNA damage, providing time for cells to repair the damage[92].

1.2 Nitric oxide and NO sensing protein H-NOX

Nitric oxide is a diatomic radical gaseous molecule of major biological importance. Micromolar NO is used by macrophages as an antimicrobial agent[93]. At lower, submicromolar concentrations, it’s used as a signaling molecule by eukaryotes to regulate physiological processes such as smooth muscle relaxation[94], platelet aggregation[95] and neurotransmissions[96]. This eukaryotic NO signaling is governed by a protein called soluble guanylate cyclase (sGC). Soluble guanylate cyclase detects NO and triggers downstream signaling via production of second messenger signaling molecules[97]. The domain of sGC responsible for NO binding is called heme nitric oxide/oxygen binding domain (H-NOX)[98,99,100]. In recent years, proteins homologous to sGC H-NOX have been identified in bacteria[98,101]. Like sGC H-NOX, bacterial H-NOX protein selectively binds NO and modulates the production of second messenger signaling molecules[102]. H-NOX mediated NO sensing and signaling has been shown to be

closely related to bacterial biofilm formation and its dispersal. Below, we will discuss the properties of bacterial H-NOX proteins and their functions.

1.2.1 Nitric oxide and soluble guanylate cyclase

Nitric oxide (NO), a gaseous radical diatomic molecule is an important signaling molecule in eukaryotic biological systems. Nitric oxide is produced by nitric oxide synthase (NOS) from L-arginine and O_2[103]. NO signaling is initiated by the prior cellular release of calcium. Released calcium binds calmodulin (CaM) then the Ca/CaM complex binds and activates NOS[104]. Synthesized NO diffuses freely through membranes and binds to the heme cofactor of soluble guanylate cyclase (sGC)[104]. Soluble guanylate cyclase, the only conclusively proven mammalian NO sensor, catalyzes the synthesis of cyclic guanosine monophosphate (cGMP)[97], a second messenger signaling molecule. Nitric oxide binding to sGC activates its cyclase activity, resulting in a few hundred folds increase in cGMP level[105]. The produced cGMP binds one of its three target proteins, cGMP-gated ion channels[106], cGMP dependent kinase[107] or cGMP-regulated phosphodiesterase[108,109] to elicit downstream cellular responses. NO/sGC signaling regulates critical biological functions including neurotransmission, smooth muscle relaxation and immune response. Malfunction in a NO/sGC signaling system is implicated with arterial hypertension[110,111], heart disease[112,113], and atherosclerosis[114,115].

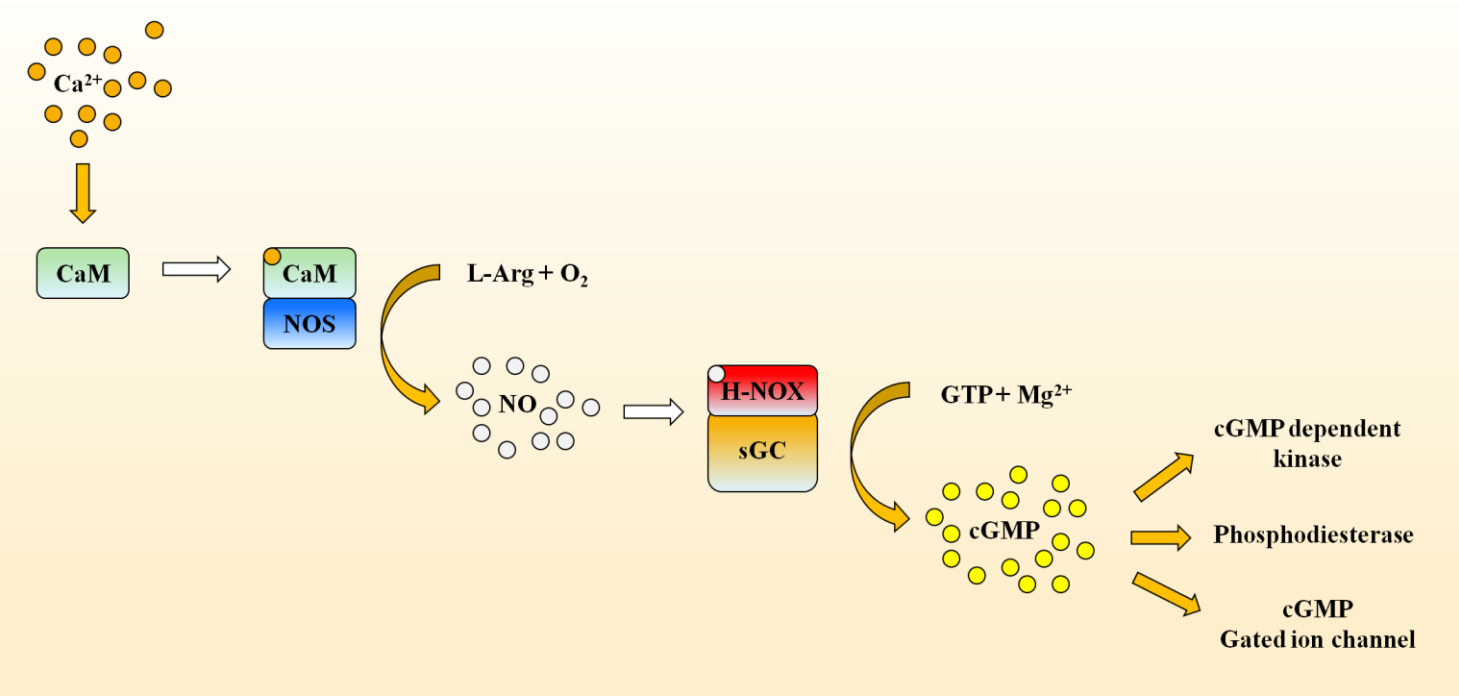

Figure 1-6. A schematic of eukaryotic NO signaling circuit. Upstream signaling releases calcium in a cell. First, calcium ion binds a calmodulin then the calcium/calmodulin complex binds NOS. The activated NOS generates NO that diffuses through a membrane then binds heme domain of sGC. NO bound sGC catalyzes the production of cGMP that binds one of its three targets: cGMP-gated ion channels, cGMP dependent kinase or cGMP-regulated phosphodiesterase.

Soluble guanylate cyclase is a dimeric protein that consists of α and β subunits. Each subunit has H-NOX domain, Per/Arnt/Sim (PAS) domain, coiled-coil (CC) domain and catalytic domain (CAT)[116]. H-NOX domain further divides into N-terminus helical subdomain and C-terminus subdomain. Heme cofactor is located in between two subdomains of H-NOX[100,99]. α and β subunits are essentially homodimers except only the β subunit H-NOX contains the heme and is thus capable of binding its ligand. This H-NOX domain of sGC is a part of conserved protein family H-NOX. H-NOX family proteins are found in both eukaryotes and bacteria[98]. All the identified H-NOX proteins bind CO and NO discriminating O_2, but some H-NOX proteins have been shown to bind O_2. In eukaryotes, H-NOX has only been found as a part of sGC. In bacteria, H-NOX are found either as a part of larger proteins or as a stand-alone protein encoded in the same operon with their partner signaling proteins[105].

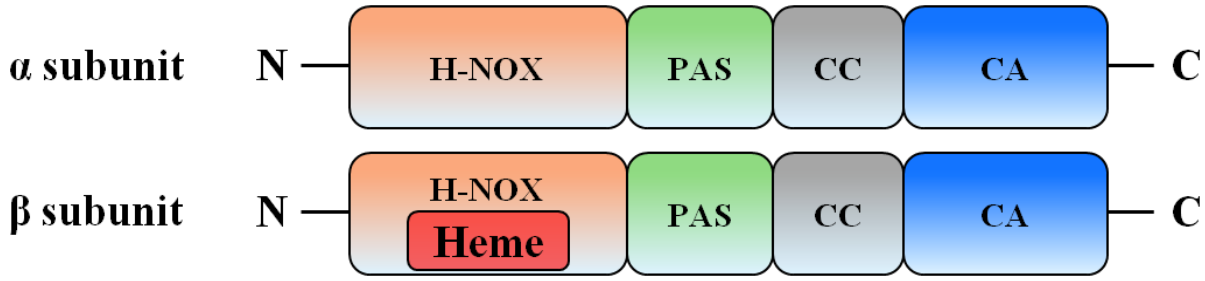

Figure 1-7. A schematic of sGC heterodimer domain organization. Each α and β subunit has a heme nitric oxide/oxygen binding (H-NOX) domain, Per/Arnt/Sim (PAS) domain, coiled-coil (CC) domain and catalytic domain (CAT), but only the β subunit H-NOX contains a heme, thus capable of binding ligands.

The first crystal structures of H-NOX protein were obtained in 2004 from *Thermoanaerobacter tengcongensis*[100]. Structural studies identified highly conserved key residues and their roles in H-NOX proteins' ligand binding. Among H-NOX proteins, highly conserved residues are H102, Y131, S133 and R135. Histidine 102 is bound to the heme central iron. The other three residues, Y131, S133 and R135 form a motif called YxSxR. YxSxR motif is conserved in all the H-NOX proteins and plays a role in stabilizing the heme binding[100]. In addition, residues I5, D45, R135, L144 and P115 are also conserved in many H-NOX proteins[99]. Other key residues are W9, N7 and Y140 in the distal heme pocket. These three residues form a hydrogen bonding network that is critical for H-NOX's O_2 binding[99,117]. Mutational studies showed Y140L mutation significantly reduces protein's O_2 binding ability whereas introduction of Tyr into the distal pocket of O_2 non-binding *L. pneumophila* H-NOX enabled the protein to bind O_2[117]. This hydrogen network has been observed only among O_2 binding H-NOX proteins. In O_2 discriminating H-NOX proteins, these H-bond network residues are substituted with non-hydrogen bond forming hydrophobic residues[117,118].

Another key structural property of H-NOX proteins is their highly distorted heme[100]. Heme distortion is due to the bonding between conserved His and heme central iron, Van der Waals interactions between the heme and conserved proline and isoleucine[100,119,120]. The mutational study showed the substitution of conserved Pro for Ala is sufficient to relax distorted heme and induces a large N-terminus shift (~11°) causing entire N-terminus sub-domain rotation and displacement[119,121]. Other studies showed that the NO binding to heme central iron significantly weakens its bonding to heme coordinating His, resulting in bond breakage[101,122]. Based on these observations, following H-NOX activation mechanism has been proposed[120]. At NO unligated inactive state, conserved proximal His is bound to the central heme iron and the heme is in a tensioned/distorted form. NO binding to the heme central iron breaks the iron-His

bond, allowing heme to be relaxed, more planar form. This heme relaxation causes H-NOX's conformational change, triggering the activation of a protein-protein interaction. The correlation between the heme conformation and H-NOX's function has been confirmed through the mutational study of *Shewanella oneidensis* H-NOX[123]. In this study, conserved P117, responsible for heme distortion was substituted with alanine. The P117A mutation caused distorted heme to flatten and the relaxed H-NOX mutant mimicked the function of an NO bound, active form of H-NOX.

1.2.2 NO sensing in bacteria

In 2003, proteins with high sequence homologies (18 to 40% identity) and key conserved residues to the H-NOX domain of sGC were identified across various phyla of bacteria[98]. As of today, H-NOX is found in over 250 bacterial species[98,101]. These bacterial H-NOX proteins to date showed similar ligand binding and spectroscopic properties as eukaryotic sGC, most of them binding CO and NO but not O_2[101,100]. Bacterial H-NOX proteins exist either as a part of a larger protein or most often, as a stand-alone protein. Stand-alone H-NOX protein coding genes are most commonly found in the same operon with genes that code for signaling proteins such as sensory histidine kinase or a c-di-GMP metabolizing protein. Histidine kinase, together with a response regulator, constitutes the two-component regulatory system. Cyclic-di-GMP metabolizing proteins are either GGDEF domain containing diguanylate cyclase (DGC) or EAL/HD-GYP domain containing phosphodiesterase (PDE). Diguanylate cyclase catalyzes the synthesis of, and phosphodiesterase catalyzes the degradation of a bacterial second messenger signaling molecule c-di-GMP. Cyclic-di-GMP has been shown to regulate bacterial biofilm formation, in many cases high c-di-GMP concentrations promote biofilm formation. H-NOX is also found as a part of methyl accepting chemotaxis protein (MCP). MCP fused H-NOX proteins have conserved Tyr, the key residue for O_2 sensing, and it's hypothesized that these proteins function as an O_2 sensor to navigate anaerobic bacteria away from O_2[124]. H-NOX's function in these signaling cascades is to detect NO and regulate the activities of their associated signaling proteins. Most commonly, H-NOX suppresses partner proteins' kinase or cyclase activities upon NO binding.

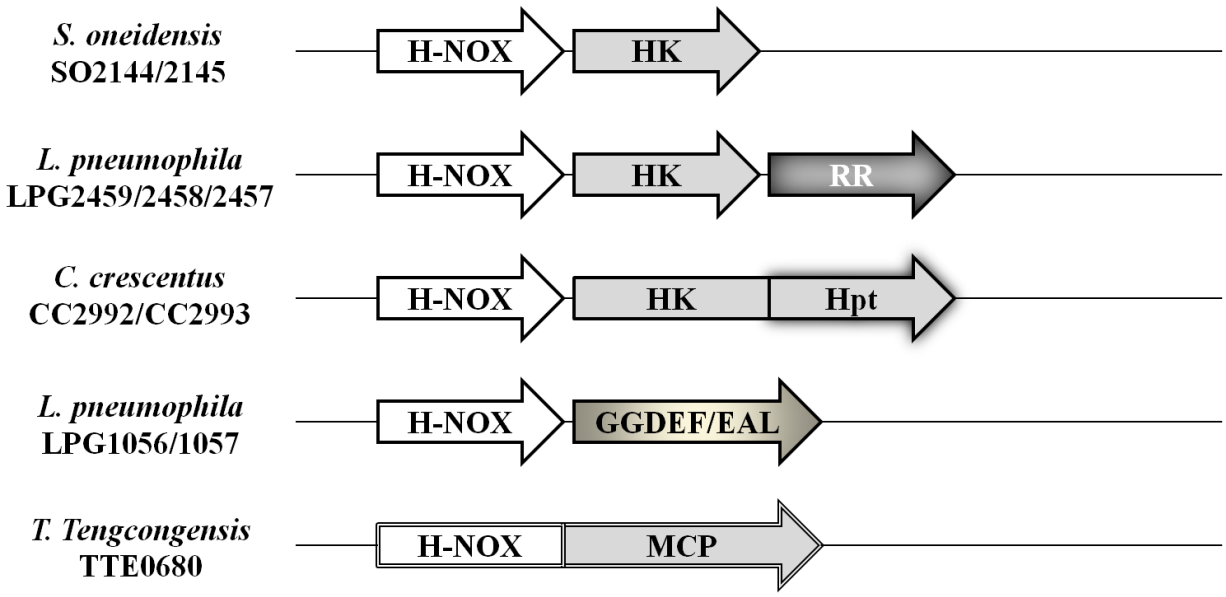

Figure 1-8. Gene organization of selected H-NOX genes. H-NOX coding genes are often found in the same operon with a HK, a hybrid HK, RR or c-di-GMP metabolizing proteins. H-NOX genes are also found as part of MCP.

Recent studies have revealed various biological roles of NO/H-NOX signaling in bacteria. In a marine bacterium *Shewanella woodyi*, *hnoX* is in the same operon as genes encoding c-di-GMP metabolizing proteins, diguanylate cyclase and phosphodiesterase. Niu et al. showed that without NO, H-NOX promotes diguanylate cyclase activity and suppresses phosphodiesterase activity. This results in an increased cellular c-di-GMP level, and promotes biofilm formation. On the other hand, in the presence of NO, NO·H-NOX inhibits the activity of diguanylate cyclase and promote the activity of phosphodiesterase, resulting in decreased c-di-GMP levels and suppressing biofilm formation[102] (Figure 1-9). The same NO/H-NOX regulation of c-di-GMP metabolizing protein activity has been observed in *Legionella pneumophila* where NO bound H-NOX suppresses DGC activity[125].

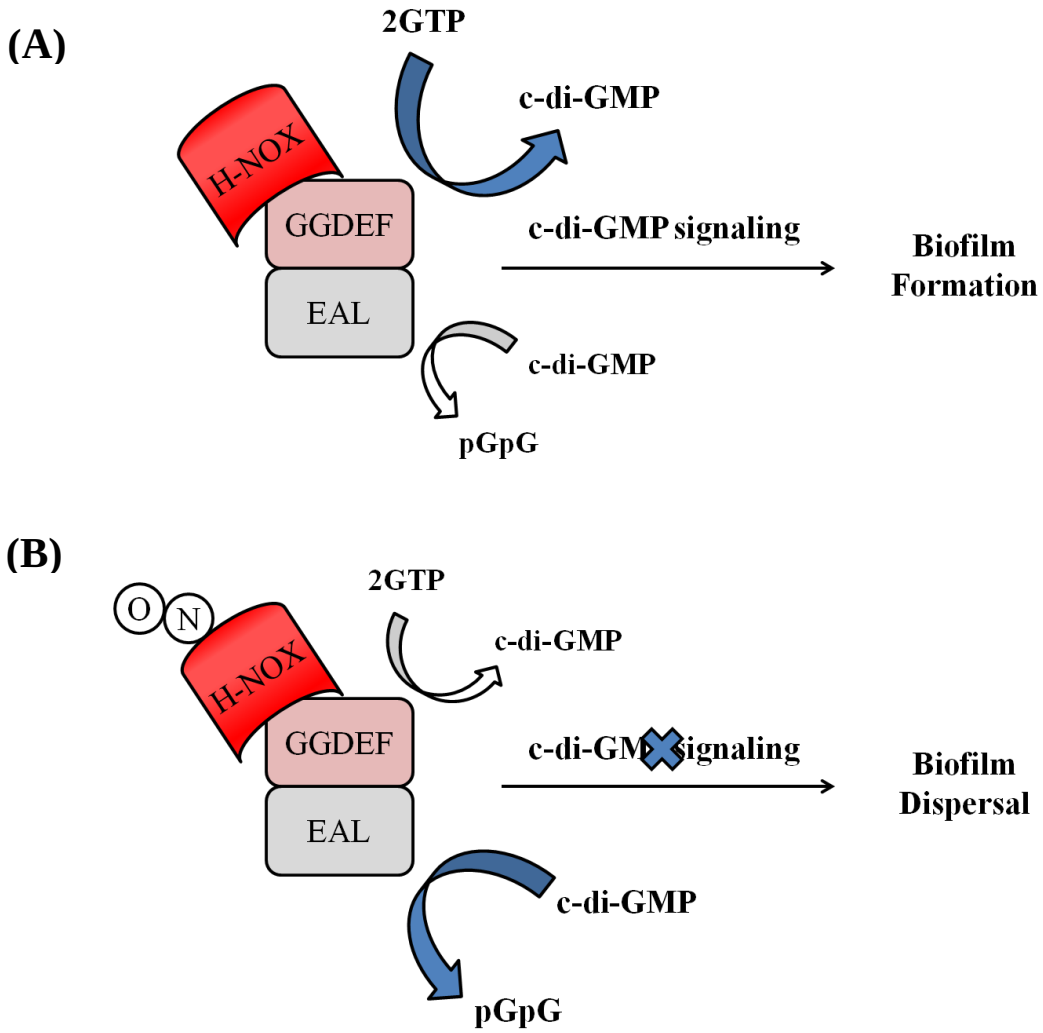

Figure 1-9. Schematics of NO regulated DGC/PDE activities in *S. woodyi*. In the absence of NO, DGC activity predominates. Diguanylate cyclase catalyzes the synthesis of c-di-GMP, promoting biofilm formation. In the presence of NO, the NO·H-NOX complex suppresses DGC activity but promotes PDE activity. Phosphodiesterase degrades c-di-GMP, resulting in decreased c-di-GMP concentrations and biofilm dispersal. Figures adapted from Liu et al. 2012.

In other cases, H-NOX proteins are coded in the same operon with a HK coding gene and regulate their activities. This H-NOX/HK regulatory system has been seen in *S. oneidensis*[126], *V. harveyi*[127] and *P. atlantica*[128]. In all of these cases, NO bound H-NOX inhibits its partner HK's kinase activities. In *Shewanella oneidensis*, H-NOX associated HK (HahK) transfers phosphate to three response regulators, HnoC, HnoD and HnoB[129]. HnoB is a phosphodiesterase that is activated upon phosphorylation. HnoD is an allosteric inhibitor of HnoB and is active only when phosphorylated. HnoC is a transcription factor that provides transcriptional feedback to all the components in the circuit. The NO binding to H-NOX inhibits HahK

autophosphorylation/phosphotransfer, resulting in decreased phosphodiesterase activity, higher c-di-GMP levels and increased biofilm formation[129,130] (Figure 1-12).

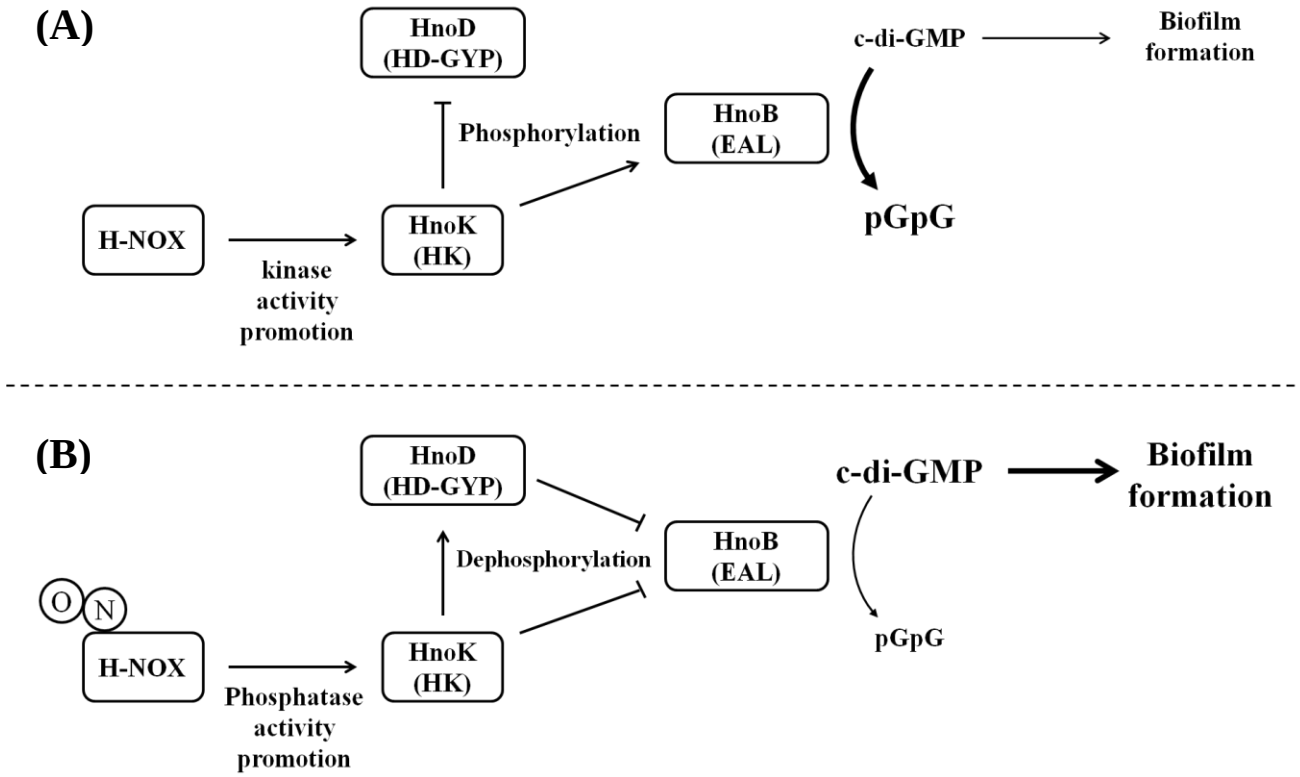

Figure 1-10. **A schematic of NO/H-NOX mediated biofilm regulatory circuit in *S. oneidensis***. H-NOX regulates the activity of three response regulators, HnoB, HnoC and HnoD through a HK, HnoK. Contrary to the case of *S. woodyi*, NO·H-NOX inhibits PDE activity, promoting increased c-di-GMP level and biofilm formation. Figure adapted from Plate, 2012.

In *V. harveyi*, NO/H-NOX signaling has been shown to be integrated into a bacterial QS circuit. *Vh* H-NOX regulates the activity of bifunctional HK, and modulates the phosphorylation state of QS response regulator LuxU that ultimately controls the expression of master quorum regulatory protein LuxR[127]. The details of NO/H-NOX's role in *V. harveyi* QS circuit will be discussed in a later section.

1.3 Bacterial quorum sensing

Bacterial biological functions such as biofilm formation, bioluminescence, antibiotic production and virulence factor production are ineffective if these actions are taken by a single or only a few bacterial cells. Rather, bacteria undergo latency period until they have a sufficiently large bacterial population and then as a whole, execute these gene expressions in a concerted manner. What enables bacteria to communicate with each other and coordinate population-wide gene expression is bacterial quorum sensing (QS)[131]. In QS, bacteria "talk" to each other through signaling molecules called autoinducers (AI). Each bacterial cell produces, diffuses and detects these signaling molecules to assess their surrounding bacterial population and bacterial species[132]. Since AI is produced by each bacterial cell, the AI concentration in a given area is proportional to the bacterial population. When bacterial cell density is low, so is the AI concentration. As the bacterial cell density increases, so does the AI concentration. When the AI concentration exceeds a threshold level, all bacteria in the community execute certain gene expressions making these biological functions effective and meaningful. Quorum sensing regulates a wide range of bacterial biological functions including bioluminescence[133], metabolism of bacterial second messenger molecule c-di-GMP[134], biofilm formation[135], antibiotic production[136], sporulation[137,138], virulence[139], cell division[140], swarming[141] and horizontal gene transfer[142]. Although the fundamental system of QS is conserved, bacteria use different AIs and quorum sensing signaling circuits. Bacteria use intra-species, inter-species and inter-genera AIs that allow them to distinguish signals from different bacterial species[132]. Among different types of QS circuits, there are some similarities and differences. Bacteria are thought to have developed certain QS signaling molecules, detectors, signaling circuits and target outputs optimized for their particular living environment/bacterial community[132]. In the following section, relevant identified bacterial AIs and QS circuits will be discussed.

1.3.1 Types of autoinducers

In quorum sensing, it is common for bacteria to employ multiple AIs to distinguish one bacterial population from another. Among different classes of autoinducers, species specific, intragenus and interspecies AIs have been identified (Figure 1-11). Gram positive bacteria primarily use oligopeptides as their autoinducer whereas gram negative bacteria use acyl homoserine lactones (AHLs)[143,144]. Each species of gram positive bacterium synthesizes its own uniquely sequenced oligopeptide AIs whereas gram negative bacteria use conserved homoserine lactone with different side chains. These oligopeptide AIs and AHLs are species specific and used for intraspecies communication. An autoinducer called AI-2 is used by several bacteria[145] and considered to be a universal autoinducer since its synthase, LuxS, homologue have been identified in hundreds of bacterial genomes[146,147]. Another autoinducer CAI-1 has been found to be used only among *Vibrios*, thus it's considered to be intragenus AI[148,149].

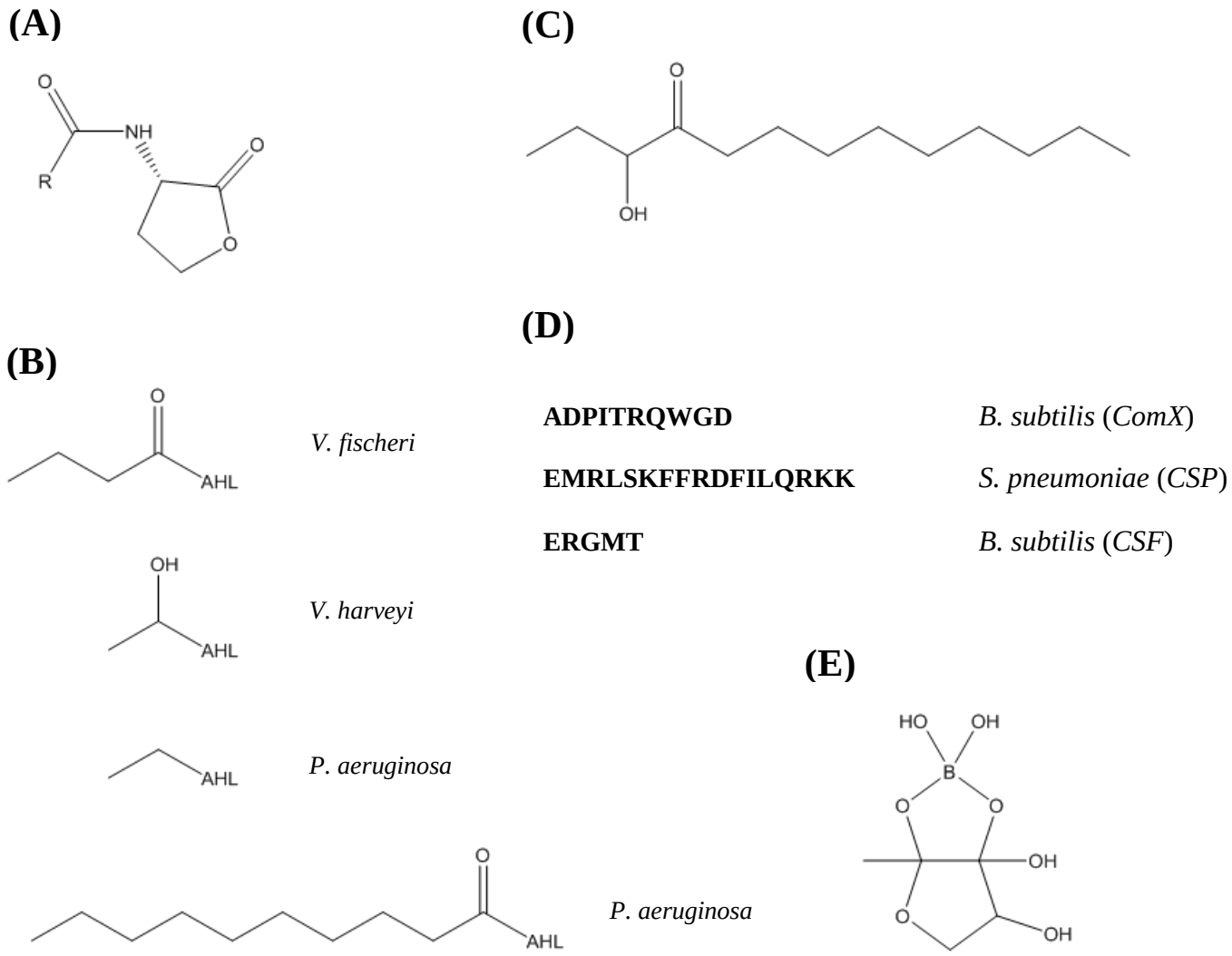

Figure 1-11. Structures of bacterial autoinducers. Structure of gram negative bacterial AI, acyl homoserine lactone (A). Acyl homoserine lactone side chains (B). Inter-*Vibrio* AI, CAI-1 (C). Peptide sequence of gram positive bacterial oligopeptide AI (D). Universal AI, AI-2 (E) Figures adapted from Ng, 2009.

1.3.2 Quorum sensing in gram positive bacteria

Gram positive bacteria primarily use small oligopeptides as their AIs (Figure 1-11-D)[150,151]. Since these peptide based AIs (autoinducing peptide or AIP) are non-membrane permeable, they are secreted by a specialized membrane bound transporter[152]. Following the secretion, AIPs are detected and processed through two-component regulatory systems (Figure 1-12). In a simplified scheme, a gram positive QS works as follows: the AIP concentration in the given environment increases as the bacterial population increases. When the AIP concentration

reaches a certain threshold (~1-10 µg/mL), it binds the membrane bound sensory HK[143]. The AI bound active HK autophosphorylates and then transfers the phosphoryl group to its partner RR. The phosphorylated RR, most often a transcription factor, dimerizes and binds its target genes to execute certain gene expressions[153,154]. The structures of autoinducing peptides differ in bacteria from species to species and thus peptide based QS circuits are considered intra-species communication[132].

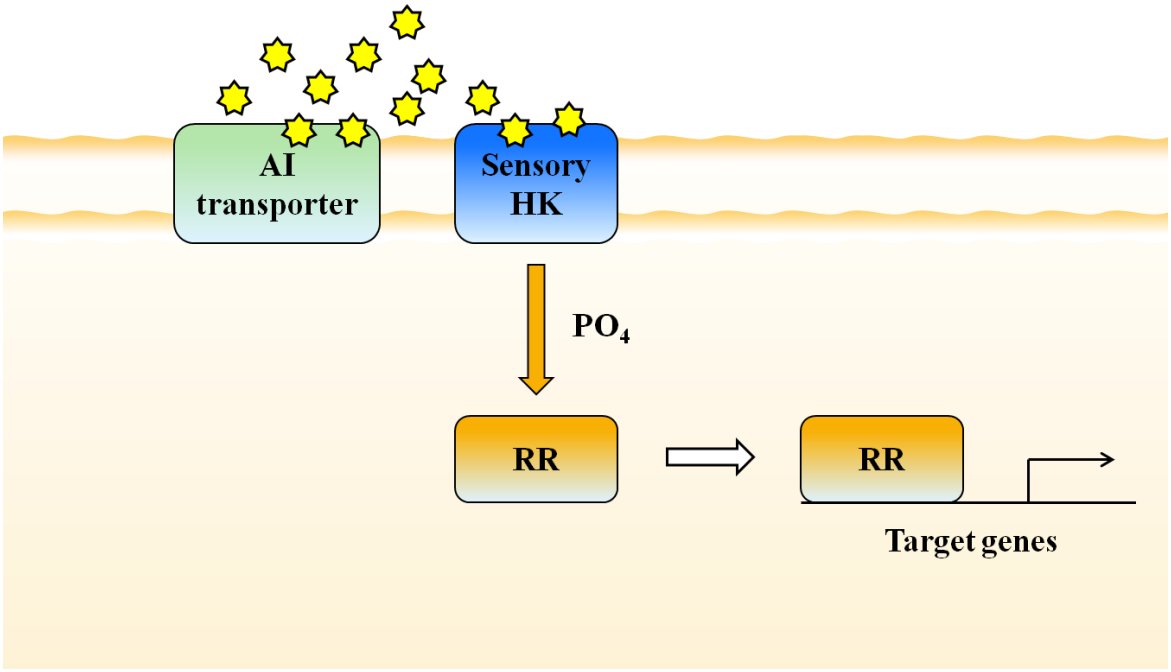

Figure 1-12. **A schematic of a canonical gram positive bacterial QS circuit**. Yellow stars denote autoinducers. Synthesized oligopeptide AI is released into the environment by an AI transporter. AI is detected by a cognate membrane bound HK and the signal is processed via TCS.

1.3.3 Quorum sensing in gram negative bacteria

A marine bioluminescent bacterium, *Vibrio fischeri*, is the first bacterium for which a QS system has been identified and thought to be the paradigm for most of the gram negative bacteria[133]. *V. fischeri* uses an acyl homoserine lactone (AHL) called *N*-3-(oxo-hexanoyl)-homoserine lactone (3OC6HSL, Figure 1-11-A, B) as its AI[143,144]. The autoinducer is synthesized by a cytoplasmic AI synthase called LuxI (Figure 1-13). The produced AHLs, being lipophilic, diffuse through membranes and bind a cytoplasmic AI receptor called LuxR[155]. LuxR is an AI receptor and also a response regulator that upon AI binding, dimerizes and binds its target operon, *luxICDABE* to activate its transcription[153]. There are a few safeguards in this QS

circuit to ensure its signaling fidelity. First, AI binds its receptor only if its concentration, thus the bacterial population, is above the threshold[156,157]. Second, the AI receptor/response regulator LuxR is unstable without AI and degrades quickly[158]. Third, the LuxR target operon *luxICDABE* activates the transcription of luciferase and AI synthase luxI, providing positive feedback in the QS circuit[153]. LuxI/R type proteins have been found in a large number of gram negative bacteria[159]. Each bacterium uses an acyl homoserine lactone with various side chains as their own unique AI[160].

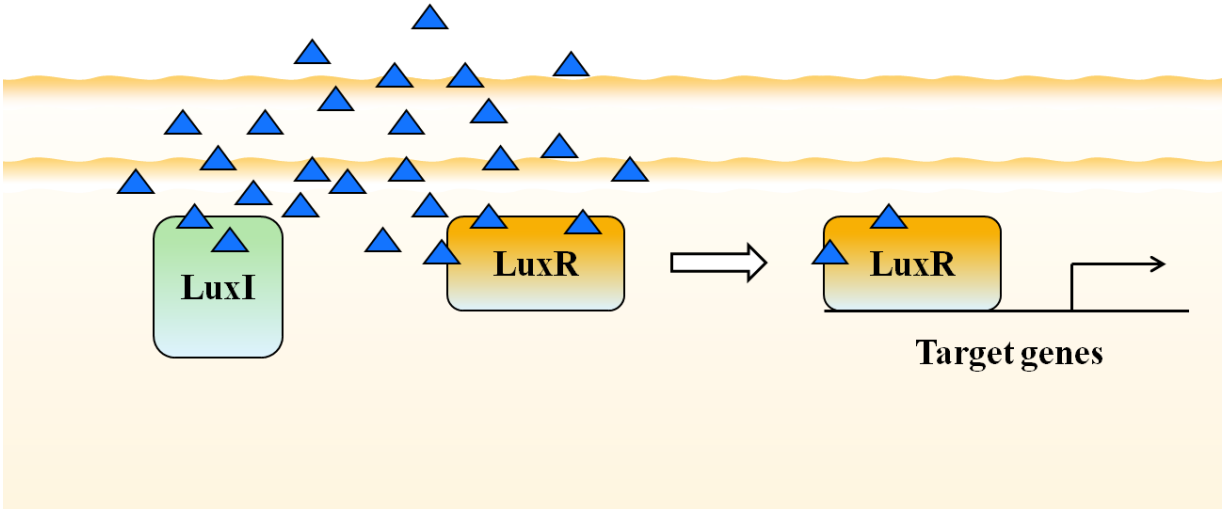

Figure 1-13. A schematic of canonical gram negative bacterial QS circuit in *V. fischeri*. Blue triangles represent AI, *N*-3-(oxo-hexanoyl)-homoserine lactone. LuxI is 3OC6HSL synthase. 3OC6HSL diffuses through membrane and binds the cytoplasmic AI sensor, LuxR. LuxR is also a transcription factor, but unstable and degrades rapidly on its own. AI binding stabilizes LuxR and AI ligated LuxR binds its target genes to activate gene expressions.

1.3.4 Hybrid quorum sensing system in *Vibrio cholerae*

A group of bacteria have a hybrid of gram positive and gram negative bacterial QS circuits described above. This hybrid QS system has a few additional QS components. First, the sensory HK has a receiver domain (internal kinase receiver domain, IKR). Second, there is an additional protein involved in the system called histidine containing phosphotransfer protein (HPt). *Vibrio cholera*, the causal agent of diarrhoeal disease cholera[161], is one such example that employs two autoinducers AI-2 and CAI-1[162]. AI-2 is produced by an AI synthase LuxS, and detected by a sensing protein/HK pair, LuxPQ[163]. CAI-1 is produced by CqsA and detected by a sensory HK, CqsS. At low cell density, two hybrid kinases LuxPQ and CqsS function as kinases. They autophosphorylate on a conserved His residue in a DHp domain, then transfer phosphates to conserved Asp in an IKR domain. Phosphates are then funneled into a single, common Hpt

protein called LuxU. At last, phosphates are transferred to the receiver domain of the response regulator[164]. The response regulator, LuxO, is a transcription factor that upon phosphorylation, activates the transcription of small non-coding RNAs, called quorum regulatory RNAs (Qrrs)[165]. Transcribed Qrrs, with the assistance of RNA chaperone Hfq, base pair with the master quorum regulatory protein mRNA to prevent its transcription[166]. The master quorum regulatory protein of *V. cholerae*, HapR, regulates a number of gene expressions, involved in biofilm formation[167], virulence factor production[168] and protease production[169].

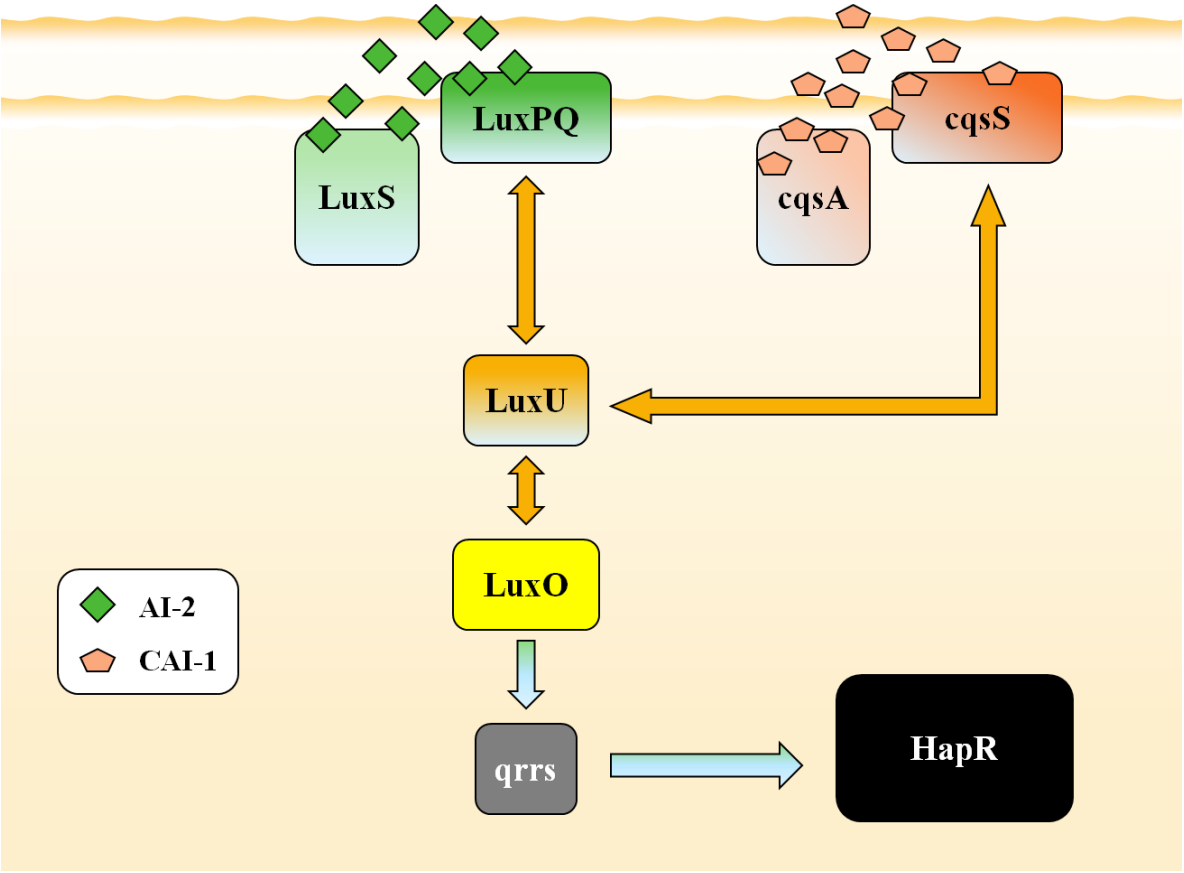

Figure 1-14. A schematic of QS circuit in *V. cholerae*. Two AIs, AI-2 and CAI-1, are detected by membrane bound HKs. The phosphoryl groups from two HKs are funneled into LuxU, then are further transferred to a RR LuxO. At low cell density, HKs' kinase activities predominate whereas at high cell density phosphatase activities predominate.

1.3.5 Hybrid quorum sensing system in *Vibrio harveyi*

Bioluminescent marine bacterium *Vibrio harveyi* is another organism that employs hybrid QS. The general QS architecture of *V. harveyi* is identical to that of *V. cholerae*, except V.

harveyi uses one additional AI, HAI-1. This intraspecies AI is produced by an AIS, LuxM, and is detected by the sensory HK LuxN (Figure 1-15). At low cell density, three QS HKs function as kinases, phosphorylating the RR LuxO through multi-step phosphorelay. In the same mechanism as *V. cholerae* QS, phosphorylated LuxO disrupts transcription of the master quorum regulatory protein LuxR. At high cell density, AIs bind their corresponding sensory HKs, shifting their functions from kinase to phosphatase, removing phosphate from RR LuxO. Now LuxR is transcribed and elicits gene expressions including bioluminescence, typeIII secretion and biofilm formation[170,139,72].

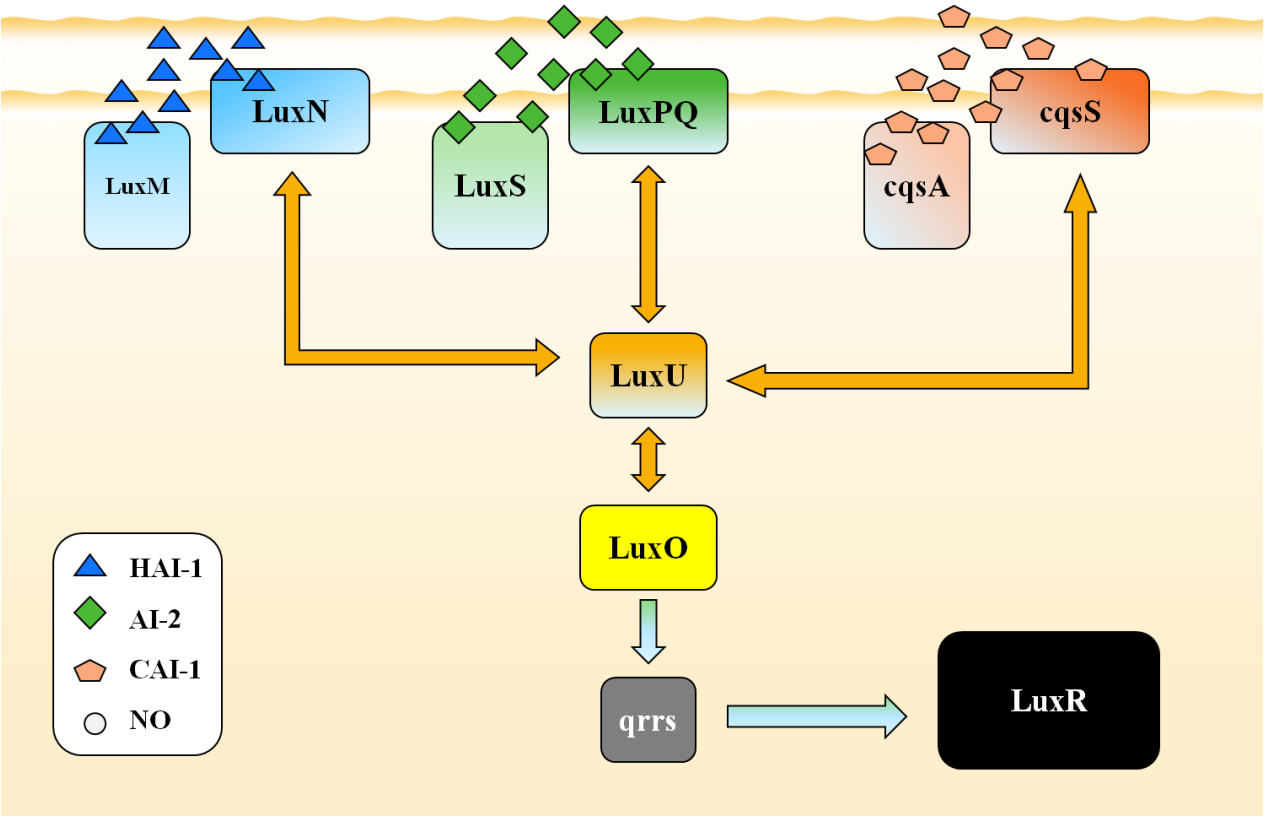

Figure 1-15. A schematic of a QS circuit in *V. harveyi*. Three AIs, HAI-1, AI-2 and CAI-1 are synthesized and detected by corresponding membrane bound hybrid HKs. The phosphoryl group is funneled into a common phosphotransfer protein LuxU, then to a RR LuxO. LuxO regulates the transcription of the master quorum regulatory protein LuxR that regulates hundreds of gene expressions.

1.3.6 Quorum sensing circuit in series

Pseudomonas aeruginosa uses two AHL-type AIs (Figure 1-11-B). Its QS circuit consists of two LuxI/R homogolues, LasI/R[171] and RhlI/R[172]. These two AI synthase/receptor pairs are built in series so that activation of one QS system successively activates the other synthase/receptor pair (Figure 1-16). At low cell density, the LasI/R pair is expressed but RhlI/R is not. As bacterial cell density increases, LasI produced AHL concentration increases and eventually binds LasR. The AHL bound LasR activates transcription of *lasI*, providing positive feedback[173], and also an AIS/sensory HK pair, *rhlI* and *rhlR*[174]. AHLs synthesized by RhlI bind RhlR, which then activates its own target genes. Microarray analysis revealed that different groups of genes are expressed in response to only one or both AIs[175,176]. In addition, transcriptome analysis showed that a different set of genes are expressed at different bacterial growth cycles, indicating that this tandem QS network provides bacteria a method to organize the set of gene expression sequences that may be critical for effective infection[176].

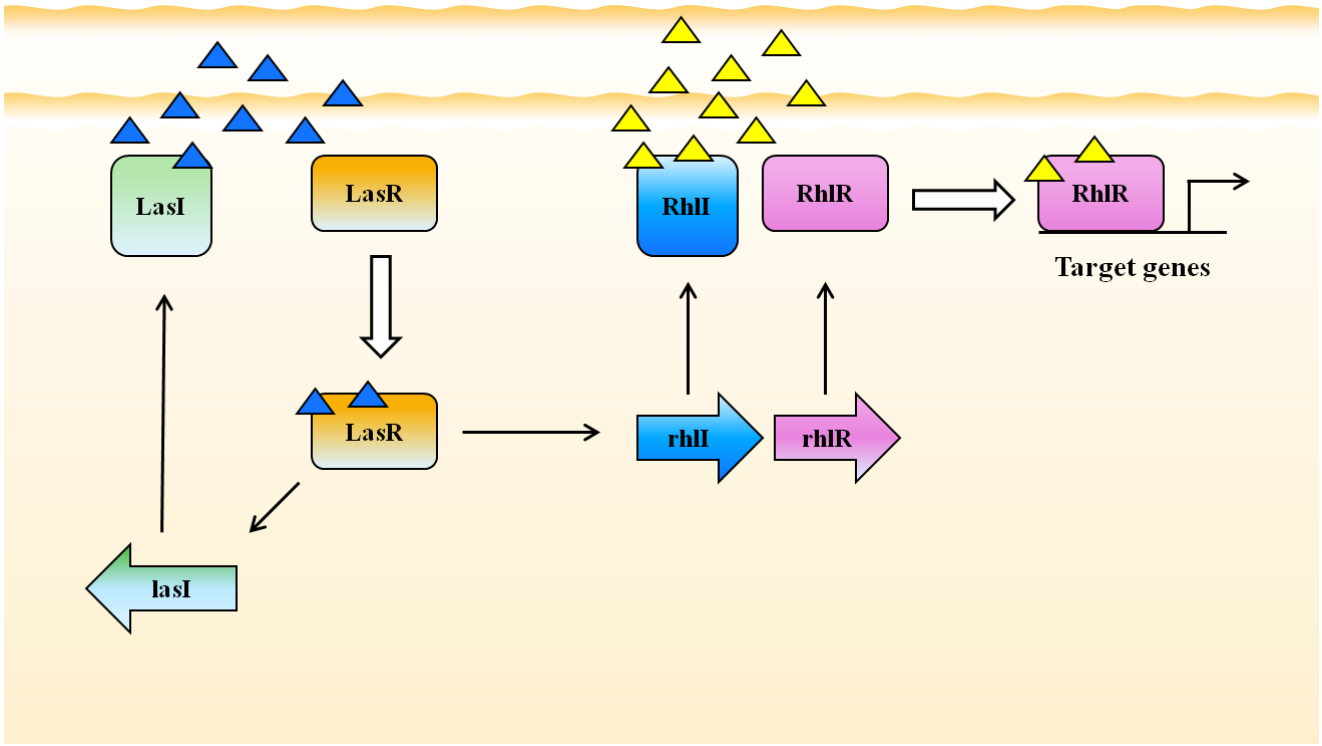

Figure 1-16. Tandem quorum sensing circuit of *P. aeruginosa*. The expression of an AIS/sensory HK pair (RhlI/RhlR) is regulated by another AI sensory HK (LasR). Activation of first RR, LasR activates the expression of the second AIS/sensory HK. Each response regulators have a different group of target genes.

1.3.7 Inter-kingdom QS

All the QS systems discussed above were regulated solely by bacteria originated AIs. However, there are QS systems that require both an AI and a host-organism originated substance to activate the QS response. A soil-dwelling bacterium *Agrobacterium tumefaciens* is one such example: its QS requires a molecule originated from its host plant. *A. tumefaciens* causes crown gall tumor in plants by inserting transferring tumor-inducing (TI) plasmid into plants[177]. Crown gall tumor secretes opine that *A. tumefaciens* uses as a nutrient for its growth[178]. *A. tumefaciens* has a LuxI/R homologous QS system called TraI/TraR[179,180]. *A. tumefaciens* senses proximity of a host plant by detecting small amounts of opine produced by a plant. Opine is being detected by a membrane bound sensory protein called AccR (or OccR)[181]. Opine binding to AccR activates the expression of the LuxR homologue RR, TarR[160]. Expressed TarR binds TraI produced AI and executes gene expressions including TI plasmid replication and bacterial conjugation[180,158].

1.3.8 Quorum quenching

Quorum sensing regulates the physiology of the global bacterial population by modulating numerous gene expressions. Bacteria dwell in environments where hundreds of different bacterial species compete against each other for limited resources. It is not surprising that bacteria evolved tools to disrupt other bacteria's QS communication to benefit its survival against others. This interruption of quorum sensing is called quorum quenching and various forms have been reported[182,183]. For example, different strains of *Staphylococcus aureus* produce uniquely structured AIP[184]. Their AIPs can bind and activate its own cognate AIP receptor, but also be able to bind other strains' non-cognate AIP receptors competitively and inhibit the binding[185]. In this manner, a strain of *S. aureus* disrupts other *S. aureus* strains' QS circuits[186]. Other bacteria, as seen in many *Bacillus* species, *Variovorax paradoxus* and some *Ralstonia species* disrupt other bacteria's QS by degrading AIs with specialized enzymes[183,187]. Quorum quenching is also seen by eukaryotes. The Australian red algae *Delisea pulchra* use quorum quenching to prevent bacteria from forming biofilm on its surface[188]. *D. pulchra* secretes and coats its surface with a mixture of halogenated furanones that resemble AHL[188]. This AHL analogue binds bacteria's LuxR type proteins and degrade them[189]. A legume *Medicago truncatula* detects AHL and secretes compounds that inhibit AI-2 signaling but stimulate AHL signaling[190]. A study shows human cells also have quorum quenching activity. Some primary immortalized human epithelial cell lines show degradation of one of *P. aeruginosa*'s AHL-type AI, 3OC12-HSL over time[191]. The mechanism of AHL degradation is unknown, but the data suggests it is due to protein activity[191].

1.3.9 NO responsive quorum sensing circuit in *V. harveyi*

As shown in the earlier section, *Vibrio harveyi* uses a hybrid QS circuit that consists of three AIs and corresponding HKs. A recent study conducted by our group identified the fourth pathway in *V. harveyi* QS circuit (Figure 1-17). In this pathway, gaseous signaling molecule nitric oxide (NO) from an unidentified source is integrated into a QS signaling cascade via H-NOX and its partner HK[127]. The membrane permeable NO is detected by cytoplasmic H-NOX. H-NOX regulates the activity of its partner signaling protein called H-NOX associated quorum sensing kinase (HqsK). HqsK is a bifunctional hybrid kinase that without NO, functions as a kinase transferring phosphate to the RR LuxO via LuxU. Upon NO binding to H-NOX, H-NOX inhibits HqsK's autophosphorylation activity, shifting HqsK's function from kinase to phosphatase. HqsK reverses the phosphate flow in the circuit, removing phosphate from LuxO. Dephosphorylation of LuxO inactivates the protein, leading to the expression of master quorum regulatory protein LuxR.

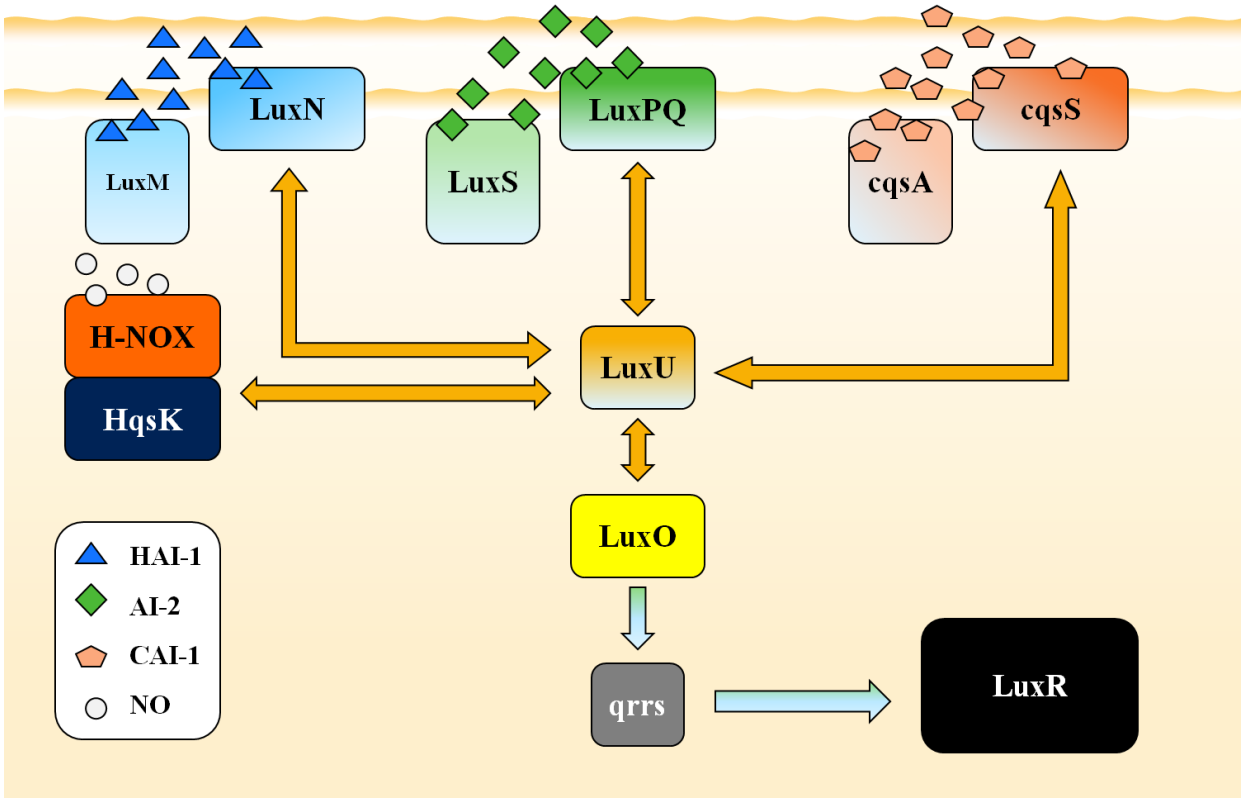

Figure 1-17. A schematic of a NO responsive QS circuit in *V. harveyi*. NO is detected by an NO sensor H-NOX that modulates the activity of its partner protein, H-NOX associated quorum sensing kinase (HqsK). NO bound H-NOX represses the kinase activity of HqsK, shifting its activity from kinase to phosphatase, promoting the dephosphorylation of RR LuxO. LuxO dephosphorylation inactivates the protein, resulting in the transcriptional activation of LuxR.

NO/H-NOX signaling has been shown to be involved in bacterial biofilm formation/dispersal through the regulation of c-di-GMP metabolism in a number of bacteria (See above section "NO sensing in bacteria")[102,125,128,129]. The identified NO responsive QS circuit in *V. harveyi* was the first proven case that NO/H-NOX signaling was integrated into bacterial QS signaling. This discovery suggests that bacteria detect and integrate environmental cues, not only AI signals, into QS circuits to regulate bacterial group behaviors. However, NO responsive QS circuits have only been identified in *Vibrio harveyi* and it has yet to be determined whether this circuit exists in other bacteria and how ubiquitous this circuit is.

1.4 Overview of research projects in this dissertation

The theme of this dissertation is bacterial two-component signaling - How bacteria detect and process diverse environmental cues through complex signaling cascades and modulate their group behaviors in response. In chapter 2, we will discuss a research project that was directed to develop a novel method to quantify autophosphorylation activities of bacterial histidine kinases. In search of an effective HK activity quantification method, we designed an acid based filter binding assay. We tested the proposed assays' validity by testing phosphorylated histidine kinases' stabilities under the proposed assay conditions. Following the confirmation of the assay's validity, we monitored kinase activity's dependence to time, enzyme and substrate concentrations. In the end, we determined kinetic parameters of four bacterial histidine kinases using the proposed assay. In chapter 3, we will discuss the discovery and the characterization of a NO responsive quorum sensing circuit in *Vibrio parahaemolyticus*. The goal of the project was to answer the question of whether a NO responsive quorum sensing circuit is a signaling circuit unique to *V. harveyi* or is it a conserved signaling circuit in other species of bacteria. To address this issue, we conducted successive studies on a human pathogenic marine bacterium *V. parahaemolyticus*. We conducted a spectrophotometric study and identified *V. parahaemolyticus* H-NOX is an NO sensing protein. The kinase/phosphatase properties of H-NOX's partner signaling protein HqsK has been analyzed. In addition, the effect of various oxidation/ligation states of H-NOX on HqsK's activities, and NO's effect on the expression of master quorum regulatory proteins OpaR and AphA were investigated.

Chapter 2: Development of filter paper based histidine kinase activity quantification method

Abstract

Two-component signaling (TCS) is a primary means by which bacteria detect and respond to environmental stimuli. In a typical TCS system, the phosphorylation state of a histidine kinase (HK) is responsive to a change in concentration of its cognate stimulus. This initial sensory event leads to downstream signaling and an adaptive response upon phosphoryl transfer from a His residue in the HK to an Asp residue in a cognate response regulator (RR). Although HKs and two-component signaling are essential for many aspects of bacteriology and pathology, they are poorly characterized. In particular, rates of autophosphorylation are only reported for a handful of HKs. This is in part due to the fact that phosphorylated His residues are inherently unstable in aqueous acidic solution. Here we report the detailed kinetic parameters of previously uncharacterized HKs from *Vibrio haveyi*, *Vibrio parahaemolytius*, *Shewanella oneidensis* and *Legionella pneumophila*. In characterizing these kinases, we effectively double the number of kinetically characterized HKs that have been reported in the literature. We also report optimized conditions for detecting His phosphorylation using a medium-throughput filter paper-binding assay.

2.1 Introduction

Two-component signaling (TCS) is a predominant mechanism for stimulus response in bacteria[24,2,44,4]. TCS consists of a sensor histidine kinase (HK) and a response regulator (RR)[5]. The variable sensor domain of the HK is responsible for detecting a stimulus, which results in a change in the phosphorylation state of the HK. The signal is relayed downstream by means of phosphoryl transfer from the HK histidine to an aspartic acid in the receiver domain of the RR. The activated RR then elicits a response to the initial stimulus[192,193]. Many TCS systems deviate from this canonical system, however. In three-component systems, an accessory protein that detects a signal and regulates HK auto-phosphorylation *in trans* replaces the HK sensor domain[22,23]. In hybrid TCS, the HK has a receiver domain, thus a His-to-Asp phosphotransfer takes place within the hybrid HK, and then a histidine-containing phosphotransfer protein (Hpt) is required to relay the signaling phosphate from the HK to the appropriate RR in two additional phosphotransfer steps[59,194,195]. TCS signaling is widely prevalent in bacteria; bacteria encode HKs capable of detecting a wide range of environmental stimuli that regulate biological functions essential for survival[24,30,196].

In vitro TCS studies that analyze basal HK autophosphorylation rates, phosphotransfer, and changes in these rates upon detection of environmental stimuli, are most commonly achieved employing [γ-^{32}P]-ATP as the HK substrate and analysis of phosphorylation by polyacrylamide gel electrophoresis (PAGE)[197,198]. Although these PAGE-based assays are labor intensive, time-consuming, and have limited sample capacities, they remain the primary means for analysis of phosphorylated His (pHis)[199,200,201]. In part this is due to the inherent lability of pHis[202,203,204,205], which hinders the application of techniques widely used for analysis of phosphorylated serine, threonine, and tyrosine residues[206]. Although several alternative analysis methods have been proposed to overcome the instability of pHis[207,208], each is nonetheless a PAGE-based assay. Here we report a carefully optimized filter paper-binding assay to determine the kinetic parameters of several previously uncharacterized HKs, nearly doubling the total number of kinetically characterized HKs.

2.2 Materials and methods

Unless otherwise noted, all the reagents were purchased at their highest available qualities and used as received.

2.2.1 Protein expression and purification

All the bacterial strains, plasmids and primers used in this work are shown in Table 2-2. *Shewanella oneidensis* MR-1 was a gift from Dr. Jeffrey Gralnick of University of Minnesota.

VIBHAR_01913 (*Vibrio campbellii*, strain ATCC BAA-1116) WT and its mutants were expressed then purified using methods published previously[127]. PCR was used to amplify VP1876 with Phusion High-Fidelity DNA Polymerase (New England Biolabs) from *Vibrio parahaemolyticus* genomic DNA (*Vibrio parahaemolyticus* EB101, ATCC 17802). Upstream and downstream primers contained NdeI and XhoI restrictions sites, respectively. SO_2145 was amplified by PCR from *Shewanella oneidensis* genomic DNA (*Shewanella oneidensis*, MR-1) with Phusion High-Fidelity DNA Polymerase. Upstream and downstream primers contained restriction sites EcoRI and XhoI, respectively. PCR was used to amplify lpg0278 with Phusion High-Fidelity DNA Polymerase from genomic DNA (*Legionella pneumophila* subsp. Pneumophila str. Philadelphia 1). Upstream and downstream primers contained restriction sites NdeI and XhoI, respectively. Amplified VIBHAR_01913, VP1876 and SO2145 were cloned into expression vector pET-23aHis-TEV to yield N-terminus 6× His tagged plasmids. Amplified lpg0278 was cloned into pET-20b(+) to yield C-terminus 6× His-tagged plasmid. Cloned PCR products were transformed into *E. coli* DH5α and positive transformants were verified by sequencing (Stony Brook DNA sequencing facility). Site directed mutagenesis was carried out to make VP1876 D499A following the QuikChange protocol from Stratagene. All proteins were expressed and purified as follows. Inserts containing plasmids were transformed into *E. coli* BL21(DE3) pLysS. Cells were grown in 2XYT media (16 g/L Tryptone, 10 g/L yeast extract and 5 g/L NaCl, supplemented with 100 μg/mL ampicillin and 34 μg/mL chloramphenicol) at 37 °C with 250 rpm agitation until A_{600nm} reached 0.5-1.0. Protein expression was induced with 100 μM IPTG for15 hours at 16 °C, then cells were harvested. Proteins contained a 6× His tag and were purified by Ni-NTA agarose. Protein concentrations were determined by Bradford assay with bovine serum albumin as a standard[209].

2.2.2 HK autophosphorylation

[γ-^{32}P]-ATP (6000 Ci/mmol, 10 mCi/mL) was purchased from PerkinElmer Health Sciences Incorporated. All reactions were performed at room temperature. Reaction mixtures generally contained final concentrations of 40 mM Tris-Cl, 150 mM KCl, 10% glycerol, 4 mM $MgCl_2$, 4 mM DTT, 10-25 μM histidine kinase, 2-4 mM ATP and 2-7 μCi [γ-^{32}P]-ATP at pH 7.6 – 7.9, unless otherwise noted. Histidine kinase in the reaction buffer was allowed to equilibrate at room temperature for a few minutes before initiation of the reaction. Reactions were initiated by the addition of ATP/[γ-^{32}P]-ATP mix solution and were stopped by the addition of 2.5× SDS loading dye (0.13% bromophenol blue, 0.25 M dithiothreitol, 25% Glycerol, 5% sodium dodecyl sulfate, 0.13 M Tris-Cl at pH 6.8).

2.2.3 Phospho-His visualization

Sample proteins were separated by electrophoresis on sodium dodecyl sulfate polyacrylamide gels (SDS-PAGE). Ten microliters of quenched reactions, without boiling, were loaded on a 12.5% sodium dodecyl sulfate (SDS) polyacrylamide gel. Proteins were separated by electrophoresis at 140 V for 80 min. The resulting chromatogram was fixed in fixing solution (30% methanol, 5% glycerol) for 30 min, stained by gel staining solution (10% acetic acid, 45% methanol, 0.25 g/100 mL Coomassie Brilliant Blue), and destained (10% acetic acid, 20% methanol), and then dried with Promega Gel Drying kit V7120/7131. Dried gels were exposed to a storage phosphor imaging screen (Molecular Dynamics) for 24 to 48 hours and images were scanned with the Typhoon scanner (Typhoon 9400, Amersham Biosciences). Band intensities from scanned images were quantified with image processing software, ImageJ v1.46. Resulting band intensities were normalized to the band not exposed to phosphoric acid.

2.2.4 Phosho-His stability test

Autophosphorylation reactions were performed as noted above. After 10 to 60 minutes of autophosphorylation, reactions were stopped by the addition of either 2.5× SDS loading dye (0 minute acid exposure) or ice cold 75 mM phosphoric acid (2.5 μL acid/30 μL reaction, final 5.77 mM). Quenched reaction mixtures were kept on ice, then were neutralized by the addition of 2.5× SDS loading dye at various time points to assess the effect of acid exposure. Samples were separated by SDS-PAGE. The resulting gels were treated and images were scanned as described above.

2.2.5 Filter binding assay

Whatman P81 ion exchange chromatography paper (catalog # 21426-202) was purchased from VWR international.

Reaction time: The components of the reaction mixture were the same as those used in HK autophosphorylation. Histidine kinase in the reaction buffer was incubated at room temperature for a few minutes prior to the initiation of the reaction by the addition of ATP/[γ-^{32}P] ATP mix solution. The reaction was quenched at various time points by the addition of ice cold 75 mM phosphoric acid (final 5.77 mM acid). The quenched reaction was immediately spotted onto p81 chromatography paper and the paper was dropped into a container containing ice cold 75 mM phosphoric acid (10 mL/paper). The spotted chromatography papers were then washed by rocking the acid containing container with a benchtop rotator for 10 minutes. The acid was replaced anew and washed two to three more times until no radioactivity was detected from the wash solution by a Geiger counter. After the wash, chromatography papers were rinsed briefly

with acetone then air dried for 1 hour. The ^{32}P of the dried chromatography papers was quantified by liquid scintillation spectrometry (PerkinElmer, Tri-Carb 2900TR). The specific activity of ATP solutions were determined from the radioactivity of the [γ-^{32}P]-ATP solutions relative to amount of unlabeled ATP in the reaction. The resulting values were used to quantify enzyme specific activities.

Enzyme concentration: The general composition of the reaction mixtures and procedures were the same as those used for reaction times (above). Reactions with varying histidine kinase concentrations were prepared. HK in the reaction buffer was incubated at room temperature for a few minutes then the reaction was initiated by the addition of ATP/[γ-^{32}P]-ATP mix solution. Reactions were quenched by the addition of ice cold phosphoric acid (final 5.77 mM). Quenched reaction was immediately spotted onto p81 chromatography paper, washed in ice cold 75 mM phosphoric acid, dried then counted. Incubation time was chosen based on the result of the time plot assay and the time point within the linear range was used. Product formations over varying enzyme concentrations were plotted and the linear range of the reaction as a function of enzyme concentration was determined.

ATP concentration: The composition of the reaction mixtures and the general procedures were the same as those used in studies of reaction times (above). Reactions with varying ATP concentrations were prepared. Incubation time and enzyme concentrations were chosen based on the results of the reaction time, enzyme concentration assays and the ones in the linear ranges were used. HK in the reaction mixture was incubated at room temperature for a few minutes and the reaction was initiated by the addition of ATP/[γ-^{32}P]-ATP mix solution. Reactions were quenched by the addition of ice cold phosphoric acid (final 5.77 mM). The assay was repeated at least three times and the average product formation over ATP concentrations are plotted.

Data fitting and determination of kinetic parameters: Data obtained from experiments with varying ATP concentrations, under conditions with which pHis formation was linear with respect to time and enzyme concentration, were fitted to the Michaelis-Menten model by use of KaleidaGraph software to determine V_{max}, K_m and k_{cat}/K_m values.

2.3 Results and Discussion

Two-component signaling pathways are critically important in pathogenesis, as well as many other aspects of bacteriology[210,211,5]. Enzyme kinetic analyses have proven to be essential for understanding signal transduction in many different signal transduction pathways in many different organisms, both for fundamental characterization of these signaling pathways, as well as in drug discovery efforts[212,213,214,215]. Nonetheless, only a handful of bacterial HKs have been kinetically characterized. This is in part due to the lack of effective assay methods. Here we

report the detailed kinetic parameters of several previously uncharacterized HKs as well as optimized conditions for detecting pHis using a medium-throughput filter paper-binding assay.

2.3.1 Phospho-His stability

Kinetic characterizations of HKs have primarily been accomplished using PAGE followed by autoradiography or alkali based filter binding assays, but both of these assays have critical shortcomings. The PAGE/autoradiography method is labor intensive, time consuming, and has a small sample capacity. The alkali-based filter binding assay frequently suffers from considerable background[216]. In search of a rapid and efficient HK kinase activity quantification method, we revisited an acid-based filter binding assay[217,218] and optimized the experimental conditions to overcome the inherent acid lability of pHis. We employed phosphoric acid at moderate concentration (75 mM) to both stop the phosphorylation reaction and to wash away unreacted ATP because we found this to be enough acid to stop the reaction with minimal pHis cleavage. Furthermore, reactions were kept near freezing during quenching and washing to avoid pHis degradation.

We used this assay to kinetically characterize four histidine kinases [*V. harveyi* (gene ID: 5555316), *V. parahaemolyticus* (gene ID: 1189383), *S. oneidensis* (gene ID: 1169886), and *L. pneumophila* (gene ID: 19831845)]. *S. oneidensis* and *L. pneumophila* HKs were orthodox HKs that lack receiver domains. HKs from *V. harveyi* and *V. parahaemolyticus* were hybrid histidine kinases with receiver domains. We used phospho-accepting aspartate mutant *Vh* and *Vp* HKs (D459A and D499A, respectively) since they yield more stable phosphorylated products and separate autophosphorylation activity from phosphotransfer and autophosphatase activities. In our first experiment, in order to determine the stability of pHis under these experimental conditions, each HK was incubated with ATP with trace amounts of [γ-^{32}P]-ATP for 60 mins, and then phosphorylated HKs were incubated in ice-cold 75 mM phosphoric acid. The degradation of pHis over time was measured by autoradiography of SDS-PAGE gels. All four HK tested in these experiments showed no apparent pHis degradation upon incubation in phosphoric acid for up to 60 min under our experimental conditions (Figure 2-1, Figure 2-2). This was somewhat surprising, as it is widely accepted that pHis is acid-labile[204,206], however, our results indicate that pHis degradation is negligible at a moderate acid concentration in solution near the freezing point of water.

To further characterize the extent of pHis stability in our assay, the phosphorylation state of the HK from *S. oneidensis* was monitored over a 2 h incubation period in ice-cold phosphoric acid. Consistent with our previous experiment, we observed no apparent degradation of pHis up to 60 min, followed by gradual degradation over the next 60 min. Overall, we observed a 7% reduction in phosphorylation of SoHK after 90 min of incubation in acid and a 21% reduction after 120 min of acid-incubation. In subsequent experiments, all of the enzymes reported here

were exposed to acid for significantly less than 60 min over the course of reaction quenching, filter paper binding, and successive washing steps. Therefore, we conclude that under our reported conditions, the integrity of protein phosphorylation is maintained.

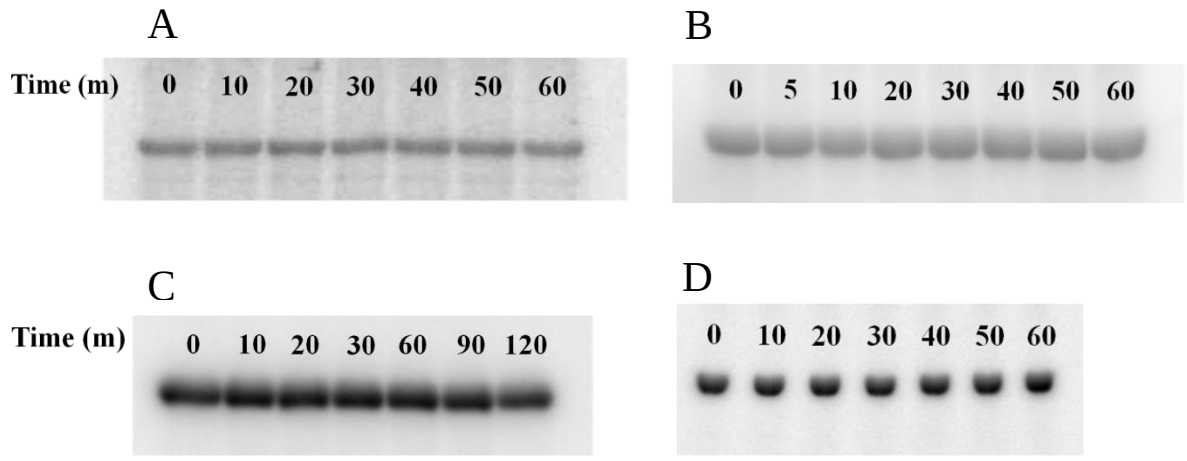

Figure 2-1. Stability of pHis on HKs from *V. harveyi* (A), *V. parahaemolyticus* (B), *S. oneidensis* (C), and *L. pneumophila* (D). The reaction mixture contained 40 mM Tris-Cl, 120 mM KCl, 10% glycerol, 4 mM $MgCl_2$, 4 mM DTT, 10 – 25 μM histidine kinase, 2 – 4 mM ATP and 2 – 7 μCi [γ-^{32}P]-ATP at pH 7.8. Autoradiography of PAGE gels shows phosphorylated histidine kinases after exposure to ice-cold 75 mM phosphoric acid for amount of time indicated. No apparent pHis degradation was observed within 60 min for all four HKs tested. Band intensities were quantified using ImageJ.

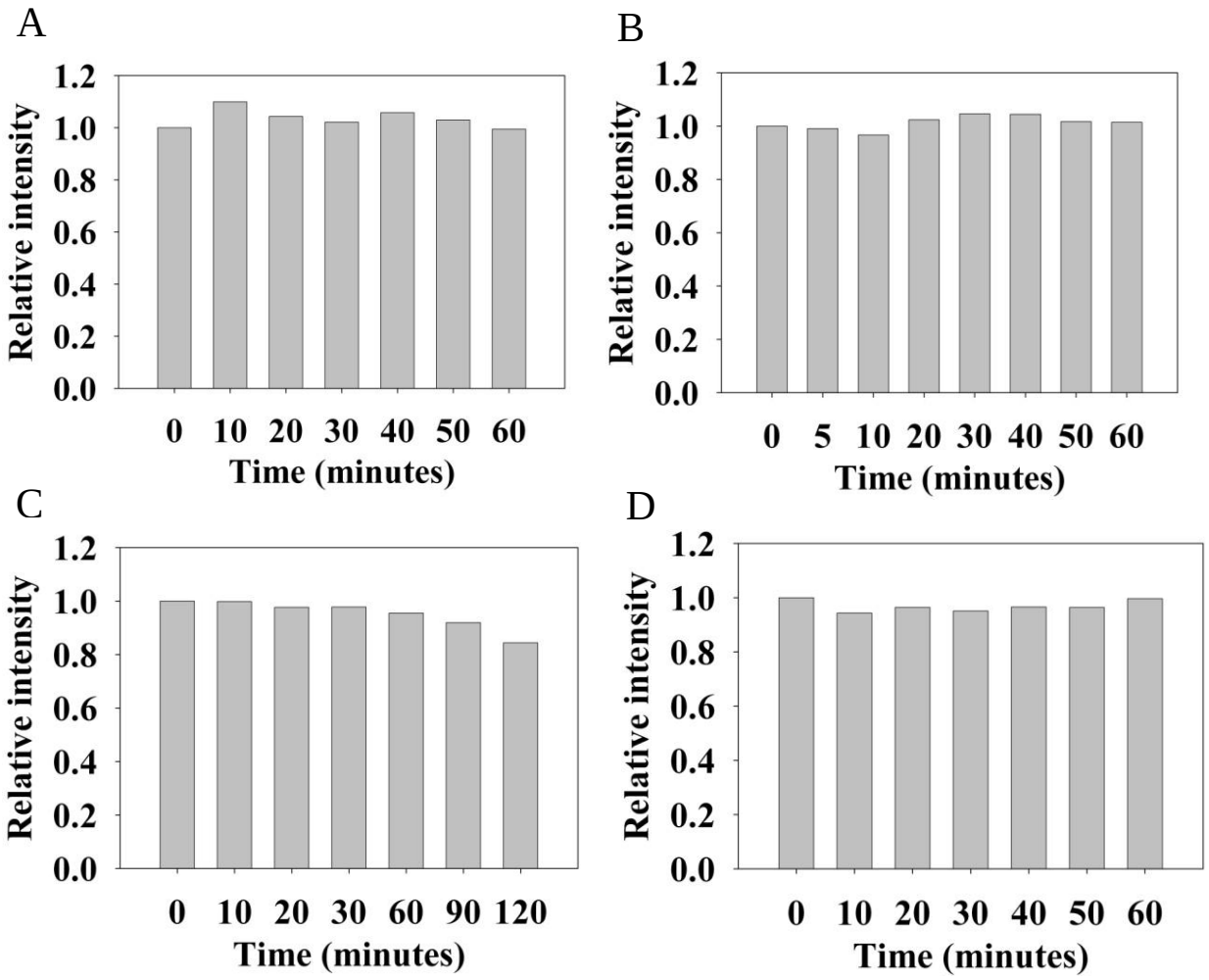

Figure 2-2. Quantified autoradiography band intensities from phospho-His stability tests (*V. harveyi* (A), *V. parahaemolyticus* (B), *S. oneidensis* (C), *L. pneumophila* (D)). No apparent pHis degradation was observed within 60 minutes for all HKs. *S. oneidensis* pHis was exposed to acid for additional 60 minutes in which it showed gradual degradation overtime – 7% degradation at 90 minutes and 21% degradation at 120 minutes.

2.3.2 Effect of time and enzyme concentration

In order to measure accurately the kinetic parameters of each HK enzyme studied here, the linear range of HK enzyme activity, as a function of time and enzyme concentration, was determined. HKs (5 – 20 μM) were incubated with 2 – 4 mM ATP with trace amounts of [γ-^{32}P]-ATP, and at various time points the phosphorylated HKs were subjected to ice-cold 75 mM phosphoric acid to quench the reaction. A plot of phosphorylation over time, for all four HKs tested here, showed the expected enzyme saturation curves, with reactions reaching saturation between 15 min (*L. pneumophila*) and 100 min (*V. harveyi*) (Figure 2-3). The linear range of the autophosphorylation reaction with respect to time was determined from these plots. To determine the linear range of the HK autophosphorylation activity as a function of enzyme concentration, pHis formation at varying enzyme concentrations was measured with fixed incubation time and ATP concentration (Figure 2-4). As expected, product formation increased linearly as a function of enzyme concentrations for all HKs tested.

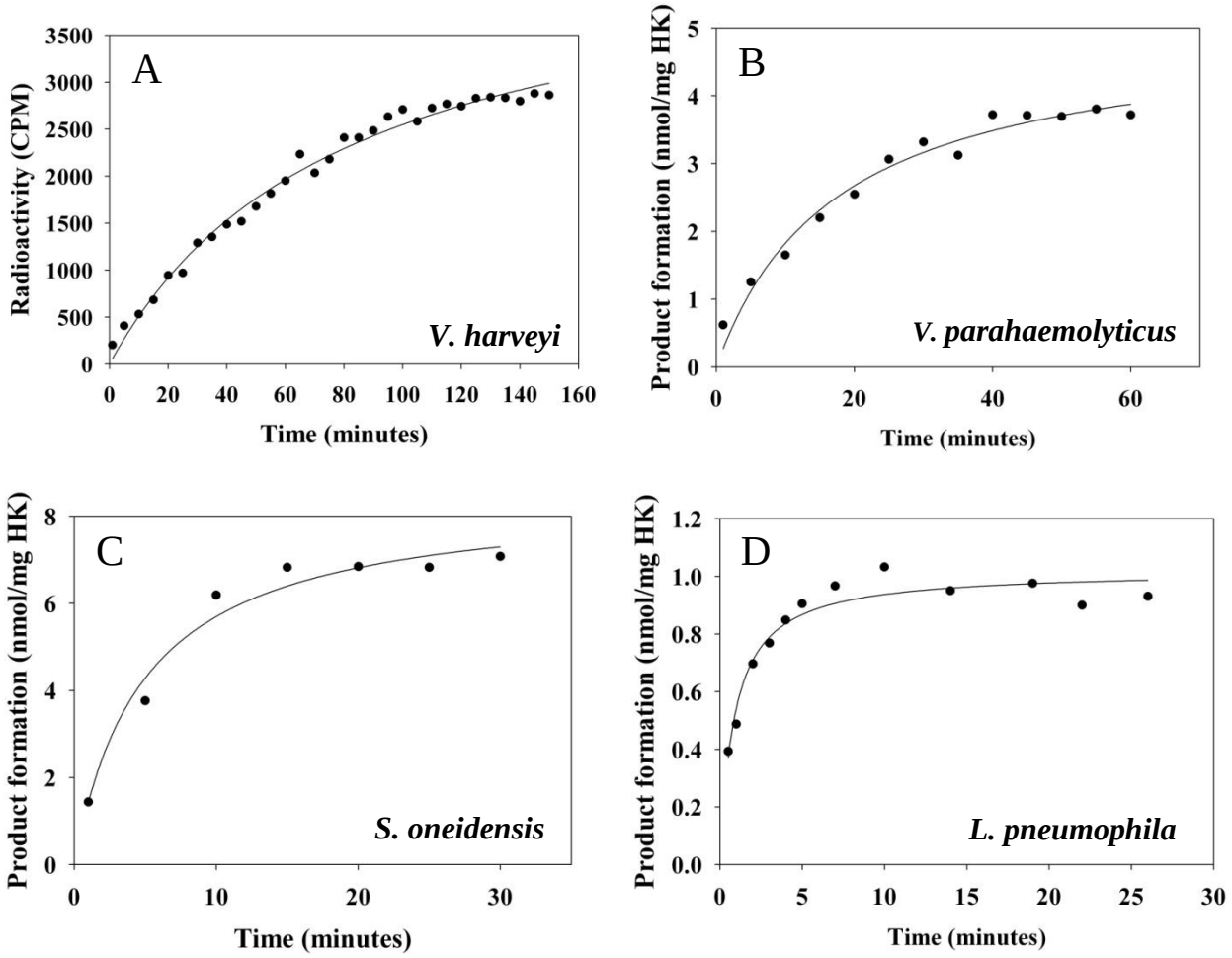

Figure 2-3. Time-dependent autophosphorylation of HKs from *V. harveyi* (A), *V. parahaemolyticus* (B), *S. oneidensis* (C), and *L. pneumophila* (D). Reactions were carried out at 23 °C ± 1 °C. ATP concentrations and enzyme concentrations, respectively, were 0.9 mM and 16 μM for *V. harveyi*, 2.1 mM, 14 μM for *V. parahaemolyticus*, 2.1 mM, 14 μM for *S. oneidensis*, and 2.1 mM, 50 μM for *L. pneumophila*. Product formation was monitored over time using the filter-paper binding assay described in the materials and methods section. All four tested HKs showed saturation curves in a time dependent manner.

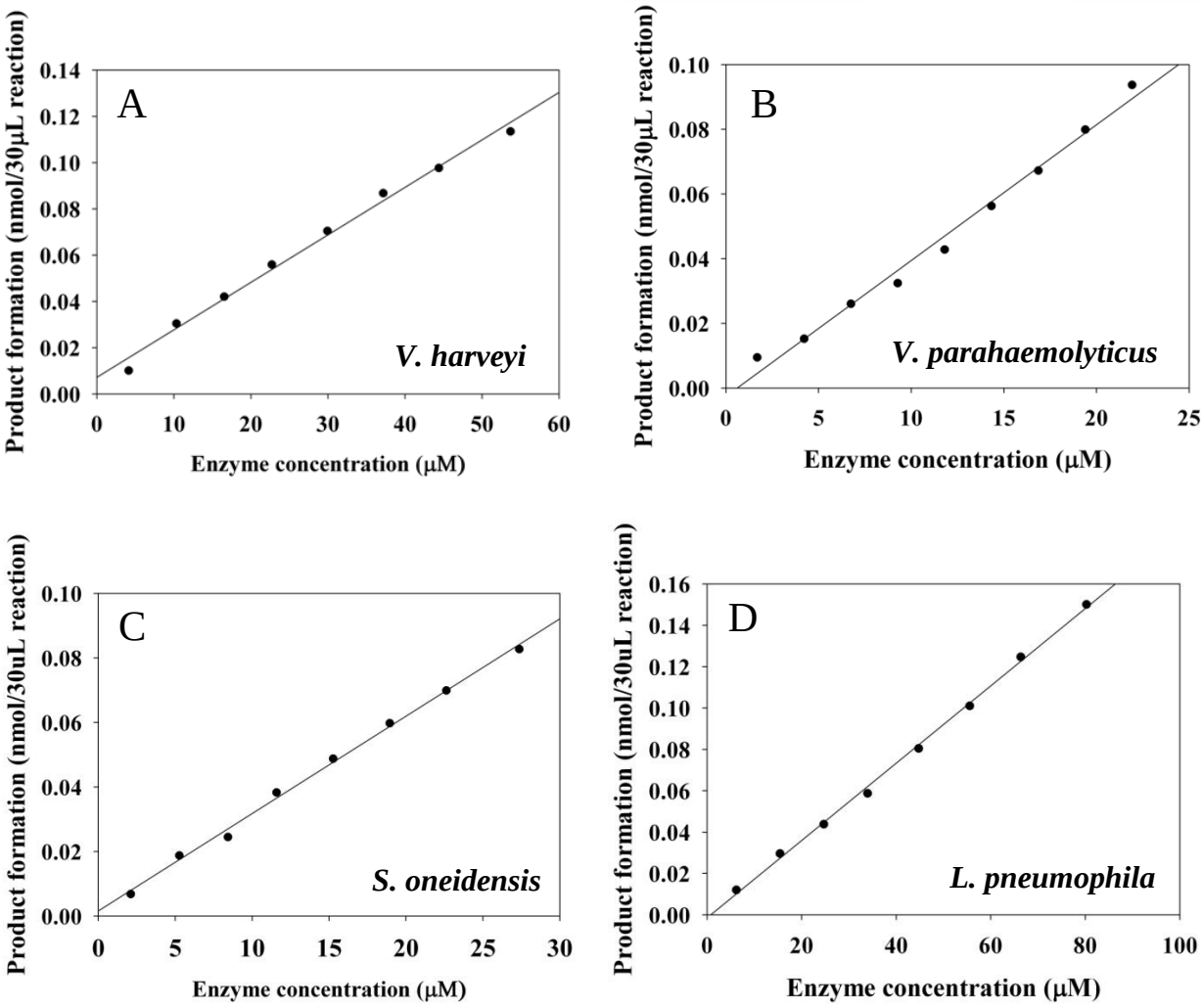

Figure 2-4. Enzyme concentration-dependent autophosphorylation of HKs from *V. harveyi* (A), *V. parahaemolyticus* (B), *S. oneidensis* (C), and *L. pneumophila* (D). ATP concentrations and incubation times were 2 mM and 40 min for *V. harveyi*, 2 mM and 20 min for *V. parahaemolyticus*, 2 mM and 5 min for *S. oneidensis*, and 2 mM and 1 min for *L. pneumophila*. Reactions were carried out at 23 °C ± 1 °C.

2.3.3 Substrate kinetics

Finally, in order to determine the k_{cat} and K_m for each HK, pHis formation as a function of ATP concentration was measured for each HK. Incubation time and enzyme concentration for each HK was chosen based on the results of time/enzyme plots (Figures 2-3 and 2-4). As illustrated in Figure 2-5, all four HKs showed the expected linear double reciprocal plot with increasing ATP concentration. Data were fitted to the Michaelis-Menten model to determine the kinetic parameters. The kinetic parameters for each HK studied here, as well as those of previously characterized HKs, are summarized in Table 2-1.

Kinetic constants of *V. parahaemolyticus, S. oneidensis,* and *L. pneumophila* were reasonably similar to those of many previously characterized *E. coli* HKs. *V. harveyi* HK had relatively low catalytic efficiency (0.02 $M^{-1}sec^{-1}$) and a large K_m (2.26 mM). The reason for the high K_m and low catalytic efficiencies of *V. harveyi* remains unclear. However, since many HKs are dual-function enzymes with both kinase and phosphatase activities[22], the primary function of VhHK may be phosphatase activity, with low kinase activity. It is also possible that the autophosphorylation activities of VpHK may be up-regulated upon detection of a ligand through its partner sensory protein.

The method provided in this paper provides an optimized method for analyzing the autophosphorylation activity of histidine kinases. The most commonly used PAGE-based method for analysis of HK-autophosphorylation is labor intensive, limits the sample number, and is time consuming. Our method is facile. It is less labor-intensive and allows a researcher to process a significantly larger number of samples in a short period of time, without risking degradation of pHis. The method proved to be effective for determining the kinetic parameters of four previously uncharacterized HKs. We propose that this assay can be used to determine the rate of autophosphorylation of any HK and may be applied further to determine the effect of ligands on HK kinase activity.

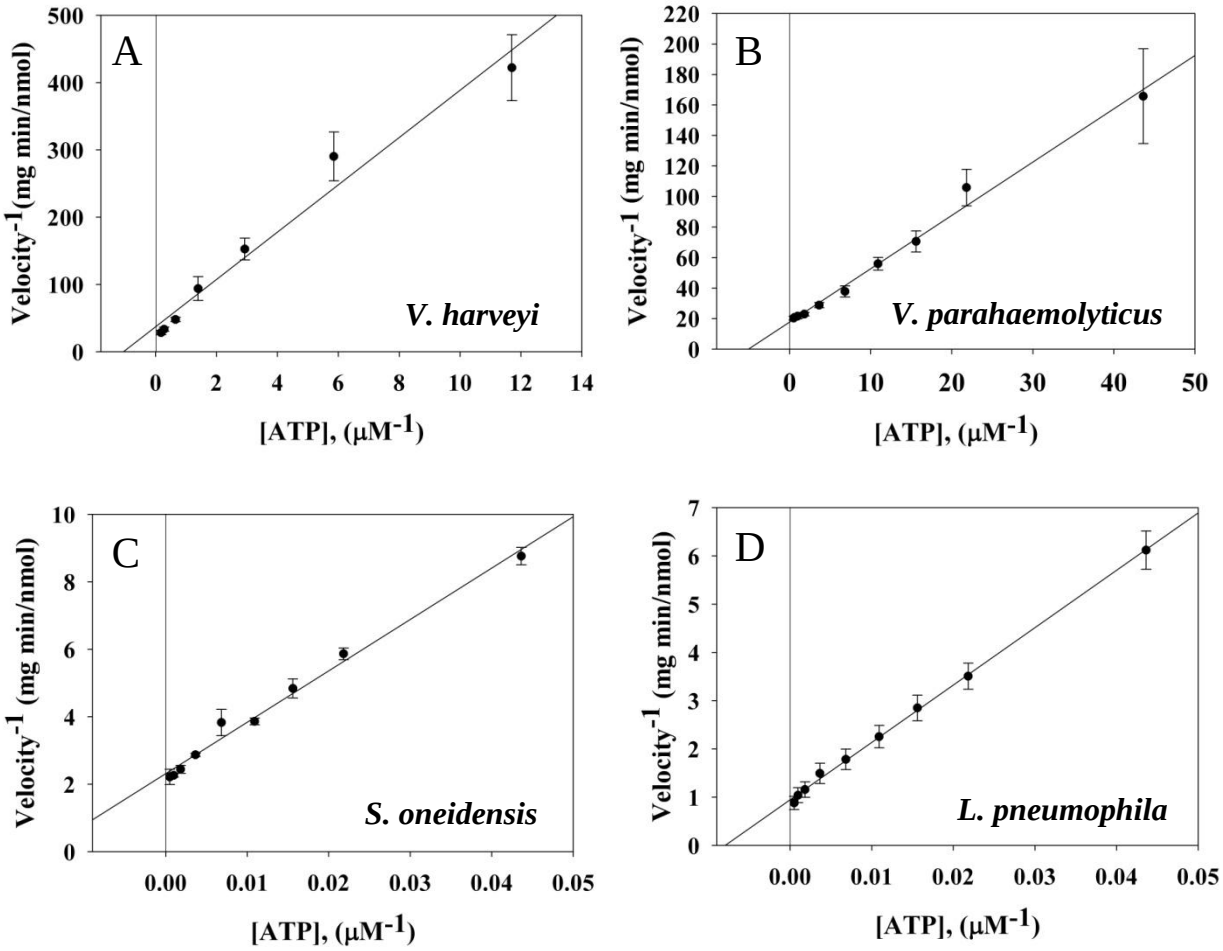

Figure 2-5. Substrate concentration-dependent autophosphorylation of HKs from *V. harveyi* (A), *V. parahaemolyticus* (B), *S. oneidensis* (C), and *L. pneumophila* (D). Double reciprocal plots are shown. Reactions were carried out at 23 °C ± 1 °C. Enzyme concentrations and incubation times, respectively, were 35 μM and 40 min for *V. harveyi*, 14 μM and 20 min for *V. parahaemolyticus*, 18 μM and 5 min for *S. oneidensis*, and 52 μM and 1 min for *L. pneumophila*. Error bars represent the standard error from the mean of a minimum of three assays.

Characterized protein	V_{max} (nmol/mg·min)	k_{cat} (/sec)	K_m (μM)	k_{cat}/K_m (/Msec)	Reference
V. harveyi, HahK	0.050 ± 0.006	4.95E-05 ± 6.30E-06	2256 ± 339	0.02	This work
V. parahaemolyticus, HahK	0.056 ± 0.003	6.01E-05 ± 3.30E-06	177 ± 12	0.34	This work
S. oneidensis, HahK	0.476 ± 0.032	2.83E-04 ± 1.90E-05	88 ± 14	3.23	This work
L. pneumophila, HK	1.320 ± 0.218	1.18E-03 ± 2.00E-04	173 ± 19	6.80	This work
E. coli, EnvZ	-	8.10E-05	218	0.37	218
E. coli, NarQ	-	2.20E-04 ± 1.10E-04	23 ± 9	9.65	219
B. subtilis, KinA	-	1.90E-03 ± 5.00E-04	74 ± 11	25.7	199
E. coli, CheA	-	2.60E-02 ± 4.00E-03	770	33.8	200
E. coli, NRII (NtrB)	-	2.37E-02 ± 5.00E-04	31 ± 1	763.4	220
E. coli, PhoQ	-	1.70E-03 ± 8.10E-04	21 ± 13	81.2	201

Table 2-1. Summary of histidine kinase autophosphorylation kinetic parameters for all characterized HK enzymes to date[201,200,199,219,220,221]**.**

Table 2-2. Bacterial strains, plasmids and primers used in this work

Strains, plasmids and primers	Genotype	Reference
Bacterial strains		
V. harveyi		
WT	*Vibrio harveyi* , BB120, ATCC BAA-1116	ATCC
V. parahaemolyticus		
WT	*Vibrio parahaemolyticus* , EB101, ATCC 17802	ATCC
S. oneidensis		
WT	*Shewanella oneidensis* , MR-1	
L. pneumophila		
WT	*Legionella pneumophilla* , Philadelphia-1, ATCC 33152	ATCC
E. coli		
DH5α	Cloning competent cell	Invitrogen
BL21(DE3)pLysS	Expression competent cell	Invitrogen
Plasmids		
pVh_HqsK(D459A)	pET-23aHis-Tev with VIBHAR_01913, N-terminus 6x His-tag, Amp^r	[28]
pVp_HqsK(D499A)	pET-23aHis-Tev with VP1876, N-terminus 6x His-tag, Amp^r	This work
pSo_HK(WT)	pET-23aHis-Tev with SO_2145, N-terminus 6x His-tag, Amp^r	This work
pLp_HK(WT)	pET-20b(+) with lpg0278, C-terminus 6x His-tag, Amp^r	This work
Primers		
pVh_HqsK(WT)-Fwd	GCG AAT TCG TGG CGT TAA AGA AAC TCG	
pVh_HqsK(WT)-Rvs	CAA TGA AGC TTT TCG CCG AGC CAT TTA CAC	
pVp_HqsK(WT)-Fwd	GGA TCC ATA TGA TGA CGG GTA ACT CC	
pVp_HqsK(WT)-Rvs	GCA TTC TCG AGC TAC TGC TCA AGC	
pSO_HK(WT)-Fwd	CCA TCC GAA TTC ATG ACT GAC AGC GAA AAT CCC	
pSO_HK(WT)-Rvs	CCA GCA GAG CTC CTA GGT TAT CGA GCT AGA AGT	
pLp_HK(WT)-Fwd	NNN CAT ATG ACA GAA ATG CAT CGG TTG TTG CAG	
pLp_HK(WT)-Rvs	NNN CTC GAG CCT CGT ACT CAA GGT TTT GGG ATT G	

Abbreviation: Amp^r: Ampicillin resistance

Chapter 3: Characterization of NO responsive QS circuit in *V. parahaemolyticus*

Abstract

Nitric oxide (NO) plays a major role in the regulation of mammalian biological functions. In recent years, NO has also been implicated in bacterial life cycles, including in the regulation of biofilm formation and the metabolism of the bacterial second messenger signaling molecule cyclic-di-GMP. In a previous study, we reported the discovery of an NO-responsive quorum sensing (QS) circuit in *Vibrio harveyi*. Here we characterize the homologous QS pathway in *Vibrio parahaemolyticus*. Spectroscopic analysis shows *V. parahaemolyticus* H-NOX is an NO sensory protein that binds NO in 5/6-coordinated mixed manner. Further, we demonstrate that through ligation to H-NOX, NO inhibits the autophosphorylation activity of an H-NOX-associated histidine kinase (HqsK; H-NOX-associated quorum sensing kinase) that is able to transfer phosphate to the Hpt (histidine-containing phosphotransfer protein) protein LuxU. Indeed, among the three Hpt proteins encoded by *V. parahaemolyticus*, HqsK transfers phosphate only to the QS-associated phosphotransfer protein LuxU. Finally, we show that NO promotes expression of the master quorum sensing regulatory protein OpaR at low cell density.

3.1 Introduction

Quorum sensing (QS) refers to a cell-to-cell communication system utilized by bacteria to assess their population density and to coordinate population-wide changes in gene expression. In QS, bacterial cells produce, secrete, and detect small signaling molecules called autoinducers (AI). Many types of autoinducers have been identified, some that are unique to a particular species and some that are shared by multiple bacterial species[143,144,145,148]. In a simplified scheme, a QS circuit consists of an AI synthase, a corresponding AI-sensing histidine kinase (HK) and a cytoplasmic response regulator (RR). The QS-associated HKs in many bacteria are hybrid histidine kinases that have both kinase and phosphatase activities that can thus phosphorylate and remove phosphate from the cognate response regulator[27,28,29]. Frequently, response regulators are transcription factors that are active only when they are phosphorylated[32,40,41] Quorum sensing is able to control gene expression patterns as a function of population density because at low cell density, AI concentrations are also low and therefore the HKs are not complexed with AI. Under these conditions, kinase activity predominates, and phosphate is transferred to the RR. The phosphorylated RR then facilitates changes in gene expression patterns, resulting in an adaptive cellular response. At high cell density, elevated AI concentrations result in HK binding, which switches the function of the kinase to phosphatase, leading to the removal of phosphate from the RR, and corresponding changes in gene expression.

Vibrio parahaemolyticus is a marine bacterium widely distributed in sea water around the world[222,223] and the leading cause of seafood-borne illnesses[224,225]. *V. parahaemolyticus* produces a number of virulence factors, including the type III secretion system 1 (T3SS1), that are regulated by quorum sensing[226]. *V. parahaemolyticus* shares a QS architecture with *Vibrio harveyi*, which is composed of three AIs (AI-2, HAI-1 and CAI-1), their synthases, and cognate membrane-bound sensory histidine kinases (LuxM/N, LuxS/PQ and cqsA/cqsS, respectively)[139,131]. All three AI-sensing kinases engage in phosphotransfer with an Hpt (histidine-containing phosphotransfer protein) called LuxU. The phosphorylation state of LuxU regulates the phosphorylation state of the response regulator LuxO. LuxO is a transcription factor that regulates the transcription of small regulatory RNAs, qrrs 1-5. Along with sigma-factor Hfq, these qrrs regulate the translation of two master quorum sensing regulatory proteins, AphA and OpaR. AphA and OpaR are both transcription factors that regulate the expression of various genes, including many involved in motility, surface sensing, biofilm formation and virulence.

A recent study conducted in our laboratory identified a fourth arm in the *V. harveyi* QS circuit. In this pathway, the signaling molecule nitric oxide (NO) gas is integrated into QS via ligation to the hemoprotein H-NOX and its partner, an H-NOX-associated hybrid HK called HqsK (H-NOX-associated quorum sensing kinase)[127]. Membrane-permeable NO is detected by H-NOX in the cytoplasm. The ligation state of H-NOX regulates the activity of HqsK. When NO is not present, HqsK functions as a kinase, transferring phosphate to LuxO via LuxU. Upon NO binding to H-NOX, HqsK switches from a kinase to a phosphatase, causing a reverse in

phosphate flow and contributing to dephosphorylation of LuxO. In this work, we further characterize the NO-responsive QS circuit in the pathogenic marine bacterium *V. parahaemolyticus*.

3.2 Materials and methods

Unless otherwise noted, all the reagents were purchased at their highest available qualities and used as received.

3.2.1 Bacterial strains and culture method

E. coli strain DH5α was used for cloning and *E.coli* BL21(DE3)pLysS was used for protein expression. DH5α was cultured in LB medium supplemented with 100 μg/mL ampicillin. BL21(DE3)pLysS was cultured in 2XYT media (16 g/L Tryptone, 10 g/L yeast extract and 5 g/L NaCl) supplemented with 100 μg/mL ampicillin and 34 μg/mL chloramphenicol. Both cultures were grown at 37 °C with 250 rpm agitation. At A_{600nm} between 0.5-1.0, protein expression was induced with 100 μM isopropyl-β-D-thiogalactopyranoside (IPTG) for 15 hours at 16 °C, then cells were harvested. *Vibrio parahaemolyticus* strain EB101 (ATCC17802) was purchased from American Type Culture Collection and was grown by following the supplier's culture method. In *Vibrio parahaemolyticus* growth curve and qPCR experiment, an overnight culture of *V. parahaemolyticus* was diluted 1:500 into fresh media (BD234000 Nutrient broth with 3% NaCl), supplemented with 100 μg/mL ampicillin with various DETA NONO concentrations (Cayman Chemical). Cultures were grown at 37 °C with agitation at 250 rpm. Bacterial growth was monitored by measuring A_{600nm} and harvested at designated ODs.

3.2.2 Molecular cloning and mutagenesis

Genome of *V. parahaemolyticus* strain EB101 has not been sequenced. Instead, we referred to the genome sequence of *V. parahaemolyticus* strain RIMD 2210633 for gene annotations and primer designing. *V. parahaemolyticus* genomic DNA was extracted using Zymo Research Quick-gDNA MiniPrep (D3006), by following the manufacturer's instructions. Extracted *V. parahaemolyticus* gDNA was used as a template to amplify *Vp* H-NOX (VP1877, gene ID: 1189384), HK (VP1876 gene ID: 1189383), LuxU (VP2098, gene ID: 1189609), and Hpt proteins (VP1472, gene ID: 1188978 and VP2127, gene ID: 1189639) by PCR. Primers for VP1877, VP1876 kinase domain only, VP1876 internal kinase domain only and VP2098 contained NdeI and XhoI up-stream/down-stream restriction sites respectively. VP1472 and VP2127 primers contained NdeI and NotI restriction sites respectively. For all PCR reactions,

Phusion High-Fidelity DNA Polymerase (New England Biolabs, M0530S) was used. Amplified products were double digested then ligated into pET-20b(+) vector (Novagen) or pET-23aHis-TEV and sequenced (Stony Brook DNA sequencing facility). Site-directed mutagenesis to generate VP1876 HK H214A and D499A was carried out following the QuikChange Site-directed Mutagenesis kit protocol (Stratagene). The primer sequence used for cloning and site-directed mutagenesis will be provided upon request.

3.2.3 Protein expression and purification

All proteins contained a 6× His tag on either the N or C-terminus and were purified by immobilized metal ion affinity chromatography using Ni-NTA agarose. Protein concentrations were determined by Bradford assay with bovine serum albumin as a standard[209].

3.2.4 H-NOX complex preparation and electronic microscopy

In an anaerobic glove bag, purified *Vp* H-NOX protein was incubated with 10 mM potassium ferricyanide for 5 minutes to make Fe(III) H-NOX. Potassium ferricyanide was then removed using PD10 desalting column (GE Healthcare). Prepared *Vp* Fe(III) H-NOX was incubated with 20 mM sodium dithionite for 30 minutes then desalted to prepare Fe(II) H-NOX. Fe(II) H-NOX was further incubated with 3 mM DPTA NONOate (Cayman Chemicals) for 30 minutes then desalted to prepare Fe(II) NO·H-NOX. To make CO bound H-NOX, Fe(II) H-NOX was bubbled with CO for 10 minutes in a closed Reacti-Vial (Thermo Scientific). Electronic spectra of all samples were measured by a Cary 100 UV-Vis spectrophotometer (Agilent) equipped with Cary temperature controller set at 20 °C. For temperature dependent 5, 6-coordinate NO·H-NOX distribution analysis, the sample's temperature was varied from 4 to 40 °C utilizing the temperature controller.

3.2.5 NO dissociation rate

Procedure has been described previously[227]. Briefly, in an anaerobic glove bag, NO bound *Vp* Fe(II) H-NOX was diluted in 40 mM Tris-Cl, 150 mM KCl, 10% glycerol and 4 mM DTT buffer at pH 7.6-7.9, then was rapidly mixed with an equal amount of the same buffer at 3, 30 or 300 mM of sodium dithionite saturated with CO. The absorption spectra were obtained by Cary 100 UV-Vis spectrophotometer (Agilent) equipped with a Cary temperature controller set at 20 °C. Nitric oxide dissociation was monitored by tracking increasing Fe(II) CO peak at 424 nm and decreasing Fe(II) NO peak at 399 nm. The resulting data was fitted to a two-phase exponential association equation, $y = y^0 + A_1*(1 - e^{-x/t1}) + A_2*(1 - e(^{-x/t2})$ to determine the NO

dissociation rate. The experiments were repeated a minimum of three times for each sodium dithionite concentration. The resulting average k_{off} (NO) rates were reported with SEM. The dissociation rates were independent of sodium dithionite concentrations.

3.2.6 HK autophosphorylation assay

[γ-^{32}P]-ATP (6000 Ci/mmol, 10 mCi/mL) was purchased from PerkinElmer Health Sciences Incorporated. All reactions were performed at room temperature. Reaction mixtures contained final concentrations of 40 mM Tris-Cl, 150 mM KCl, 10% glycerol, 4 mM $MgCl_2$, 4 mM DTT, 5-10 μM histidine kinase, 2-4 mM ATP and 2-7 μCi [γ-^{32}P]-ATP at pH 7.6 – 7.9. Histidine kinase in the reaction buffer was allowed to equilibrate at room temperature for a few minutes then reactions were initiated by the addition of an ATP/[γ-^{32}P]-ATP mix solution. Reactions were quenched by adding 5× SDS loading dye (0.25% bromophenol blue, 0.5 M dithiothreitol, 50% Glycerol, 10% sodium dodecyl sulfate, 0.25 M, pH 6.8 Tris-Cl) at indicated time points. Quenched reactions were separated by SDS-PAGE. After gel drying, the sample radioactivity was detected by a Typhoon scanner (Typhoon 9400, Amersham Biosciences) then quantified with image processing software ImageJ.

3.2.7 HK phosphatase activity assay

Purified *Vp* HK was mixed with the final concentration of 250 μM 3-O-methyl-fluorescein phosphate (OMFP) in the reaction buffer (40 mM Tris-HCl, 150 mM KCl, 10% glycerol, 4 mM DTT at pH 7.6-7.9) at room temperature. HK's phosphatase activity was quantified by measuring the absorbance of OMFP hydrolysis product, O-methylfluorescein (OMF) at 450 nm. All data acquisition was done by VICTO X5 Multilabel Plate Reader (PerkinElmer).

3.2.8 HK/LuxU phosphotransfer assay

The components of the reaction mixture were the same as those used in the HK autophosphorylation assay. Reactions were performed at room temperature. The final concentration of 9.4 μM HK in the reaction buffer was incubated with ATP/[γ-^{32}P]-ATP mix solution for 40 minutes to autophosphorylate HK. The final concentration of 40.7 μM LuxU was then added to the reaction mixture to initiate phosphotransfer. Reactions were quenched by the addition of 5× SDS loading dye at various time points followed by gel electrophoresis, gel drying and image scanning. Histidine kinase only with ATP mix solution, LuxU only with ATP mix solutions were run along with HK + LuxU as controls.

3.2.9 HK autophosphorylation activity inhibition by H-NOX

All reactions were carried out at room temperature. The components of the reaction mixture were the same as those used in the HK autophosphorylation assay. In an anaerobic glove bag, different oxidation/ligation states of H-NOX (final concentration 69.4 μM or varying [NO·H-NOX] for the titration) were incubated with *Vp* HK (D499A, final concentration 5.3 μM) for 30 minutes. Reactions were initiated by the addition of ATP/[γ-^{32}P]-ATP mix solution. Thirty minutes after the initiation of the reaction, reactions were terminated by adding 5× SDS loading dye, followed by SDS-PAGE, gel drying and image scanning.

3.2.10 Phosphotransfer profiling

The procedure followed what's been described by Laub[228]. All reactions were performed at room temperature. The components of the reaction mixture were the same as those of the HK autophosphorylation assay. Final concentrations of 3.3 μM HK DHp domain and 3.3 μM IKR domains were incubated with ATP/[γ-^{32}P]-ATP mix solution for 60 minutes. Final concentrations of 33 μM histidine containing phosphotransfer proteins (VP1472, VP2098 or VP2127) were added to the reaction mixtures to initiate phosphotransfer. At various time points, reactions were quenched by adding 5× SDS loading dye. Proteins were separated by electrophoresis on polyacrylamide gels, followed by gel drying and image scanning.

3.2.11 Phosphotransfer specificity test

All reactions were carried out at room temperature and the components of the reaction mixtures were the same as those used in phosphotransfer profiling. Reaction mixtures with various components, DHp only, IKR only, VP1472 only, VP2098 (LuxU) only, VP2127 only, DHp + IKR, DHp + IKR + VP2098 (LuxU), DHp + VP1472, DHp + VP2098 (LuxU), DHp + VP2127, were incubated with ATP/[γ-^{32}P]-ATP mix solution for 60 minutes. Reactions were terminated by the addition of 5× SDS loading dye, followed by gel electrophoresis, gel drying and image scanning.

3.2.12 RNA extraction, cDNA synthesis and qPCR

RNA was extracted from bacterial cultures using the PureLink RNA Mini Kit (Ambion). Extracted RNA was treated with dsDNase (Thermo Scientific). cDNA synthesis and qPCR were carried out using either DyNAmo SYBR Green 2-Step qRT-PCR Kit or Maxima First Strand

cDNA Synthesis Kits for RT-qPCR and DyNAmo HS SYBR Green qPCR Kit (Thermo Scientific). qPCR was carried out using primers listed in table 3-2 and SecY (VP0277) as a reference gene. Data were analyzed by ΔΔCT method (BIO-RAD).

3.3 Results and Discussion

3.3.1 *Vp* H-NOX is an NO-binding protein

To begin investigating the NO/H-NOX-mediated QS circuit in *V. parahaemolyticus*, we cloned, expressed, and purified *Vp* H-NOX (VP1877, gene ID: 1189384) and analyzed its spectroscopic and ligand-binding properties (Figure 3-1 and Table 3-1). The absorption peaks of purified H-NOX from *V. parahaemolyticus* in various oxidation/ligation states are similar to those of the eukaryotic H-NOX homolog sGC, as well as *V. harveyi*, *Shewanella oneidensis*, and other previously characterized H-NOX proteins[229,101,127,227]. The reduced-unligated (Fe^{II}-unligated) and CO-bound (Fe^{II}-CO) *Vp* H-NOX complexes have Soret band maxima at 426 nm and 424 nm respectively (Figure 3-1). Interestingly, NO-bound (Fe^{II}-NO) *Vp* H-NOX has two Soret peaks, at 399 and 417 nm, which indicates the protein is a mixture of 5- and 6-coordinate heme at 20 ºC. In previous work on the H-NOX from *Nostoc punctiforme*, it was shown that the distribution of the Fe^{II}-NO coordination state is temperature dependent, with lower temperatures favoring the 6-coordinate complex and higher temperature favoring the 5-coordinate state[227]. We tested if this was also the case for *Vp* H-NOX by varying the temperature from 4 to 40 °C. Indeed, we observed that the distribution of the 5- and 6-coordinate complexes was temperature dependent, being predominately 6-coordinate at 4 °C with a shift towards 5-coordinate as the temperature was increased (Figure 3-2). We also determined the NO dissociation rate for *Vp* H-NOX using a sodium dithionite/carbon monoxide trap[117,230]. We determined k_{off} to be $(4.3 \pm 0.5) \times 10^{-4}$ s^{-1} at 20 ºC, indicating a slow NO dissociation rate, similar to those of other previously characterized H-NOX proteins (Table 3-1). All of these results support that *Vp* H-NOX is a NO-binding protein.

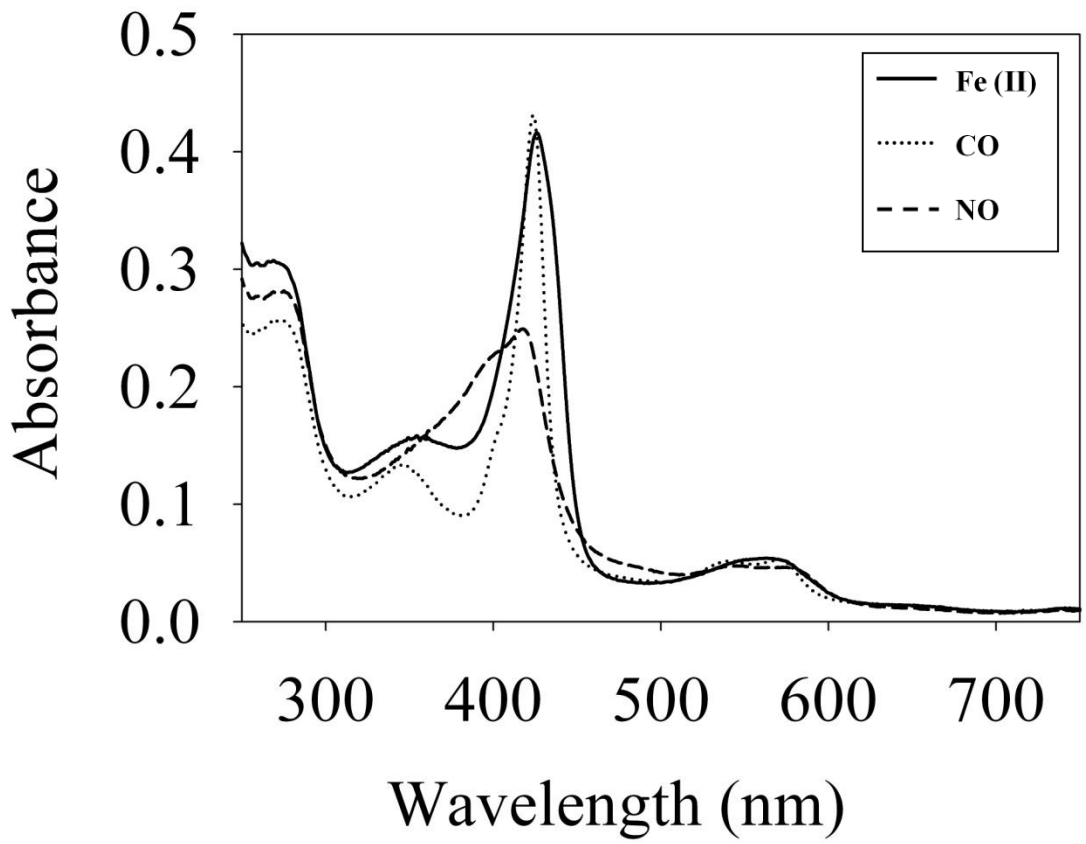

Figure 3-1. **Absorption spectra of *Vibrio parahaemolyticus***. Soret peaks of *Vp* H-NOX Fe(II), Fe(II)·CO and Fe(II)·NO H-NOX at 20 °C. Their Soret maxima are 426, 424 and 399/417nm respectively.

Protein	Soret peaks (nm)			k_{off} (NO)	Reference
	Fe^{II} unligated	Fe^{II}-CO	Fe^{II}-NO	$\times 10^{-4}$ s^{-1}	
sGC[a]	431	423	398	3.6 ± 0.8	228
Tt H-NOX[b]	431	424	420	5.6 ± 0.5	101
Vp H-NOX	426	424	399/417	4.3 ± 0.5	This work
Vh H-NOX[c]	429	423	399	4.6 ± 0.9	127
Np H-NOX[d]	430	423	400/416	-	226

[a]H-NOX domain from soluble guanylate cyclase from bovine lung. [b]H-NOX from *Thermoanaerobacter tengcongensis*. [c]H-NOX from *Nostoc punctiforme*. [d]H-NOX from *Nostoc punctiforme*.

Table 3-1. Electronic absorption spectra Soret peaks and NO dissociation rates of various H-NOX proteins.

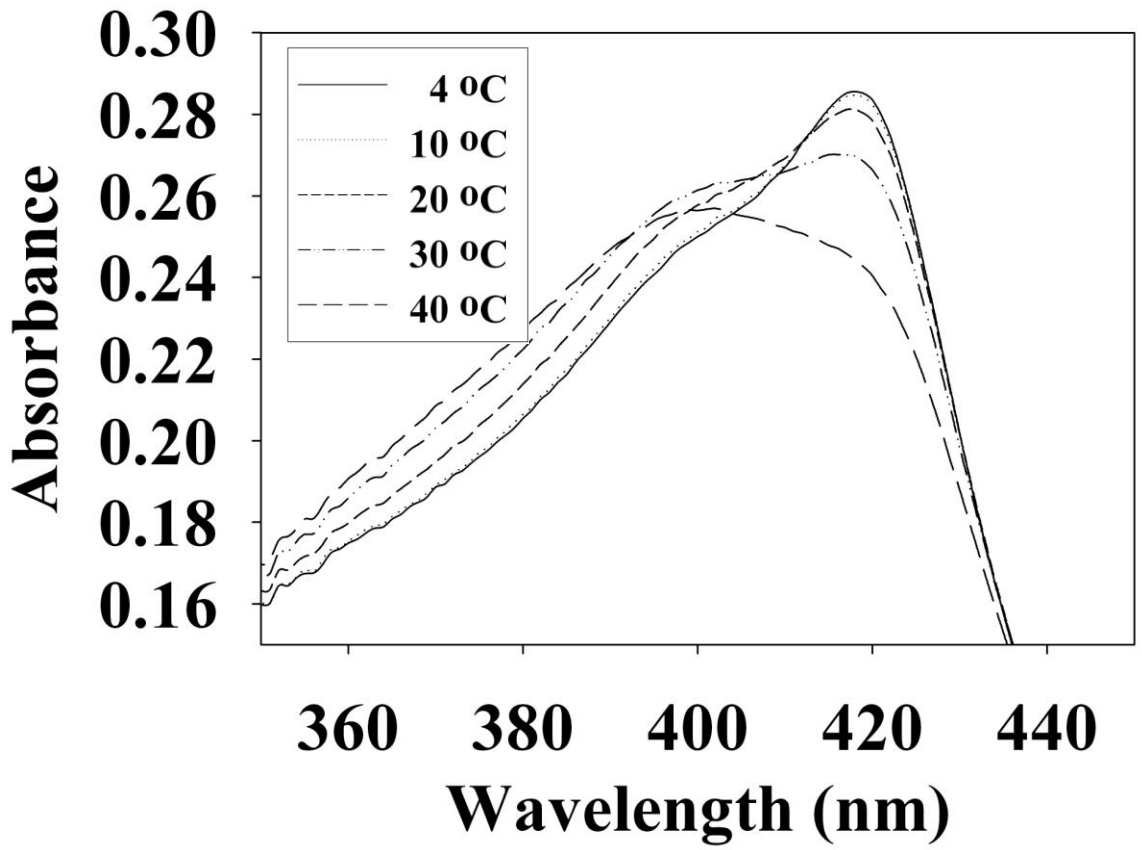

Figure 3-2. Temperature dependent absorption spectra of *V. parahaemolyticus* Fe^{II}-NO H-NOX. The absorption spectrum shows the shift in the 5/6-coordinate Fe^{II}-NO H-NOX ratio by temperature, lower temperatures favoring 6-coordinate (417 nm) and higher temperatures favoring 5-coordinate (399 nm). Absorption spectra were taken at 4 °C (—), 10 °C (·····), 20 °C (- - -), 30 °C (— · —) and 40 °C (– – –).

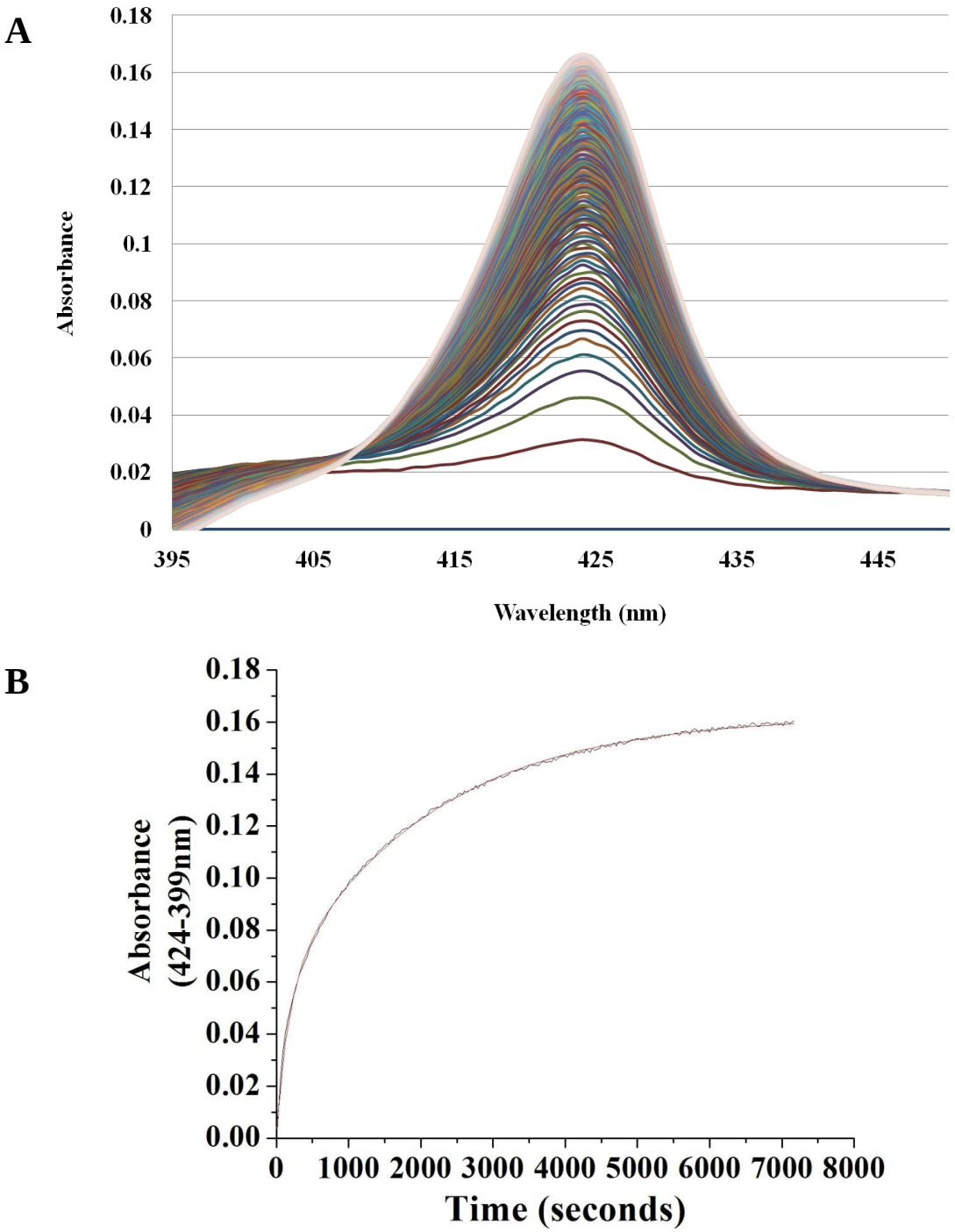

Figure 3-3. Continuous absorption spectra during *Vp* H-NOX Fe^{II}-NO dissociation rate determination. Rate of NO dissociation was measured by electronic absorption spectroscopy using saturating CO and 3-300 mM $Na_2S_2O_4$ as a released NO trap. The assay was conducted at 20 °C and the dissociation rate was $Na_2S_2O_4$ concentration independent. Absorbance difference (B) spectrum shows the absorbance difference (absorbance at 0 sec subtracted from each subsequent absorbance) versus time along with the exponential fit of the data.

3.3.2 *Vp* HqsK is an active hybrid kinase with kinase and phosphatase activities

Bacterial *hnoX* genes often neighbor genes that code for signaling proteins, such as HKs, cyclic-di-GMP metabolizing proteins, or methyl accepting chemotaxis proteins[98]. In all H-NOX homologs characterized to date, H-NOX has been demonstrated to regulate the activity of its associated signaling protein as a function of NO binding. In *V. parahaemolyticus*, *hnoX* is encoded in the same operon as a hybrid HK predicted to be involved in QS. We named this kinase HqsK (H-NOX-associated QS kinase). To identify whether HqsK (VP1876, gene ID: 1189383) is a functional kinase, we cloned, expressed, and purified the protein, and then conducted autophosphorylation activity assays. As illustrated in Figure 3-4 and 3-5, when HqsK is incubated with ATP containing trace [γ-^{32}P]-ATP over time, the resulting autoradiography shows accumulating radiolabeled phosphate on the HK in a time-dependent manner, confirming kinase activity of *Vp* HqsK.

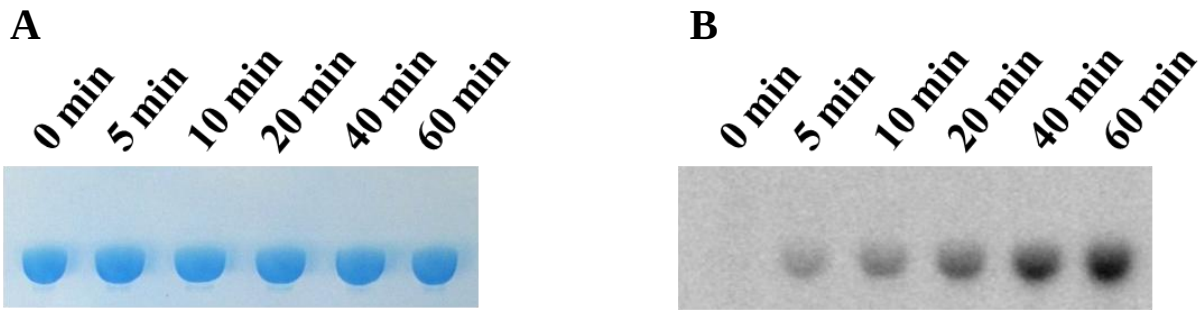

Figure 3-4. *In vitro* autophosphorylation activity assay of *Vp* HqsK (D499A). Autophosphorylation activity was detected by autoradiography following SDS-PAGE. Stained polyacrylamide gel shows uniform protein loading (A). Autoradiography shows increasing phosphate accumulation on *Vp* HqsK over time (B)

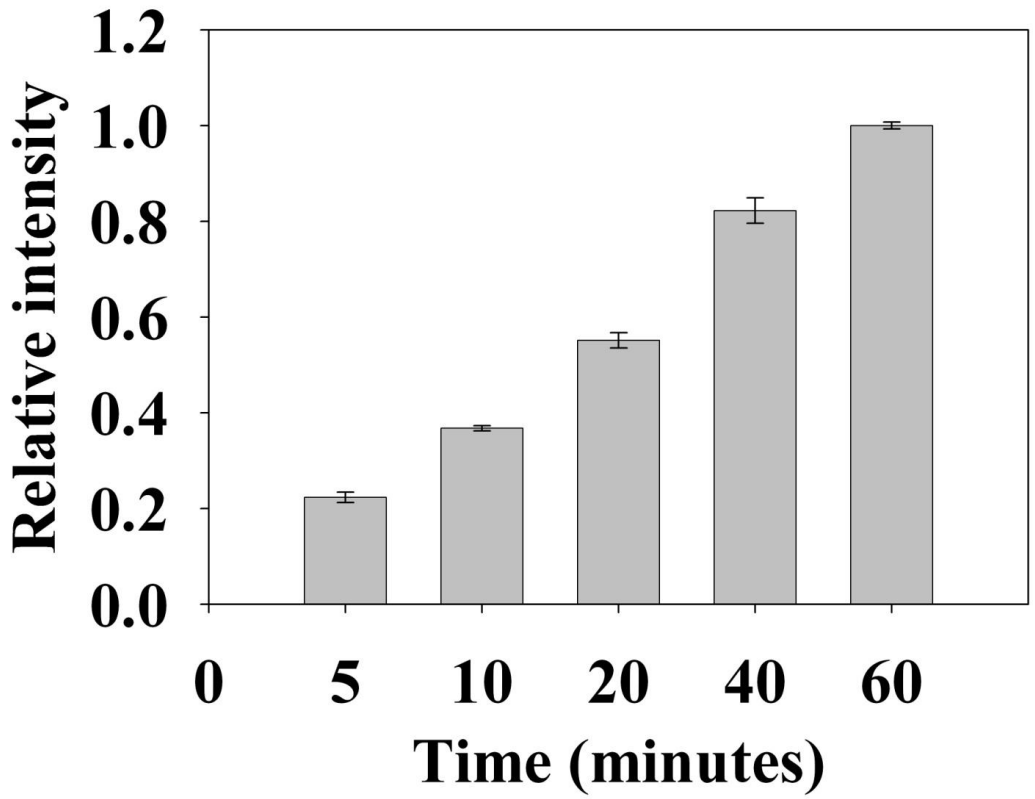

Figure 3-5. *In vitro* autophosphorylation activity assay of *Vp* HqsK (D499A) (Plot). Band intensity from *Vp* HqsK kinase activity assay (Figure 3-4) was quantified with imageJ. Average ± SEM from three independent assays are shown.

Many hybrid HKs are dual-functioning enzymes that have phosphatase activity in addition to kinase activity, in order to regulate the phosphorylation state of a partner response regulator[5]. To test whether *Vp* HqsK is such an enzyme, phosphatase activity was monitored using a generic phosphatase substrate 3-O-methyl-fluorescein phosphate (OMFP), that yields O-methylfluorescein (OMF) upon dephosphorylation. Wild-type HqsK displays increasing OMF fluorescence over time, indicating *Vp* HqsK has phosphatase activity (Figure 3-6).

The kinase and phosphatase activities of hybrid HKs are dependent on conserved His and Asp residues, respectively[231,232,233]. To demonstrate the importance of these residues for phosphatase activity, we generated H214A and D499A mutant HqsKs and repeated the phosphatase assay. Wild-type and H214A HKs have the same level of phosphatase activity as the wild-type enzyme, whereas D499A has significantly reduced phosphatase activity, indicating conserved D499 in the internal kinase receiver domain (IKR) is required for *Vp* HqsK phosphatase activity.

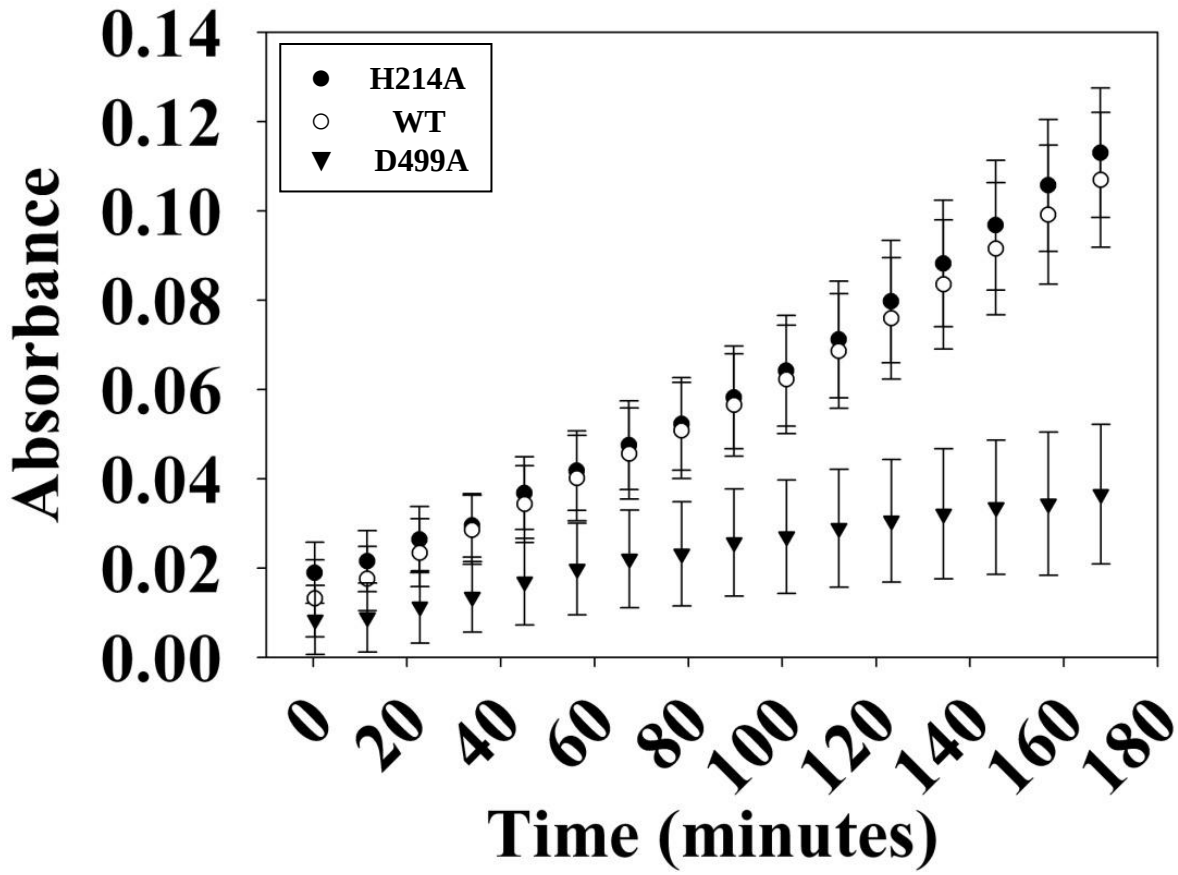

Figure 3-6. Phosphatase activity of *Vp* HK. *Vibrio parahaemolyticus*' phosphatase activity over time was monitored using OMFP as a substrate. *Vp* HK has phosphatase activity, which was diminished upon the mutation of conserved aspartic acid (D499A) in the kinase receiver domain. The plot shows the average of three independent assays ± SEM.

3.3.3 *Vp* HqsK transfers phosphate to the quorum sensing phosphotransfer protein LuxU

To establish the phosphotransfer circuit between *Vp* HqsK and the quorum sensing histidine-containing phosphotransfer protein LuxU, a phosphotransfer assay was conducted. Purified HqsK was incubated with ATP containing trace [γ-^{32}P]-ATP, followed by the addition of purified LuxU. The resulting autoradiography shows an accumulation of radiolabeled phosphate on LuxU over time, indicating *Vp* HqsK transfers phosphate to LuxU (Figure 3-7). We also tested HqsK/LuxU phosphotransfer using the H214A and D499A HqsK mutants to confirm the transfer is occurring, as predicted, via phosphotransfer from H214 to D499 in HqsK followed by transfer to H56 in LuxU. As expected, H214A HqsK showed neither autophosphorylation nor phosphotransfer activities, whereas D499A HqsK exhibited only autophosphorylation activity (Figure 3-8).

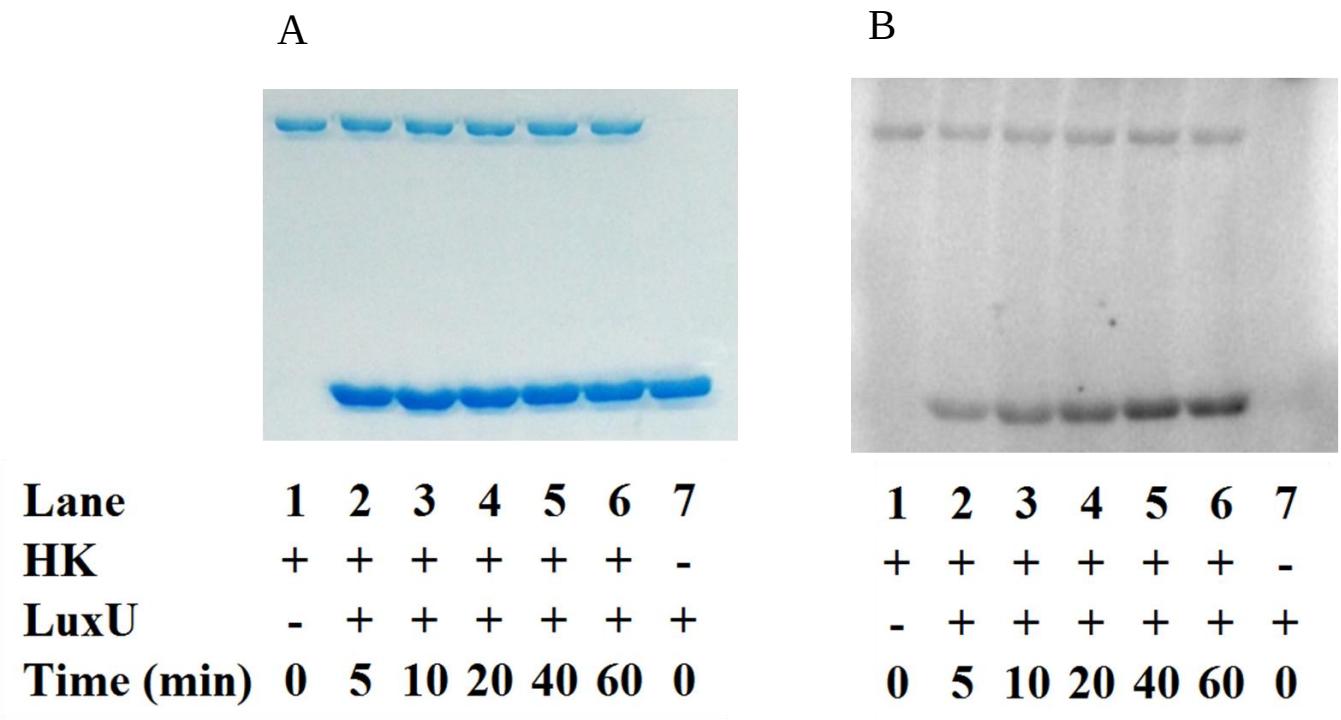

Figure 3-7. *In vitro* phosphotransfer assay of *Vp* HqsK to LuxU. Phosphotransfer activity was detected by SDS-PAGE and autoradiography. Stained polyacrylamide is shown for uniform protein loading (A). *Vp* HqsK transfers phosphate to LuxU over time in the presence of ATP (B).

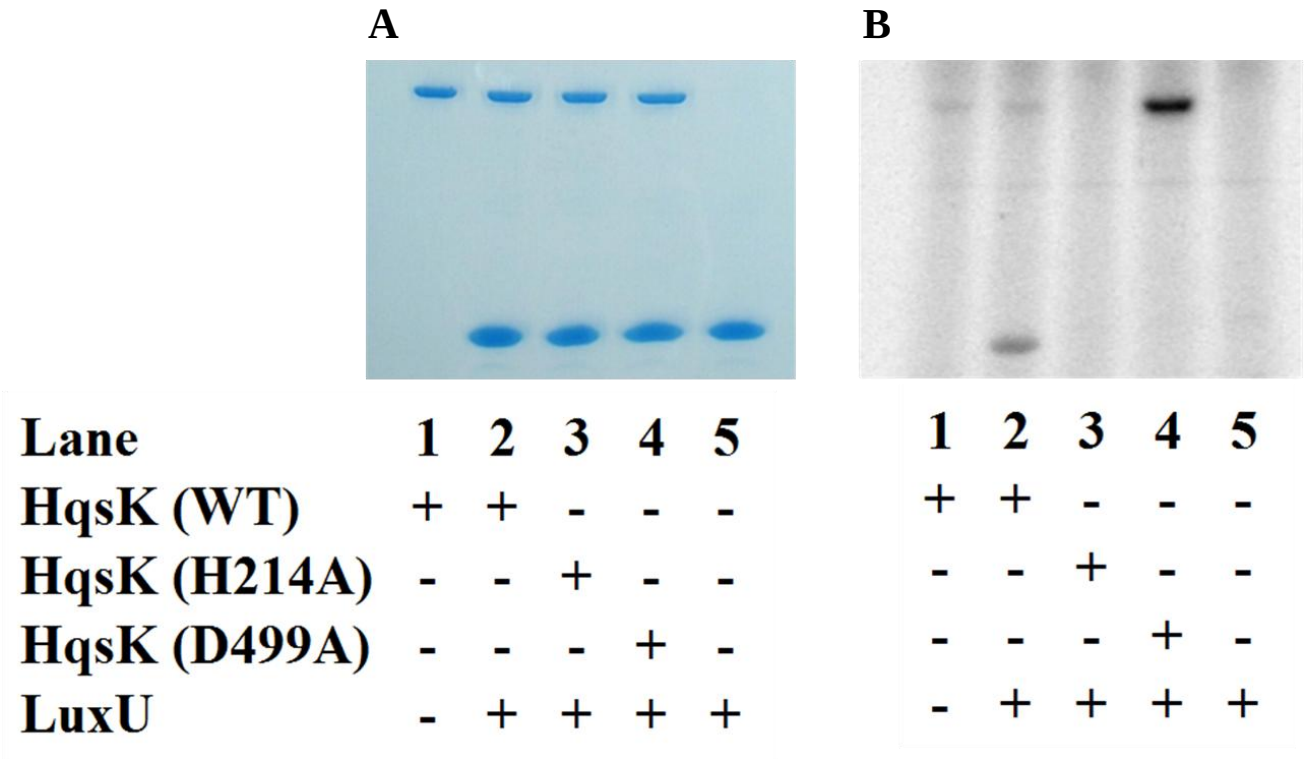

Figure 3-8. Phosphotransfer specificity test. *In vitro* phosphotransfer assay from HqsK to LuxU with H214A, WT and D499A HqsK. Stained polyacrylamide gel (A) and autoradiography (B) are shown. H214A HqsK has no autophosphorylation activity due to the phosphorylation site mutation. D499A, kinase receiver domain mutant autophosphorylates, but does not phosphotransfer to receiver domain nor LuxU.

3.3.4 LuxU is the cognate phosphotransfer protein for *Vp* HqsK

V. parahaemolyticus has three stand-alone Hpts. As described above, we have demonstrated that *Vp* HqsK transfers phosphate to LuxU, but since many HKs can transfer phosphate to multiple partners, there remained a possibility that this HqsK/LuxU phosphotransfer was not exclusive and/or that LuxU is not a cognate phosphotransfer partner for HqsK. It has been demonstrated that *in vitro*, an HK will have a kinetic preference for its *in vivo* cognate response regulator, exhibiting a much faster rate of phosphotransfer with its cognate partner[228]. This preference is determined in an experiment called phosphotransfer profiling, in which either loss of phosphate from the HK or the appearance of a preferentially phosphorylated Hpt is detected using PAGE followed by autoradiography[228].

The dimerization and histidine phosphotransfer domain (DHp) and IKR domains from *Vp* HqsK were separately cloned and expressed to isolate the kinase and receiver domains[228]. We also purified all three stand-alone Hpt proteins from *V. parahaemolyticus*: LuxU (VP2098, gene

ID: 1189609), VP1472 (gene ID: 1188978), and VP2127 (gene ID: 1189639). Then each Hpt was separately added to a mixture of *Vp* HqsK DHp and IKR domains that had been preincubated with radiolabeled ATP. The resulting autoradiography showed no apparent band intensity loss from any of the kinase domains, nor band appearance for VP1472 or VP2098. However, a band corresponding to phosphorylated LuxU appears after 15 minutes and increases in intensity over time, indicating the accumulation of phosphate on LuxU (Figure 3-9). To verify this accumulation of phosphate on LuxU is not due to non-specific phosphorylation, but due to phosphotransfer through the HqsK DHp/IKR domains, we conducted a phosphotransfer specificity test (Figure 3-10). The results indicate that LuxU does not phosphorylate itself, nor can it directly receive phosphate from the HqsK DHp domain, but it can only be phosphorylated via a His-Asp-His phosphotransfer through the HqsK DHp and IKR domains. Overall, these results show LuxU is the cognate phosphotransfer Hpt protein for HqsK.

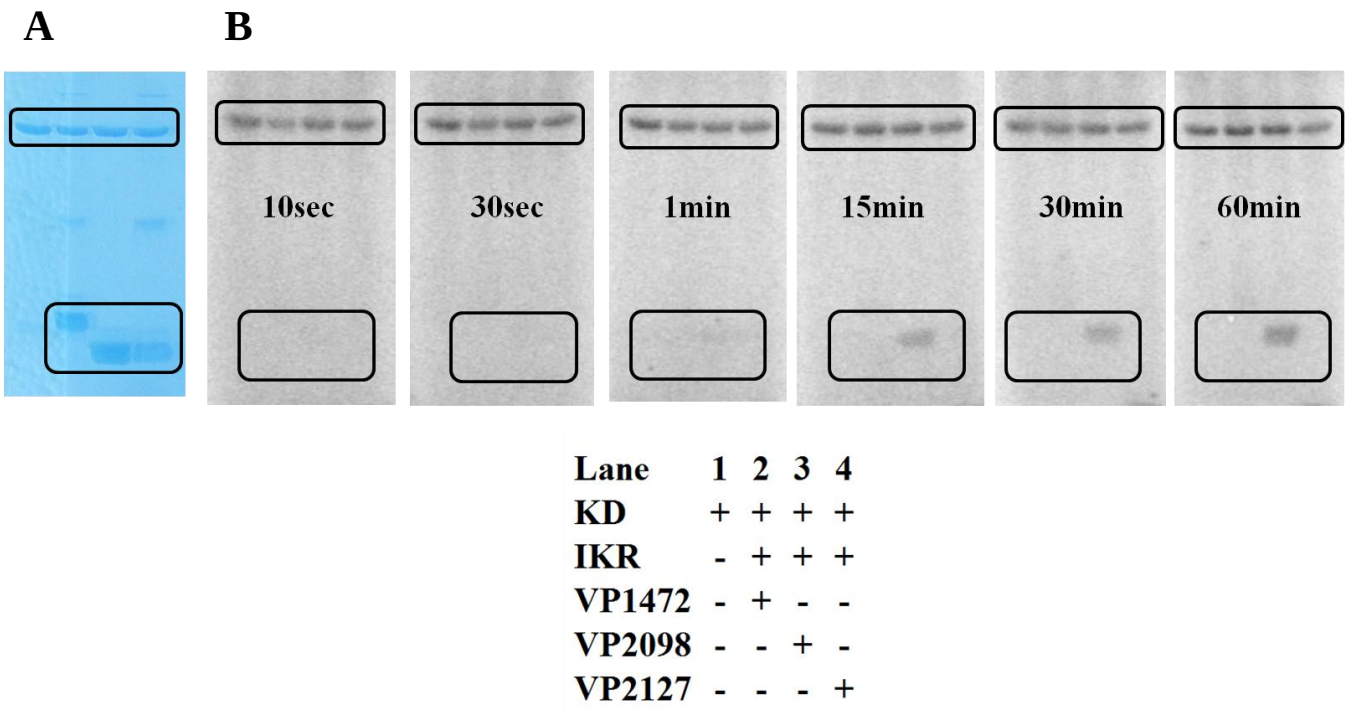

Figure 3-9. Phosphotransfer profiling of *Vp* HqsK and three stand-alone *Vp* Hpt proteins (VP1472, VP2098 and VP2127). Stained polyacrylamide gel (A) and autoradiography are shown (B). 1 µM each of KD and IKR were incubated with 10 µM each of Hpts. KD/IKR were loaded with phosphoryl group by preincubating with ATP for 90 min. Hpt proteins were then added to initiate the phosphotransfer. Phoshoryl group accumulation was observed only for VP2098 (LuxU) among three Hpts.

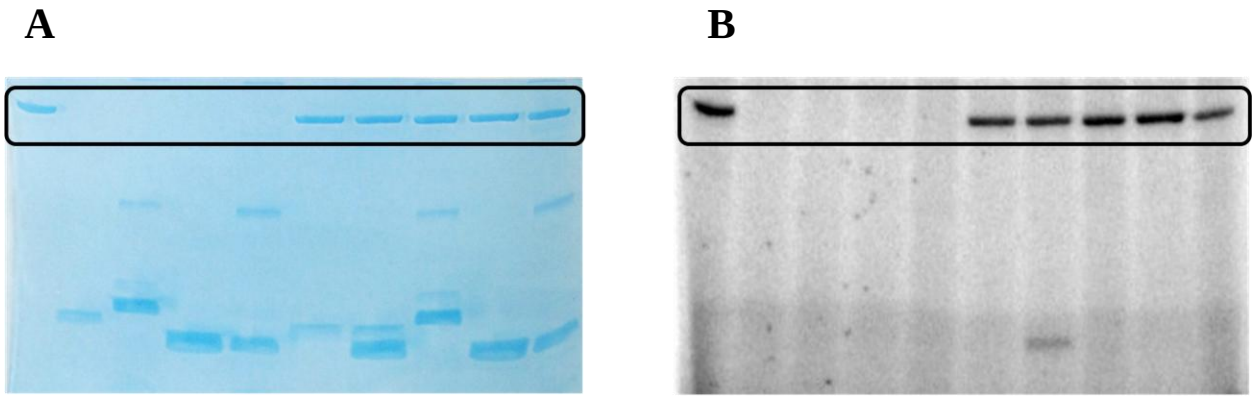

Lane	1	2	3	4	5	6	7	8	9	10
KD	+	-	-	-	-	+	+	+	+	+
IKR	-	+	-	-	-	+	+	-	-	-
VP1472	-	-	+	-	-	-	-	+	-	-
VP2098	-	-	-	+	-	-	+	-	+	-
VP2127	-	-	-	-	+	-	-	-	-	+

Figure 3-10. *V. parahaemolyticus* HK, Hpt phosphotransfer specificity test. Stained polyacryl amide gel (A) and autoradiography (B) are shown.

3.3.5 H-NOX suppresses *Vp* HqsK autophosphorylation upon NO binding

In the NO-responsive QS circuit in *V. harveyi*, the basal kinase activity of *Vh* HqsK was repressed by H-NOX upon NO binding[127]. To test whether *Vp* HqsK is regulated in a similar manner, various ligation states of *Vp* H-NOX were incubated with HqsK and the effects on autophosphorylation were observed. *Vp* HqsK and Fe^{II}-unligated, Fe^{II}-CO or Fe^{II}-NO *Vp* H-NOX were incubated in an anaerobic chamber, and then ATP with trace [γ-^{32}P]-ATP was added to initiate HqsK autophosphorylation. The resulting autoradiography showed significant kinase activity inhibition with all *Vp* H-NOX complexes, with the most inhibition (74%) by Fe^{II}-NO H-NOX (Figure 3-11, Figure 3-12). We also titrated HqsK with Fe^{II}-NO H-NOX and observed decreasing *Vp* HqsK autophosphorylation in an Fe^{II}-NO H-NOX concentration-dependent manner (Figure 3-13, Figure 3-14). Our data indicate that *Vp* H-NOX suppresses the kinase activity of the associated HqsK upon NO binding, similar to what has been observed in *V. harveyi*.

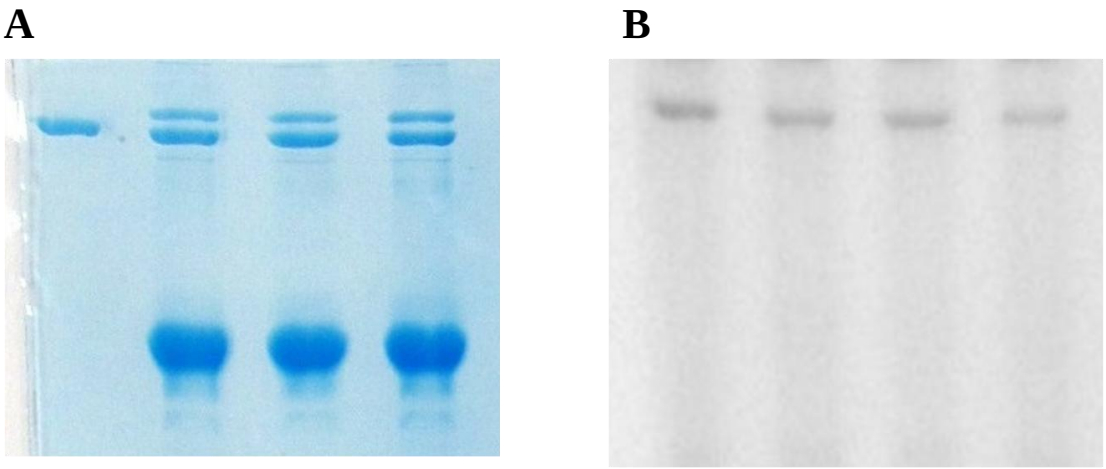

Lane	1	2	3	4
HqsK (D499A)	+	+	+	+
Fe^{II} H-NOX	-	+	-	-
Fe^{II} H-NOX·CO	-	-	+	-
Fe^{II} H-NOX·NO	-	-	-	+

Figure 3-11. ***Vp*** **H-NOX inhibits kinase activity of HqsK**. Stained polyacryl amide gel (A) and autoradiography (B) are shown. Unligated and CO bound H-NOX showed the same degree of kinase activity inhibition (30%). NO bound H-NOX most strongly inhibited (60%) HqsK activity.

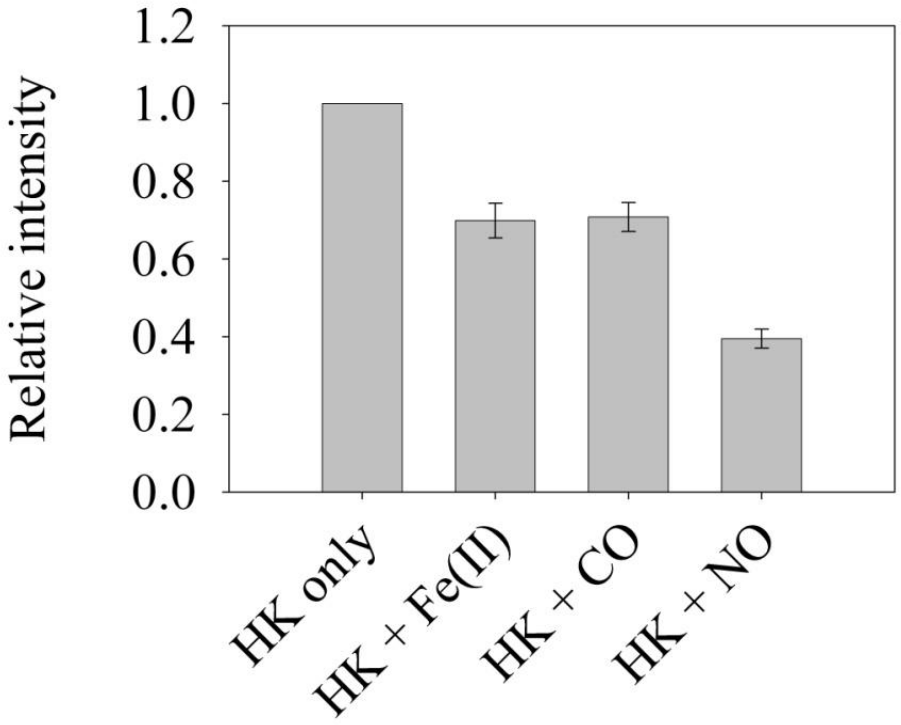

Figure 3-12. *Vp* H-NOX inhibits kinase activity of HqsK (Plot). Band intensity of Figure 3-11 was quantified with ImageJ then plotted. The plot shows the average of four independent assays ± SEM.

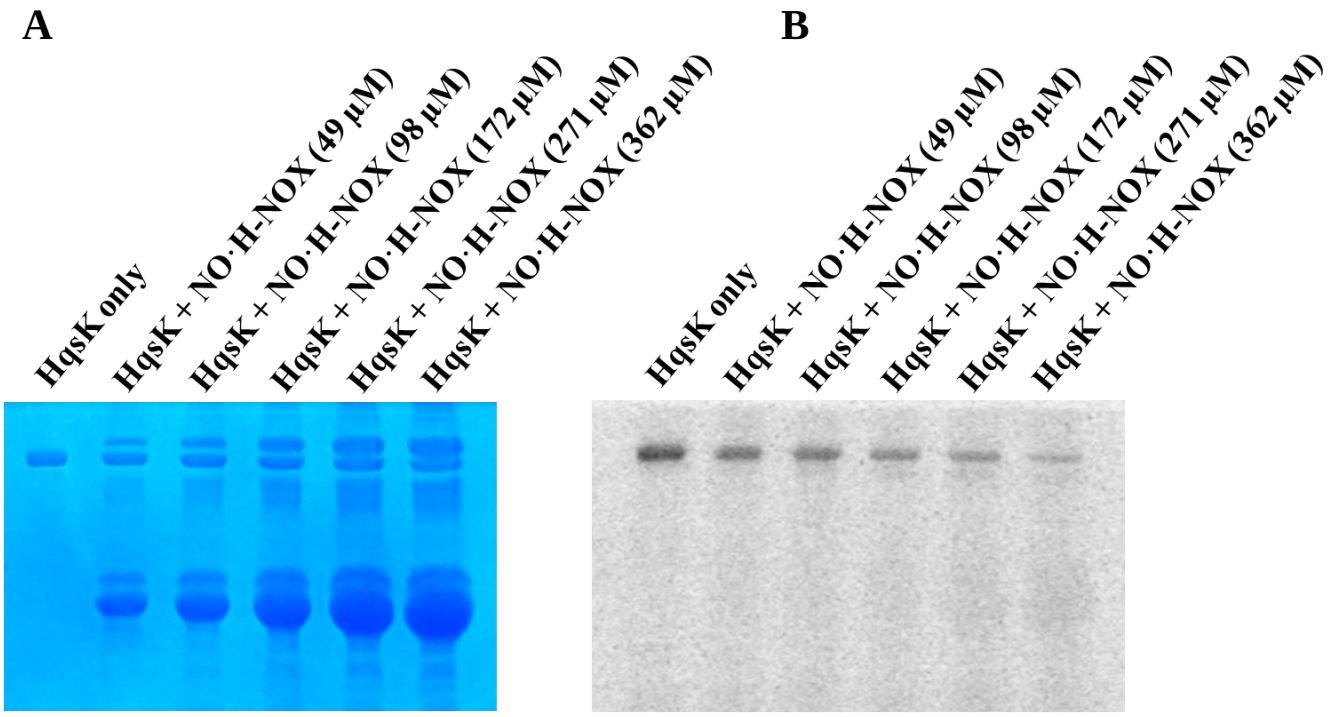

Figure 3-13. *Vp* HqsK autophosphorylation inhibition by various [NO·H-NOX]. NO bound H-NOX inhibits HqsK kinase activity in a dose-dependent manner. 2.67 µM *Vp* HqsK (D499A) was incubated with varying concentrations of NO·H-NOX for 30 min then another 30 min after the addition of ATP. Stained polyacryl amide gel (A) shows uniform protein loading. Autoradiography (B) shows dose dependent HqsK kinase activity inhibition by NO·H-NOX.

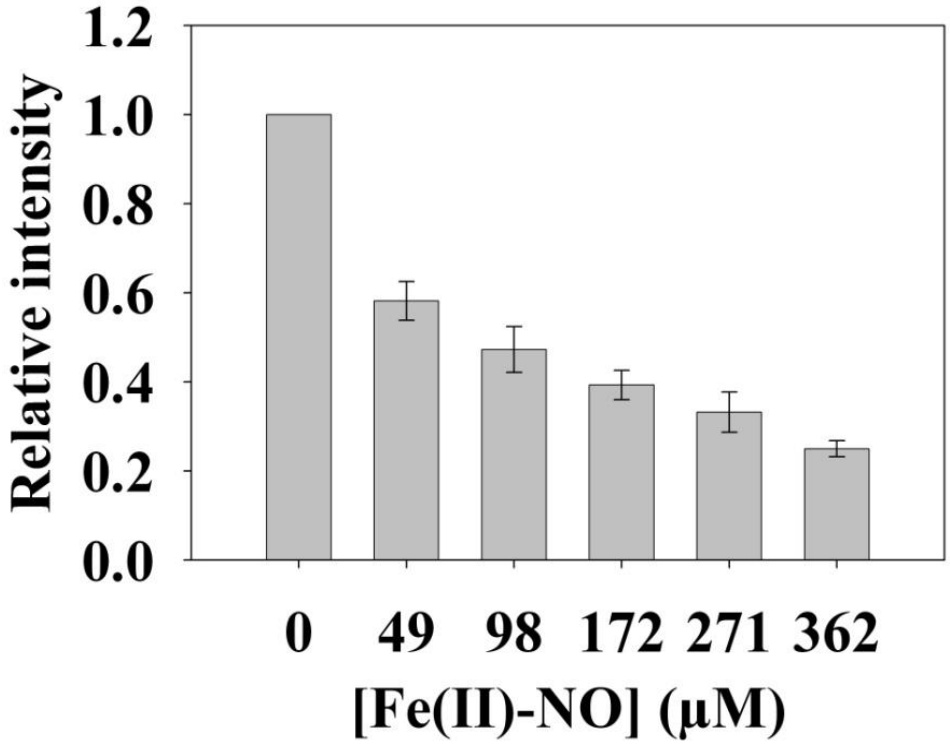

Figure 3-14. *Vp* HqsK autophosphorylation inhibition by various [NO·H-NOX] (Plot). Quantified band intensities of HqsK titration with Fe^{II}-NO H-NOX (Figure 3-13). Average of three independent assays ± SEM is plotted.

3.3.6 5 and 6-coordinate NO-bound H-NOX complexes both inhibit HqsK kinase activity

As described above, we have shown that *Vp* H-NOX binds NO in both a 5- and a 6-coordinate complex, and the equilibrium between the two complexes can be shifted with temperature. To test whether or not the 5- and 6-coordinate complexes differentially inhibit HqsK activity, we conducted HqsK autophosphorylation reactions with NO-bound H-NOX at 10 ºC and 40 °C (Figure 3-15). Based on our electronic absorption spectra experiments (Figure 3-2), NO-bound H-NOX is mostly 6-coordinate at 10 °C, whereas a significant percentage of the population is 5-coordinate at 40 °C. *Vp* HqsK and various concentrations of NO-bound H-NOX were incubated at the designated temperatures, then an autophosphorylation reaction was initiated by the addition of ATP with trace [γ-^{32}P]-ATP. Quantification of the resulting autoradiography bands indicates comparable degrees of autophosphorylation in the presence of 5- and 6-coordinate *Vp* H-NOX (Figure 3-15, Figure 3-16). These data are consistent with the conclusion that the 5- and 6-coordinate NO-bond H-NOX complexes have virtually the same degree of HqsK inhibition.

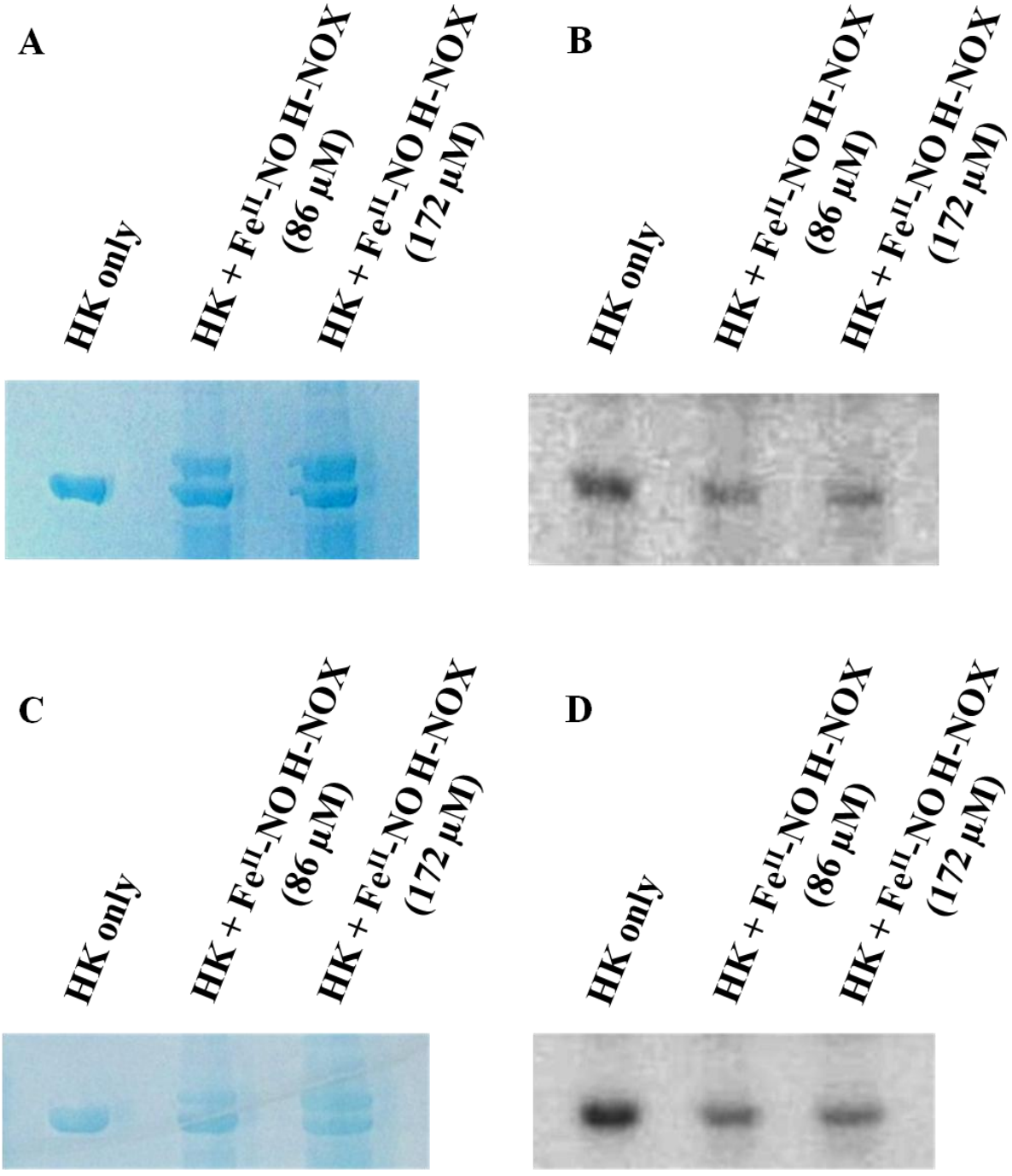

Figure 3-15. *Vp* HqsK autophosphorylation activity inhibition by 5-, 6-coordinate NO·H-NOX. *Vp* HqsK was incubated with various concentrations of 6-coordinate NO·H-NOX (10 °C) or 5-coordinate NO·H-NOX (40 °C). Figures A and B show polyacrylamide gel and autoradiography of HqsK incubated with 6-coordinate NO·H-NOX. Figures C and D show that with 5-coordinate NO·H-NOX.

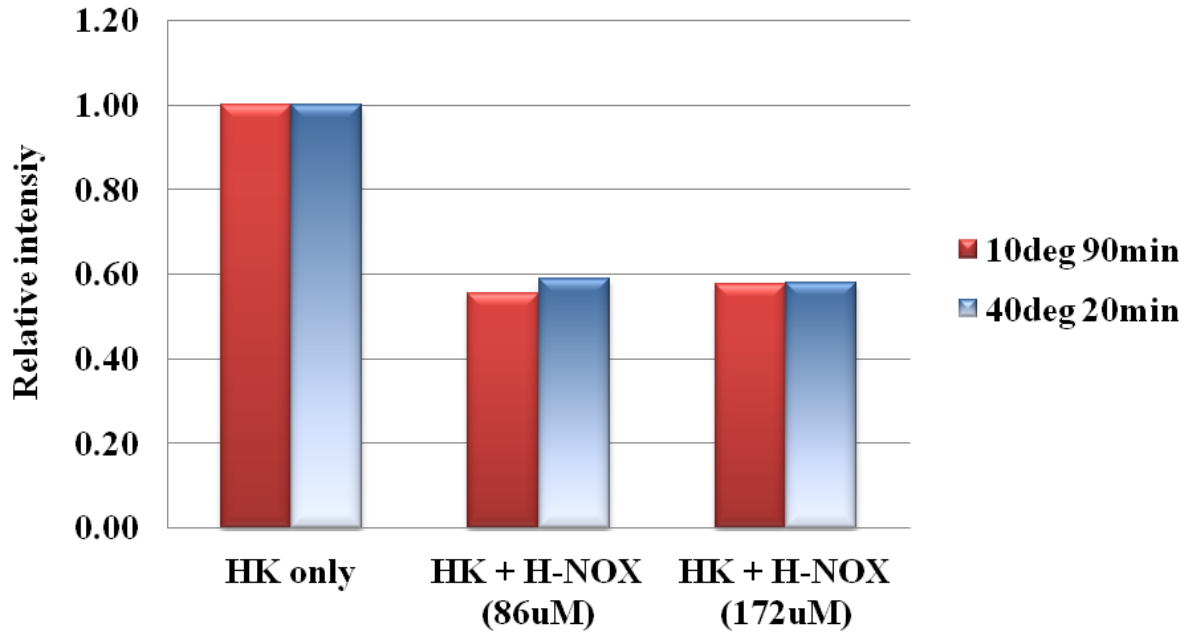

Figure 3-16. *Vp* HqsK autophosphorylation activity inhibition by 5-, 6-coordinate NO·H-NOX (Plot). Quantified band intensity of *Vp* HqsK autophosphorylation activity inhibition by 5-, 6-coordinate H-NOX (Figure 3-15). Band intensity was quantified by imageJ. 5- and 6-coordinate NO·H-NOX inhibit HqsK kinase activity equally.

3.3.7 The effect of NO on the master quorum regulatory proteins OpaR and AphA

In the *V. parahaemolyticus* QS circuit, LuxU and LuxO ultimately regulate transcription of two master quorum regulatory proteins, OpaR and AphA[234]. In *V. harveyi* and *V. cholerae*, these two master quorum regulatory proteins have been shown to regulate each other's expressions reciprocally. At low cell density, AphA is expressed and it directly suppresses expression of OpaR. At high cell density, OpaR is expressed, and in turn, represses expression of AphA[234,235]. Here we analyze the effect of various concentrations of NO (delivered with the NO donor DETA NONOate) on the expression of these two master quorum regulatory proteins at low (OD600 = 0.2) cell density using qRT-PCR.

First, the growth rate of *V. parahaemolyticus* in the presence of various concentrations of DETA NONOate was monitored to determine the NO toxic threshold (Figure 3-17). The growth curve for cultures with 0, 50, 100, and 200 DETA NONOate (equivalent to 0, 190, 380, 760 nM NO[236]) showed an almost identical growth rate, but almost no cell growth was seen with 500 µM DETA NONOate (1900 nM NO). Accordingly, *V. parahaemolyticus* cultures grown with 0-200 µM DETA NONOate were used to monitor AphA and OpaR expression. The gene expression levels of OpaR and AphA were quantified using *secY* (VP0277, gene ID: 1187744) as a reference gene. We observed a trend of increasing expression of OpaR as a function of NO (1.22-, 1.71- and 2.04-fold change with 50, 100 and 200 µM DETA NONOate, respectively). The fold-change of 2.04 with 200 µM NONOate was significantly different ($p < 0.05$) with respect to no NONOate, but the other two were not ($p > 0.05$). Expression of AphA remained almost constant with increasing NO, although at 200 µM NONOate, there was an increase of 1.56 ($p < 0.05$) with respect to no NONOate. An NO-dependent increase in both AphA and OpaR expression is unexpected since OpaR suppresses AphA expression. The mechanism of this increased AphA expression at higher NO concentration is unknown. It is possible that although 200 µM NONOate did not hinder the bacterial growth, it is causing stress to bacteria, and increased AphA expression is a part of the stress response. Also, it is possible that NO may be activating an unidentified signaling cascade that is turned on only at higher NO concentrations.

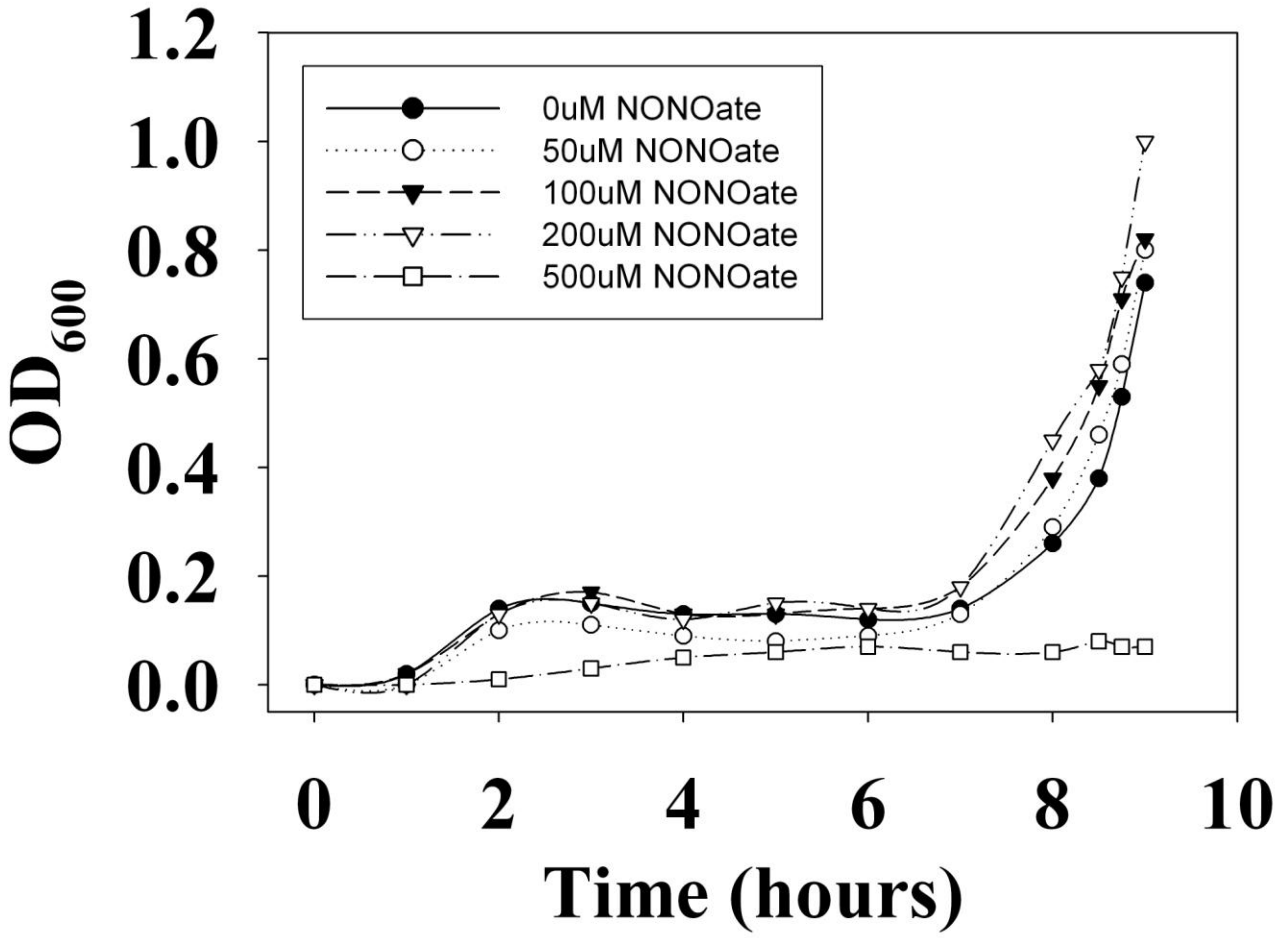

Figure 3-17. Growth curve of *V. parahaemolyticus*. *V. parahaemolyticus* was grown with 0, 50, 100, 200, and 500 µM DETA NONOate (equivalent to 0, 190, 380, 760 and 1900 nM NO, respectively). Almost no growth was observed with 500 µM NONOate. For the detailed growth condition, see the materials and methods section.

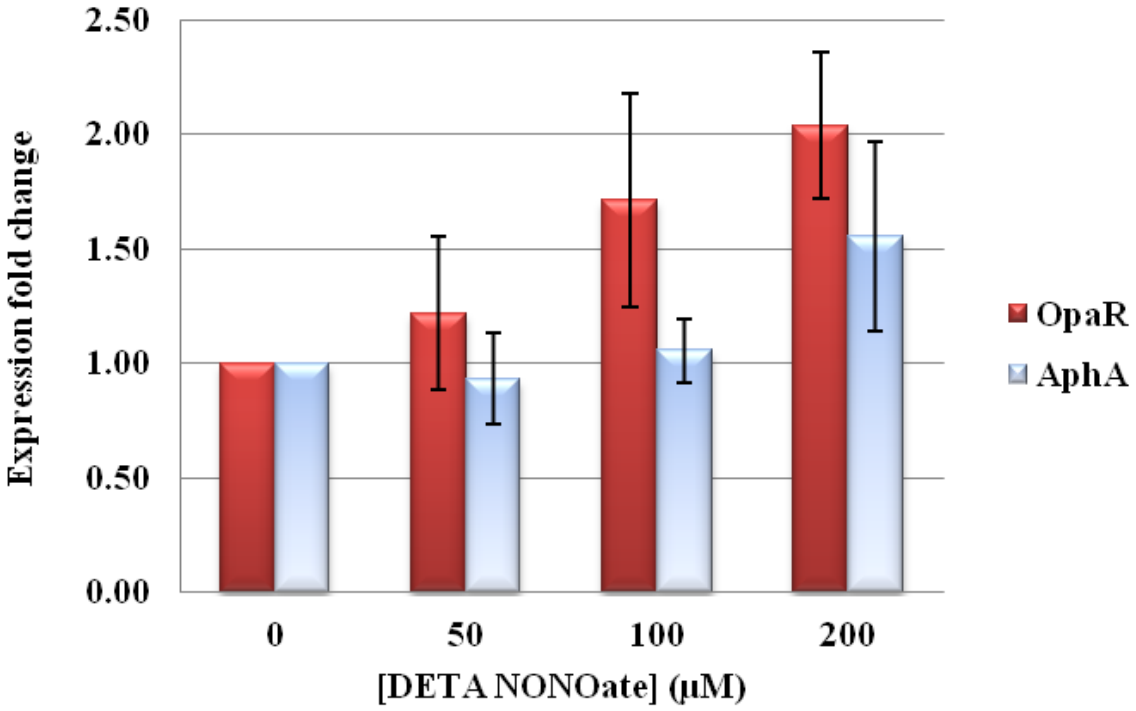

Figure 3-18. *Vp* master quorum regulatory protein expression analysis by qPCR. Expression of two *Vp* master quorum regulatory proteins, AphA and OpaR in the presence of various concentrations of DETA NONOate was analyzed. 0, 50, 100 and 200 µM NONOate is equivalent to 0, 190, 380 and 760 nM NO respectively. Error bars represent SEM from four independent assays.

Table 3-2. Bacterial strains, plasmids and primers used in this work

Strains, plasmids and primers	Genotype	Reference
Bacterial strains		
V. parahaemolyticus		
WT	*Vibrio parahaemolyticus*, EB101, ATCC 17802	ATCC
E. coli		
DH5α	Cloning competent cell	Invitrogen
BL21(DE3)pLysS	Expression competent cell	Invitrogen
Plasmids		
pVp_H-NOX	pET-20b(+) with VP1877, C-terminus 6x His-tag, Ampr	This work
pVp_HqsK(WT)	pET-23aHis-Tev with VP1876, N-terminus 6x His-tag, Amp^r	This work
pVp_HqsK(H214A)	pET-23aHis-Tev with VP1876 (H214A), N-terminus 6x His-tag, Amp^r	This work
pVp_HqsK(D499A)	pET-23aHis-Tev with VP1876 (D499A), N-terminus 6x His-tag, Amp^r	This work
pVp_HqsK(KD)	pET-23aHis-TEV with VP1876(KD), N-terminus 6x His-tag, Amp^r	This work
pVp_HqsK(IKR)	pET-23aHis-TEV with VP1876(IKR), N-terminus 6x His-tag, Amp^r	This work
pVp_LuxU	pET-20b(+) with VP2098, C-terminus 6x His-tag, Ampr	This work
pVp_VP1472	pET-20b(+) with VP1472, C-terminus 6x His-tag, Ampr	This work
pVp_VP2127	pET-20b(+) with VP2127, C-terminus 6x His-tag, Ampr	This work
Primers		
pVp_H-NOX-Fwd	GGG GGG GGG CAT ATG ATG AAA GGG ATA ATC	
pVp_H-NOX-Rvs	GGA ACC TCA GTT ATT GTG CCT CCA GC	
pVp_HqsK(WT)-Fwd	GGA TCC ATA TGA TGA CGG GTA ACT CC	
pVp_HqsK(WT)-Rvs	GCA TTC TCG AGC TAC TGC TCA AGC	
pVp_HqsK(KD)-Fwd	CAA CAA CAT ATG ATG ACG GGT AAC TCC TCA TTA GAA AGG AAA CTC	
pVp_HqsK(KD)-Rvs	GTT GTT CTC GAG AGC TTG CCC CTC TTT TAA AGG GAT GGA AAC	
pVp_HqsK(IKR)-Fwd	CAA CAA CAT ATG CGC TCG ATA TTG GTG GTG GAT GAT ATA CG	
pVp_HqsK(IKR)-Rvs	GTT GTT CTC GAG CTG CTC AAG CCA CTT ACA CAT GAT CTG CTC	
pVp_LuxU-Fwd	CAA CAA CAT ATG ATG ACG ATA TTG AAT CAA CAA AAA ATA GAT GAA C	
pVp_LuxU-Rvs	GTT GTT CTC GAG TTG AGT CCA AGA GCG ATA CGC GTC GCG TGT TTC	
pVp_VP1472-Fwd	CCG CTT CAT ATG TTG GTT GAT GAG CTC ATT CTC CAG CAA ATG	
pVp_VP1472-Rvs	TTG TTG CGG CCG CCT CAA AAC CTT GAG CCT TGC GCA GGT TGA GCG	
pVp_VP2127-Fwd	CAA CAA CAT ATG ATG CTG GAT TCG CTT TCT GGC GAT GAA GGC GC	
pVp_VP2127-Rvs	GTT GTT GCG GCC GCA TCT GTT AGC ACT TCT CGT ATC TTT TCA C	

Abbreviation: Amp^r: Ampicillin resistance

3.4 Perspectives

Quorum sensing is a key signaling system used by bacteria to orchestrate population-wide gene expression patterns appropriate for different stages of growth or environmental conditions. Bacteria employ various types of QS circuits, AIs and AI receptors that are most suitable for their particular lifestyle or the environment in which they live. Not only do bacteria monitor other AI concentrations of their own and other bacterial species, many actively interfere with QS circuits of competing species through a process called quorum quenching. Some pathogenic or symbiotic bacteria also integrate host-organism-originated signals into QS to manage effective colonization and pathogenicity. Similarly, eukaryotes monitor bacterial AIs to detect their presence and activate an immune response. Autoinducer-mediated quorum sensing is a dynamic communication system that spans across different bacterial species and even across kingdoms.

In this work, we showed NO/H-NOX is the fourth signaling cascade of *Vp* QS and plays a critical role in regulating its communal behavior. *V. parahaemolyticus* detects NO with H-NOX. NO ligated H-NOX switches activity of HqsK from kinase to phosphatase and removes phosphate from the response regulator LuxO. Dephosphorylation of LuxO leads to expression of OpaR and suppression of AphA and thus changes in hundreds of gene expressions appropriate for the cell density. We characterized each component of this NO responsive QS circuit to demonstrate that *V. parahaemolyticus* integrates NO into its QS signaling. We also showed, using qPCR that at low cell density, submicromolar NO promotes expression of OpaR in a dose dependent manner. In *V. harveyi* and *V. cholerae,* LuxR (OpaR homolog) and AphA are expressed reciprocally at high and low cell densities respectively. Thus, if this relationship between two master quorum regulatory proteins is conserved in *V. parahaemolyticus*, we expect increasing OpaR expression and decreasing AphA expression with increasing NO concentration. Our qPCR analysis confirmed that *Vp* OpaR expression is promoted with increasing concentration of NO in the submicromolar range. However, the AphA expression also increased at a high NO concentration (200 μM). This discrepancy may be due to NO's toxicity at higher submicromolar levels or an unidentified NO signaling cascade. We are currently investigating the mechanism behind the increased AphA expression by NO and the alternative NO signaling cascade in *V. parahaemolyticus*.

Chapter 4: Summary and future directions

In this thesis, we presented two research projects: development of a filter-binding assay for histidine kinase phosphorylation and identification and characterization of NO responsive QS circuits in *V. parahaemolyticus*. The first project was intended to provide a solution to the lack of effective assay methods for HK activity quantification, especially since TCS is an important signaling cascade in bacteria. However, the commonly used method was labor intensive, time consuming and could process only a small number of samples at a time. As a result, there are only a few HKs for which kinetic parameters are known. The proposed acid based filter-binding assay was developed through carefully adjusting experimental conditions. We demonstrated that the acid-labile pHis exhibits almost no degradation under the described experimental conditions. Subsequent experiments that monitored HKs' time, enzyme concentration and substrate concentration dependency showed expected enzymatic activities. The kinetic parameters we determined were mostly in accordance with previously characterized HKs. We hope this study provides an alternative method to effectively quantify HK phosphorylation activity and promote the study of HK. A possible future direction for this project is quantifying other types of HKs using the developed method. Characterized HKs with the proposed assay were all H-NOX (or putative NO sensing protein) associated HKs. Although this assay is expected to work on any given HKs due to their highly conserved domain organizations, it may be beneficial to employ the method to quantify other non-H-NOX associated HKs to verify the method is effective for all types of HKs.

The second project, the identification and characterization of NO responsive QS circuits in *V. parahaemolyticus* was a follow-up of a previous study, the discovery of NO responsive QS circuits in *V. harveyi*. In the previous study, we established that in a marine bioluminescent bacterium, *V. harveyi*, there exists a fourth QS circuit that is regulated by NO. NO binds H-NOX then H-NOX inhibits kinase activity of its partner protein HqsK. Since HqsK transfers a phosphate to QS phosphotransfer protein LuxU, we concluded that NO/H-NOX regulates QS through modulation of phosphotransfer. There are only a few cases reported of non-AI signals being integrated into QS. In addition, the NO responsive QS circuit was the first discovery that NO signaling was integrated into QS. The goal of this second project was to further investigate NO responsive QS circuits. Specifically, we wanted to answer the following questions: do NO responsive QS circuits exist in bacteria other than *V. harveyi*? Is phosphotransfer from HqsK to LuxU a cognate phosphotransfer or mere crosstalk? What is the effect of NO on the master quorum regulatory protein expression? To address these questions, we conducted a study on a marine pathogenic bacterium, *V. parahaemolyticus*. *V. parahaemolyticus* has the same QS component as *V. harveyi*, along with an H-NOX/HK pair in an operon. We characterized each component in the putative NO responsive QS circuit. Based on spectroscopic properties and the

NO dissociation rate, we concluded that VP1877, a protein annotated as H-NOX, is a selective NO sensor. VP1866, the HK encoded in the same operon with H-NOX, is an active hybrid kinase that has both kinase and phosphatase activities with its phosphorylation sites H214 and D499. VP1866 HK transfers phosphate to QS Hpt protein LuxU through a successive phosphotransfer. Phosphotransfer from VP1866 HK to LuxU is not a non-specific phosphotransfer, but takes place only through the conserved residues H214, D499 and then to H56 on LuxU. VP1866 HK's kinase activity is repressed by NO bound H-NOX in a dose dependent manner. Out of three stand-alone Hpt proteins, VP1866 HK transfers phosphate only to LuxU, thus the phosphotransfer from Vp1866 HK to LuxU is not a crosstalk, but a cognate phosphotransfer. Lastly, by using qPCR, we demonstrated that NO promotes the expression of master quorum regulatory protein LuxR at low cell density. In conclusion, NO responsive QS circuits exist not only in *V. harveyi*, but also in *V. parahaemolyticus*. We elucidated the signaling cascade of a *Vp* NO responsive QS circuit as follows: NO binds H-NOX and NO·H-NOX inhibits the kinase activity of HqsK. HqsK's function switches from kinase to phosphatase, resulting in dephosphorylation of the response regulator LuxO. The dephosphorylated, inactive LuxO leads to the expression of master quorum regulatory protein OpaR. Expressed OpaR controls hundreds of gene expressions. Although we characterized many aspects of NO responsive QS circuits in *V. parahaemolyticus*, there are more to be further investigated. For example, we analyzed the change in HqsK's kinase activity using various forms and concentrations of H-NOX. However, the effect of H-NOX on HqsK's other function, phosphatase activity, was not analyzed. Also, based on the spectroscopic properties and NO dissociation rate, we concluded that *Vp* H-NOX is an NO sensor. However, for more detailed characterization, H-NOX's NO association rate and K_D should also be determined. In addition, it will be beneficial to see the importance of NO signals relative to other AIs to modulate overall QS cascade. Finally, and most importantly, are there any other non-AI signals that modulate QS?

Through this work we revealed yet another complex layer of bacterial signaling. Quorum sensing was first thought to be controlled only by bacteria originated AIs, but as seen in *A. tumefaciens*'s inter-kingdom QS and *V. harveyi*, *V. parahaemolyticus*' NO responsive QS circuit, non-AI signals are also integrated into bacterial QS. What is apparent from these observations is that the integration of non-AI signals into QS is not an unusual phenomenon but exists in a number of different bacterial species. The detection of environmental stimuli including AIs and signal processing are done by TCS. As of today, only a few HK ligands are known and many remain unknown. In addition, TCS signaling is far more complex than its name "two-component" signaling. A single HK can interact with multiple RRs. Conversely, multiple HKs can interact with a single RR. Empirical identification of a cognate HK/RR pair is not a trivial task. Furthermore, recently discovered auxiliary proteins add further complexity to the system. TCS is not merely "two-component" signaling. Rather, it is a tangled web of multi-component signaling. This complex, multi-component TCS is interwoven with second-messenger signaling, quorum sensing to comprise overall bacterial signaling. Our discovery of NO is one of the first identified non-AI signals integrated into bacterial QS circuits. I hypothesize future studies will

identify more non-AI signals integrated into QS. For the answer to my hypothesis, we will have to wait for further advancement of the study of TCS: identification of sensory HK ligands, elucidation of signaling connection between HK, RR, auxiliary proteins and other signaling cascades. We hope our work presented here would aid the future study of TCS and bacterial QS.

References

1. Stock, A. M.; Robinson, V. L.; Goudreau, P. N., Two-component signal transduction. *Annual Review of Biochemistry* **2000,** *69*, 183-215.
2. Krell, T.; Lacal, J.; Busch, A.; Silva-Jimenez, H.; Guazzaroni, M.-E.; Ramos, J. L., Bacterial sensor kinases: diversity in the recognition of environmental signals. *Annual Review of Microbiology* **2010,** (64), 539-559.
3. Jung, K.; Fried, L.; Behr, S.; Heermann, R., Histidine kinases and response regulators in networks. *Current Opinion in Microbiology* **2011,** *15* (2), 118-124.
4. Stewart, R. C., Protein histidine kinases: assembly of active sites and their regulation in signaling pathways. *Current Opinion in Microbiology* **2010,** *13* (2), 133-141.
5. Parkinson, J. S.; Kofoid, E. C., Communication Modules in Bacterial Signaling Proteins. *Annual Review of Genetics* **1992,** *26*, 71-112.
6. Mizuno, T., His-Asp phosphotransfer signal transduction. *The Journal of Biological Chemistry* **1998,** *123* (4), 555-563.
7. Koretke, K. K.; Lupas, A. N.; Warren, P. V.; Rosenberg, M.; Brown, J. R., Evolution of two-component signal transduction *Molecular Biology and Evolution* **2000,** *17* (12), 1956-1970.
8. Cock, P. J. A.; Whitworth, D. E., Evolution of Prokaryotic Two-Component System Signaling Pathways: Gene Fusions and Fissions. *Molecular Biology and Evolution* **2007,** *24* (11), 2355-2357.
9. Heermann, R.; Jung, K., *Stimulus perception and signaling in histidine kinases*. Wiley-VCH: 2009.
10. Swanson, R. V.; Alex, L. A.; Simon, M. I., Histidine and aspartate phosphorylation: two-component systems and the limits of homology. *Trends in Biochemical Sciences* **1994,** *19* (11), 485-490.
11. Hess, J. F.; Bourret, R. B.; Simon, M. I., Histidine phosphorylation and phosphoryl group transfer in bacterial chemotaxis. *Nature* **1988,** *336*.
12. Ninfa, A. J.; Bennett, R. L., Identification of the site of autophosphorylation of the bacterial protein kinase/phosphatase NRII. *The Journal of Biological Chemistry* **1991,** *266* (11), 6888-6893.
13. Bader, M. W.; Sanowar, S.; Daley, M. E.; Schneider, A. R.; Cho, U.; Xu, W.; Klevit, R. E.; Moual, H. L.; Miller, S. I., Recognition of Antimicrobial Peptides by a Bacterial Sensor Kinase. *Cell* **2005,** *122* (3), 461-472.
14. Cheung, J.; Hendrickson, W. A., Crystal structures of C4-dicarboxylate ligand complexes with sensor domains of histidine kinases DcuS and DctB. *The Journal of Biological Chemistry* **2008,** *283* (44), 30256-30265.
15. Cheung, J.; Hendrickson, W. A., Structural analysis of ligand stimulation of the histidine kinase NarX. *Structure* **2009,** *17* (2), 190-201.
16. Kerff, F.; Charlier, P.; Colombo, M.-L.; Sauvage, E.; Brans, A.; Fre`re, J.-M.; Joris, B.; Fonze, E., Crystal structure of the sensor domain of the BlaR penicillin receptor from Bacillus licheniformis. *Biochemistry* **2003,** *42* (44), 12835-12843.
17. Purcell, E. B.; Siegal-Gaskins, D.; Rawling, D. C.; Fiebig, A.; Crosson, S., A photosensory two-component system regulates bacterial cell attachment. *Proceedings of the National Academy of Sciences of the United States of America* **2007,** *104* (46), 18241-18246.
18. Aguilar, P. S.; Hernandez-Arriaga, A. M.; Cybulski, L. E.; Erazo, A. C.; Mendoza, D. d., Molecular basis of thermosensing: a two-component signal transduction thermometer in Bacillus subtilis. *The EMBO Journal* **2001,** *20* (7), 1681-1691.
19. Mikami, K.; Kanesaki, Y.; Suzuki, I.; Murata, N., The histidine kinase Hik33 perceives osmotic stress and cold stress in Synechocystis sp. PCC 6803. *Molecular Microbiology* **2002,** *46* (4), 905-915.
20. Neiditch, M. B.; Federle, M. J.; Pompeani, A. J.; Kelly, R. C.; Swem, D. L.; Jeffrey, P. D.; Bassler, B. L.; Hughson, F. M., Ligand-induced asymmetry in histidine sensor kinase complex regulates quorum sensing. *Cell* **2006,** *126* (6), 1095-1108.

21. Neiditch, M. B.; Federle, M. J.; Miller, S. T.; Bassler, B. L.; Hughson, F. M., Regulation of LuxPQ receptor activity by the quorun1-sensing signal autoinducer-2. . *Molecular Cell* **2005,** *18* (5), 507-518.
22. Ninfa, A. J.; Magasanik, B., Covalent modification of the ginG product, NRI, by the glnL product, NRII, regulates the transcription of the glnALG operon in Escherichia coli. *Proceedings of the National Academy of Sciences of the United States of America* **1986,** *83* (16), 5909-5959.
23. Zhulin, I. B., The superfamily of chemotaxis transducers: from physiology to genomics and back. *Advances in Microbial Physiology* **2001,** *45*, 157-198.
24. Robinson, V. L.; Buckler, D. R.; Stock, A. M., A tale of two components: a novel kinase and a regulatory switch. *Nature Structural Biology* **2000,** *7* (8), 626-633.
25. Attwood, P. V., Histidine kinases from bacteria to humans *Biochemical Society Transactions* **2013,** *41* (4), 1023-1028.
26. Casino, P.; Rubio, V.; Marina, A., Structural insight into partner specificity and phosphoryl transfer in two component signal transduction. *Cell* **2009,** *139* (2), 325-336.
27. Aiba, H.; Mizuno, T.; Mizushima, S., Transfer of phosphoryl group between two regulatory proteins involved in osmoregulatory expression of the ornpF and ornpC genes in *Escherichia coli*. *The Journal of Biological Chemistry* **1989,** *264* (15), 8563-8567.
28. Makino, K.; Shinagawa, H.; Amemura, M.; Kawamoto, T.; Yamada, M.; Nakata, A., Signal transduction in the phosphate regulon of *Escherichia coli* involves phosphotransfer between PhoR and PhoB proteins. *The Journal of Biological Chemistry* **1989,** *210* (3), 551-559.
29. Tanaka, T.; Kawata, M.; Mukai, K., Altered phosphorylation o f Bacillus subtilis DegU caused by single amino acid changes in DegS. *Journal of Bacteriology* **1991,** *173* (17), 5507-5515.
30. Mizuno, T., Compilation of All Genes Encoding Two-component Phosphotransfer Signal Transducers in the Genome of Escherichia coli *DNA Research* **1997,** *4* (2), 161-168.
31. Clarke, D. J., The Rcs phosphorelay: more than just a two-component pathway. *Future Microbiology* **2010,** *5* (8), 1173-1184.
32. Galperin, M. Y., Structural Classification of Bacterial Response Regulators: Diversity of Output Domains and Domain Combinations. *Journal of Bacteriology* **2006,** *188* (12), 4169-4182.
33. Paul, R.; Weiser, S.; Amiot, N. C.; Chan, C.; Schirmer, T.; Giese, B.; Jenal, U., Cell cycle-dependent dynamic localization of a bacterial response regulator with a novel di-guanylate cyclase output domain. *Genes & Development* **2004,** *18* (6), 715-727.
34. Chang, A. L.; Tuckerman, J. R.; Gonzalez, G.; Mayer, R.; Weinhouse, H.; Volman, G.; Amikam, D.; Benziman, M.; Gilles-Gonzalez, M.-A., Phosphodiesterase A1, a regulator of cellulose synthesis in Acetobacter xylinum, is a heme-based sensor. *Biochemistry* **2001,** *40* (12), 3420-3426.
35. Galperin, M. Y., Bacterial signal transduction network in a genomic perspective. *Environmental Microbiology* **2004,** *6* (6), 552-567.
36. Ross, P.; Mayer, R.; Weinhouse, H.; Amikam, D.; Huggirat, Y.; Benziman, M., The cyclic diguanylic acid regulatory system of cellulose synthesis in Acetobacter xylinum. Chemical synthesis and biological activity of cyclic nucleotide dimer, trimer, and phosphothioate derivatives. *The Journal of Biological Chemistry* **1990,** *265* (31), 18933-18943.
37. Krasteva, P. V.; Fong, J. C. N.; Shikuma, N. J.; Beyhan, S.; Navarro, M. V. A. S.; Yildiz, F. H.; Sondermanna, H., *Vibrio cholerae* VpsT regulates matrix production and motility by directly sensing cyclic di-GMP. *Science* **2010,** *327* (5967), 866-868.
38. Beyhan, S.; Tischler, A. D.; Camilli, A.; Yildiz, F. H., Transcriptome and phenotypic responses of Vibrio cholerae to increased cyclic di-GMP level. *Journal of Bacteriology* **2006,** *188* (10), 3600-3613.
39. Tischler, A. D.; Camilli, A., Cyclic diguanylate (c-di-GMP) regulates *Vibrio cholerae* biofilm formation. *Molecular Microbiology* **2004,** *53* (3), 857-869.
40. Hoch, J. A., Two-component and phosphorelay signal transduction. *Curr Opin Microbiol* **2000,** (3), 165-170.
41. Gao, R.; Mack, T. R.; Stock, A. M., Bacterial Response Regulators: Versatile Regulatory Strategies from Common Domains. *Trends in Biochemical Sciences* **2007,** *32* (5), 225-234.

42. Zapf, J.; Madhusudan; Grimshaw, C. E.; Hoch, J. A.; Varughese, K. I.; Whitele, J. M., A Source of Response Regulator Autophosphatase Activity: The Critical Role of a Residue Adjacent to the Spo0F Autophosphorylation Active Site. *Biochemistry* **1998,** *37* (21), 7725-7732.
43. Hess, J. F.; Oosawa, K.; Kaplan, N.; Simon, M. I., Phosphorylation of three proteins in the signaling pathway of bacterial chemotaxis. *Cell* **1988,** *53* (1), 79-87.
44. Jung, K.; Fried, L.; Behr, S.; Heermann, R., Histidine kinases and response regulators in networks. *Current Opinion in Microbiology* **2012,** *15* (2), 118-124.
45. Buelow, D. R.; Raivio, T. L., Three (and more) component regulatory systems – auxiliary regulators of bacterial histidine kinases. *Molecular Microbiology* **2010,** *75* (3), 547-566.
46. Wang, L.; Grau, R.; Perego, M.; Hoch, J. A., A novel histidine kinase inhibitor regulating development in Bacillus subtilis. *Genes & Development* **1997,** *11* (19), 2569-2579.
47. Peregoa, M.; Brannigan, J. A., Pentapeptide regulation of aspartyl-phosphate phosphatases. *Peptides* **2001,** *22*, 1541–1547.
48. Tomoaki Ogino, M. M., Naoki Kato, Yoshihiro Nakamura, Takeshi Mizuno, An Escherichia coli protein that exhibits phosphohistidine phosphatase activity towards the HPt domain of the ArcB sensor involved in the multistep His-Asp phosphorelay. *Molecular Microbiology* **1998,** *27* (3), 573-585.
49. Kofoid, J. S. P. a. E. C., Communication modules in bacterial signaling proteins. *Annual Review of Genetics* **1992,** *26*, 71-112.
50. Cock, P. J. A.; Whitworth , D. E., Evolution of Prokaryotic Two-Component System Signaling Pathways: Gene Fusions and Fissions. *Molecular Biology and Evolution* **2007,** *24* (11), 2355-2357.
51. Surette, M. G.; Levit, M.; Liu, Y.; Lukat, G.; Ninfai, E. G.; Ninfai, A.; Stock, J. B., Dimerization Is Required for the Activity of the Protein Histidine Kinase CheA That Mediates Signal Transduction in Bacterial Chemotaxis. *The Journal of Biological Chemistry* **1996,** *271* (2), 939-945.
52. Dutta, R.; Qin, L.; Inouye, M., Histidine kinases: diversity of domain organization. *Molecular Microbiology* **1999,** *34* (4), 633-640.
53. Stock, J. B.; Surrette, M. G.; Levitt, M.; Park, P., *Two-component signal transduction systems: structure-function relationships and mechanisms of catalysis*. ASM Press: Washington, D.C., 1995; p 25-51.
54. Sanders, D. A.; Gillece-Castro, B. L.; Burlingame, A. L.; Koshland, D. E., Phosphorylation Site of NtrC, a Protein Phosphatase Whose Covalent Intermediate Activates Transcription. *Journal of Bacteriology* **1992,** *174* (15), 5117-5122.
55. Sanders, D. A.; Gillece-Castro, B. L.; Stock, A. M.; Burlingameg, A. L.; Koshland, D. E., Identification of the Site of Phosphorylation of the Chemotaxis Response Regulator Protein, CheY. *The Journal of Biological Chemistry* **1989,** *264* (36), 21770-21778.
56. Stock, J. B.; Koshland, D. E., A protein methylesterase involved in bacterial sensing. *Proceedings of the National Academy of Sciences of the United States of America* **1978,** *75* (8), 3659-3663.
57. Shaulsky, G.; Escalante, R.; Loomis, W. F., Developmental signal transduction pathways uncovered by genetic suppressors. *Proceedings of the National Academy of Sciences of the United States of America* **1996,** *93* (15260-15265).
58. Keener, J.; Kustu, S., Protein kinase and phosphoprotein phosphatase activities of nitrogen regulatory proteins NTRB and NTRC of enteric bacteria: Roles of the conserved amino-terminal domain of NTRC. *Proceedings of the National Academy of Sciences of the United States of America* **1988,** *85* (4976-4980).
59. Ishige, K.; Nagasawa, S.; Tokishita, S.-i.; Mizunol, T., A novel device of bacterial signal transducers. *The EMBO Journal* **1994,** *13* (21), 5195-5202.
60. Georgellis, D.; Lynch, A. S.; Lin, E. C. C., In vitro phosphorylation study of the arc two-component signal transduction system of Escherichia coli. *Journal of Bacteriology* **1997,** *179* (17), 5429-5435.
61. Burbulys, D.; Trach, K. A.; Hoch, J. A., Initiation of sporulation in B. subtilis is controlled by a multicomponent phosphorelay. *Cell* **1991,** *64* (3), 545-552.

62. Varughese, K. I., Molecular recognition of bacterial phosphorelay proteins. *Current Opinion in Microbiology* **2002,** *5* (2), 142-148.
63. Hua, J.; Chang, C.; Sun, Q.; Meyerowitz, E. M., Ethylene insensitivity conferred by Arabidopsis ERS gene. *Science* **1995,** *269* (5231), 1712-1714.
64. Busch, A.; Lacal, J.; Martos, A.; Ramos, J. L.; Krell, T., Bacterial sensor kinase TodS interacts with agonistic and antagonistic signals. *Proceedings of the National Academy of Sciences* **2007,** *104* (34), 13774-13779.
65. Busch, A.; Guazzaroni, M.-E.; Lacal, J.; Ramos, J. L.; Krell, T., The sensor kinase TodS operates by a multiple step phosphorelay mechanism involving two autokinase domains. *The Journal of Biological Chemistry* **2009,** *284* (16), 1035-1060.
66. Leonia, L.; Ascenzia, P.; Bocedib, A.; Rampionia, G.; Castellinia, L.; Zennaroa, E., Styrene-catabolism regulation in Pseudomonas fluorescens ST: phosphorylation of StyR induces dimerization and cooperative DNA-binding. *Biochemical and Biophysical Research Communications* **2003,** *303* (3), 926-931.
67. Ramos-González, M.-I.; Olson, M.; Gatenby, A. A.; Mosqueda, G.; Manzanera, M.; Campos, M. J.; Víchez, S.; Ramos, J. L., Cross-regulation between a novel two-component signal transduction system for catabolism of toluene in Pseudomonas mendocina and the TodST system from Pseudomonas putida. *Journal of Bacteriology* **2002,** *184* (24), 7062-7067.
68. Coschigano, P. W.; Young, L. Y., Identification and sequence analysis of two regulatory genes involved in anaerobic toluene metabolism by strain T1. *Applied and Environmental Microbiology* **1997,** *63* (2), 652-660.
69. Burbulys, D.; Trach, K. A.; Hoch, J. A., Initiation of Sporulation in B. subtilis Is Controlled by a Multicomponent Phosphorelay *cell* **1991,** *64*, 545-552.
70. Goulian, M., Two-Component Signaling Circuit Structure and Properties. *Curr Opin Microbiol* **2010,** *13* (2), 184-189.
71. Kirby, J. R., Chemotaxis-Like Regulatory Systems: Unique Roles in Diverse Bacteria. *Annual Review of Microbiology* **2000,** *63*, 45-59.
72. Waters, C. M.; Bassler, B. L., The Vibrio harveyi quorum-sensing system uses shared regulatory components to discriminate between multiple autoinducers. *Genes & Development* **2006,** *20* (19), 2754-2767.
73. Piggot, P. J.; Hilbert, D. W., Sporulation of Bacillus subtilis. *Current Opinion in Microbiology* **2004,** *7* (6), 579-586.
74. Alm, E.; Huang, K.; Arkin, A., The Evolution of Two-Component Systems in Bacteria Reveals Different Strategies for Niche Adaptation. *PLOS Computational Biology* **2006,** *2* (11), 1329-1342.
75. Mitrophanov, A. Y.; Groisman, E. A., Signal integration in bacterial two-component regulatory systems. *Genes & Development* **2008,** (22), 2601-2611.
76. Farris, C.; Sanowar, S.; Bader, M. W.; Pfuetzner, R.; Miller, S. I., Antimicrobial peptides activate the Rcs regulon through the outer membrane lipoprotein RcsF. *Journal of Bacteriology* **2010,** *192* (19), 4894-4903.
77. Dintner, S.; Staroń, A.; Berchtold, E.; Petri, T.; Mascher, T.; Gebhard, S., Coevolution of ABC transporters and two-component regulatory systems as resistance modules against antimicrobial peptides in Firmicutes Bacteria. *Journal of Bacteriology* **2011,** *193* (15), 3851-3862.
78. Ottemann, K. M.; Xiao, W.; Shin, Y.-K.; Jr., D. E. K., A Piston Model for Transmembrane Signaling of the Aspartate Receptor. *Science* **1999,** *285* (5434), 1751-1754.
79. Garnerone, A.-M.; Cabanes, D.; Foussard, M.; Boistard, P.; Batut, J., Inhibition of the FixL sensor kinase by the FixT protein in *Sinorhizobium meliloti*. *The Journal of Biological Chemistry* **1999,** *274* (45), 32500-32506.
80. Buelow, D. R.; Raivio, T. L., Cpx signal transduction is influenced by a conserved N-terminal domain in the novel inhibitor CpxP and the periplasmic protease DegP. *Journal of Bacteriology* **2005,** *187* (19), 6622-6630.

81. Ogino, T.; Matsubara, M.; Kato, N.; Nakamura, Y.; Mizuno, T., An Escherichia coli protein that exhibits phosphohistidine phosphatase activity towards the HPt domain of the ArcB sensor involved in the multistep His-Asp phosphorelay. *Molecular Microbiology* **1998,** *27* (3), 573-585.
82. Rowland, S. L.; Burkholder, i. F.; Cunningham, K. A.; Maciejewski, M. W.; Grossman, A. D.; King, G. F., Structure and mechanism of action of Sda, an inhibitor of the histidine kinases that regulate initiation of sporulation in Bacillus subtilis. *Molecular Cell* **2004,** *13* (5), 689-701.
83. Good, M. C.; Zalatan, J. G.; Lim, W. A., Scaffold proteins: hubs for controlling the flow of cellular information. *Science* **2011,** *332* (6030), 680-686.
84. Heermann, R.; Weber, A.; Mayer, B.; Ott, M.; Hauser, E.; Gabriel, G.; Pirch, T.; Jung, K., The Universal Stress Protein UspC Scaffolds the KdpD/KdpE Signaling Cascade of Escherichia coli under Salt Stress. *Journal of molecular Biology* **2009,** *386* (1), 134-148.
85. Eguchi, Y.; Itou, J.; Yamane, M.; Demizu, R.; Yamato, F.; Okada, A.; Mori, H.; Kato, A.; Utsumi, R., B1500, a small membrane protein, connects the two-component systems EvgS/EvgA and PhoQ/PhoP in Escherichia coli. *proceedings of the National Academy of Sciences of the United States of America* **2007,** *104* (47), 18712-18717.
86. Kato, A.; Groisman, E. A., Connecting two-component regulatory systems by a protein that protects a response regulator from dephosphorylation by its cognate sensor. *Genes & Development* **2004,** *18* (18), 2302-2313.
87. Bongiorni, C.; Ishikawa, S.; Stephenson, S.; Ogasawara, N.; Perego, M., Synergistic regulation of competence development in Bacillus subtilis by two Rap-Phr systems. *Journal of Bacteriology* **2005,** *187* (13), 4353-4361.
88. Core, L.; Perego, M., TPR-mediated interaction of RapC with ComA inhibits response regulator-DNA binding for competence development in Bacillus subtilis. *Molecular Microbiology* **2003,** *49* (6), 1509-1522.
89. Zheng, M.; Wang, X.; Templeton, L. J.; Smulski, D. R.; LaRossa, R. A.; Storz, G., DNA microarray-mediated transcriptional profiling of the Escherichia coli response to hydrogen peroxide. *Journal of Bacteriology* **2001,** *183* (15), 4562-4570.
90. Bougdour, A.; Wickner, S.; Gottesman, S., Modulating RssB activity: IraP, a novel regulator of sigma(S) stability in Escherichia coli. *Genes & Development* **2006,** *20* (7), 884-897.
91. Kato, A.; Mitrophanov, A. Y.; Groisman, E. A., A connector of two-component regulatory systems promotes signal amplification and persistence of expression. *Proceedings of the National Academy of Sciences of the United States of America* **2007,** *104* (29), 12063-12068.
92. Ruvolo, M. V.; Mach, K. E.; Burkholder, W. F., Proteolysis of the replication checkpoint protein Sda is necessary for the efficient initiation of sporulation after transient replication stress in Bacillus subtilis. *Molecular Microbiology* **2006,** *60* (6), 1490-1508.
93. Bredt, D. S.; Snyder, S. H., Nitric oxide: a physiologic messenger molecule. *Annual Review of Biochemistry* **1994,** (63), 175-195.
94. Münzel, T.; Feil, R.; Mülsch, A.; Lohmann, S. M.; Hofmann, F.; Walter, U., Physiology and pathophysiology of vascular signaling controlled by guanosine 3_,5_-cyclic monophosphate-dependent protein kinase. *Circulation* **2003,** *108* (18), 2172-2183.
95. Sanders, K. M.; Ward, S. M.; Thornbury, K. d.; Dalziel, H. H.; Westfall, D. P.; Carl, C. A., Nitric oxide as a non-adrenergic, non-cholinergic neurotransmitter in the gastrointestinal tract. *Japanese Journal of Pharmacology* **1992,** (58), 220–225.
96. Warner, T. d.; Mitchell, J. A.; Sheng, H.; Murad, F., Effects of cyclic GMP on smooth muscle relaxation. *Advances in Pharmacology* **1994,** (26), 171-194.
97. Denninger, J. W.; Marletta, M. A., Guanylate cyclase and the NO/cGMP signaling pathway. *Biochimica et Biophysica Acta* **1999,** *1411* (2-3), 334-350.
98. Iyer, L. M.; Anantharaman, V.; Aravind, L., Ancient conserved domains shared by animal soluble guanylyl cyclases and bacterial signaling proteins. *BioMed Central* **2003,** *4* (1), 1-8.
99. Nioche, P.; Berka, V.; Vipond, J.; Minton, N.; Tsai, A.-L.; Raman, C. S., Femtomolar Sensitivity of a NO Sensor from Clostridium botulinum. *Science* **2004,** *306* (5701), 1550-1553.

100. Pellicena, P.; Karow, D. S.; Boon, E. M.; Marletta, M. A.; Kuriyan, J., Crystal structure of an oxygen-binding heme domain related to soluble guanylate cyclases. *Proceedings of the National Academy of Sciences of the United States of America* **2004,** *101* (35), 12854-12859.
101. Karow, D. S.; Pan, D.; Tran, R.; Pellicena, P.; Presley, A.; Mathies, R. A.; Marletta, M. A., Spectroscopic Characterization of the Soluble Guanylate Cyclase-like Heme Domains from Vibrio cholerae and Thermoanaerobacter tengcongensis. *Biochemistry* **2004,** *43*, 10203-10211.
102. Liu, N.; Xu, Y.; Hossain, S.; Huang, N.; Coursolle, D.; Gralnick, J. A.; Boon, E. M., Nitric oxide regulation of cyclic di-GMP synthesis and hydrolysis in *Shewanella woodyi*. *Biochemistry* **2012,** *51* (10), 2087-99.
103. Whiteley, C. G., Arginine metabolising enzymes as targets against Alzheimers' disease *Neurochemistry International* **2014,** *67*, 23-31.
104. James, L.; Griffiths, C.; Garthwaite, J.; Bellamy, T., Inhibition of nitric oxide-activated guanylyl cyclase by calmodulin antagonists. *British Journal of Pharmacology* **2009,** *158* (6), 1454-1464.
105. Derbyshire, E. R.; Marletta, M. A., Structure and Regulation of Soluble Guanylate Cyclase. *Annual Review of Biochemistry* **2012,** (81), 533-559.
106. Zugotta, W. N.; Siegelbaum, S. A., Structure and function of cyclic nucleotide-gated channels. *Annual Review of Neuroscience* **1996,** (19), 235-263.
107. Lohmanna, S. M.; Vaandragerb, A. B.; Smolenskia, A.; Waltera, U.; Jonge, H. R. D., Distinct and specific functions of cGMP-dependent protein kinases. *Trends in Biochemical Sciences* **1997,** *22* (8), 307-312.
108. Degerman, E.; Belfrage, P.; Manganiello, V. C., Structure, localization, and regulation of cGMP-inhibited phosphodiesterase (PDE3). *The Journal of Biological Chemistry* **1997,** *272* (11), 6823-6826.
109. Houslay, M. D.; Milligan, G., Tailoring cAMP-signalling responses through isoform multiplicity. *Trends in Biochemical Sciences* **1997,** *22* (6), 217-224.
110. Schlaich, M. P.; Parnell, M. M.; Ahlers, B. A.; Finch, S.; Marshall, T.; Zhang, W.-Z.; Kaye, D. M., Impaired L-arginine transport and endothelial function in hypertensive and genetically predisposed normotensive subjects. *Circulation* **2004,** *110* (24), 3680-3686.
111. Taddei, S.; Virdis, A.; Mattei, P.; Ghiadoni, L.; Sudano, I.; Salvetti, A., Defective L-Arginine–Nitric Oxide Pathway in Offspring of Essential Hypertensive Patients. *Circulation* **1996,** *94* (6), 1298-1303.
112. Mitrovic, V.; Hernandez, A. F.; Meyer, M.; Gheorghiade, M., Role of guanylate cyclase modulators in decompensated heart failure. *Heart Failure Reviews* **2009,** *14* (4), 309-319.
113. Pachera, P.; Schulz, R.; Liaudet, L.; Szabód, C., Nitrosative stress and pharmacological modulation of heart failure. *Trends in Pharmacological Sciences* **2005,** *26* (6).
114. Goran K. Hansson, Inflammation, atherosclerosis, and coronary artery disease. *The New England Journal of Medicine* **2005,** (352), 1685-1695.
115. Libby, P.; Theroux, P., Pathophysiology of coronary artery disease. *Circulation* **2005,** *111* (25), 3481-3488.
116. Cary, S. P. L.; Winger, J. A.; Derbyshire, E. R.; Marletta, M. A., Nitric oxide signaling: no longer simply on or off. *Trends in Biochemical Sciences* **2006,** *31* (4), 231-239.
117. Boon, E. M.; Huang, S. H.; Marletta, M. A., A molecular basis for NO selectivity in soluble guanylate cyclase. *Nature Chemical Biology* **2005,** *1* (1), 53-59.
118. Ma, X.; Sayed, N.; Beuve, A.; Akker, F. v. d., NO and CO differentially activate soluble guanylyl cyclase via a heme pivot-bend mechanism. *The EMBO Journal* **2007,** *26* (2), 578-588.
119. Charles Olea, J.; Boon, E. M.; Pellicena, P.; Kuriyan, J.; Marletta, M. A., Probing the function of heme distortion in the H-NOX family. *ACS Chemical Biology* **2008,** *3* (11), 703-710.
120. Erbil, W. K.; Price, M. S.; Wemmer, D. E.; Marletta, M. A., A structural basis for H-NOX signaling in Shewanella oneidensis by trapping a histidine kinase inhibitory conformation. *Proceedings of the National Academy of Sciences of the United States of America* **2009,** *106* (47), 19753-19760.
121. Tran, R.; Boon, E. M.; Marletta, M. A.; Mathies, R. A., Resonance Raman spectra of an O_2-binding H-NOX domain reveal heme relaxation upon mutation. *Biochemistry* **2009,** *48* (36), 8568-8577.

122. Stone, J. R.; Marletta, M. A., Spectral and kinetic studies on the activation of soluble guanylate cyclase by nitric oxide. *Biochemistry* **1996,** *35* (4), 1093-1099.
123. Muralidharan, S.; Boon, E. M., Heme Flattening Is Sufficient for Signal Transduction in the H-NOX Family. *The Journal of the American Chemical Society* **2012,** *134* (4), 2044-2046.
124. Boon, E. M.; Marletta, M. A., Ligand specificity of H-NOX domains: from sGC to bacterial NO sensors. *Journal of Inorganic Biochemistry* **2005,** *99* (4), 892-902.
125. Carlson, H. K.; Vance, R. E.; Marletta, M. A., H-NOX regulation of c-di-GMP metabolism and biofilm formation in Legionella pneumophila. *Molecular Microbiology* **2010,** *77* (4), 930-942.
126. Price, M. S.; Chao, L.; Marletta, M. A., Shewanella oneidensis MR-1 H-NOX regulation of a histidine kinase by nitric oxide. *Biochemistry* **2007,** *46* (48), 13677-13683.
127. Henares, B. M.; Higgins, K. E.; Boon, E. M., Discovery of a nitric oxide responsive quorum sensing circuit in *Vibrio harveyi*. *ACS Chem Biol* **2012,** *7* (8), 1331-6.
128. Arora, D. P.; Boon, E. M., Nitric oxide regulated two-component signaling in Pseudoalteromonas atlantica. *Biochemical and Biophysical Research Communications* **2012,** *421* (3), 521-526.
129. Plate, L.; Marletta, M. A., Nitric oxide modulates bacterial biofilm formation through a multicomponent cyclic-di-GMP signaling network. *Molecular Cell* **2012,** *46* (4), 449-460.
130. Plate, L.; Marletta, M. A., Nitric oxide-sensing H-NOX proteins govern bacterial communal behavior. *Cell* **2013,** *38* (11), 566-575.
131. Ng, W.-L.; Bassler, B. L., Bacterial Quorum-Sensing Network Architectures. *Annual Review of Genetics* **2009,** *43*, 197-222.
132. Waters, C. M.; Bassler, B. L., Quorum sensing: cell-to-cell communication in bacteria. *Annual Review of Cell and Developmental Biology* **2005,** *21*, 319-346.
133. Nealson, K. H.; Hastings, J. W., Bacterial Bioluminescence: Its Control and Ecological Significance. *Microbiological Reviews* **1979,** *43* (4), 496-518.
134. Waters, C. M.; Lu, W.; Rabinowitz, J. D.; Bassler, B. L., Quorum Sensing Controls Biofilm Formation in *Vibrio cholerae* through Modulation of Cyclic Di-GMP Levels and Repression of vpsT. *Journal of Bacteriology* **2008,** *190* (7), 2527-2536.
135. Davies, D. G.; Parsek, M. R.; Pearson, J. P.; Iglewski, B. H.; Costerton, J. W.; Greenberg, E. P., The involvement of cell-to-cell signals in the development of a bacterial biofilm. *Science* **1998,** *280*, 295-298.
136. Dawson, M. H.; Sia, R. H. P., In vitro transformation of pneumococcal types I. A technique for inducing transformation of penumococcal types in vitro. *The Journal of Experimental Medicine* **1931,** *54* (5), 681-699.
137. Lazazzera, B. A.; Solomon, J. M.; Grossman, A. D., An exported peptide functions intracellularly to contribute to cell density signaling in *B. subtilis*. *Cell* **1997,** *89* (6), 917-925.
138. Solomon, J. M.; Lazazzera, B. A.; Grossman, A. D., Purification and characterization of an extracellular peptide factor that affects two different developmental pathways in *Bacillus subtilis*. *Genes & Development* **1996,** *10* (16), 2014-2024.
139. Henke, J. M.; Bassler, B. L., Quorum Sensing Regulates Type III Secretion in *Vibrio harveyi* and *Vibrio parahaemolyticus*. *Journal of Bacteriology* **2004,** *186* (12), 3794-3805.
140. Withers, H.; Nordstrom, K., Quorum-sensing acts at initiation of chromosomal replication in Escherichia coli. *proceedings of the National Academy of Sciences of the United States of America* **1998,** *95*, 15694-15699.
141. Sauer, K.; Camper, A.; Ehrlich, G.; Costerton, W.; Davies, D., Pseudomonas aeruginosa displays multiple phenotypes during development as a biofilm. *Journal of Bacteriology* **2002,** *184* (4), 1140-1154.
142. Antonova, E.; Hammer, B., Quorum-sensing autoinducer molecules produced by members of a multispecies biofilm promote horizontal gene transfer to Vibrio cholera. *FEMS Microbiology Lettters* **2011,** (322), 68-76.
143. Eberhard, A.; Burlingame, A. L.; Eberhard, C.; Kenyon, G. L.; Nealson, K. H.; Oppenheimer, N. J., Structural identification of autoinducer of Photobacterium fischeri luciferase. *Biochemistry* **1981,** *20* (9), 2444-2449.

144. Engebrecht, J.; Silverman, M., Identification of genes and gene products necessary for bacterial bioluminescence. *Proceedings of the National Academy of Sciences of the United States of America* **1984,** *81*, 4154-4158.
145. Miller, S. T.; Xavier, K. B.; Campagna, S. R.; Taga, M. E.; Semmelhack, M. F.; Bassler, B. L.; Hughson, F. M., Salmonella typhimurium Recognizes a Chemically Distinct Form of the Bacterial Quorum-Sensing Signal AI-2. *Molecular Cell* **2004,** *15*, 677-687.
146. Xavier, K.; Bassler , B., LuxS quorum sensing: more than just a numbers game. *Current Opinion in Microbiology* **2003,** (6), 191-197.
147. Michael J. Federle, B. L. B., Interspecies communication in bacteria. *The Journal of Clinical Investigation* **2003,** *112*, 1291-1299.
148. Henke, J. M.; Bassler, B. L., Three parallel quorum-sensing systems regulate gene expression in *Vibrio harveyi*. *Journal of Bacteriology* **2004,** *186* (20), 3794-3805.
149. Higgins, D. A.; Pomianek, M. E.; Kraml, C. M.; Taylor, R. K.; Semmelhack, M. F.; Bassler, B. L., The major Vibrio cholerae autoinducer and its role in virulence factor production. *Nature* **2007,** *450* (7171), 883-886.
150. Havarstein, L. S.; Coomaraswamy, G.; Morrison, D. A., An unmodified heptadecapeptide pheromone induces competence for genetic transformation in *Streptococcus pneumoniae*. *Proceedings of the National Academy of Sciences of the United States of America* **1995,** *92* (24), 11140-11144.
151. Ji, G.; Beavis, R. C.; Novick, R. P., Cell density control of staphylococcal virulence mediated by an octapeptide pheromone. *Proceedings of the National Academy of Sciences of the United States of America* **1995,** *92* (26), 12055-12059.
152. Ansaldi, M.; Marolt, D.; Stebe, T.; Mandic-Mulec, I.; Dubnau, D., Specific activation of the Bacillus quorum-sensing systems by isoprenylated pheromone variants. *Molecular Microbiology* **2002,** *44* (6), 1561-1573.
153. Engebrecht, J.; Nealson, K.; Silverman, M., Bacterial bioluminescence: Isolation and genetic analysis of functions from *Vibrio fischeri*. *Cell* **1983,** *32* (3), 773-781.
154. Engebrecht, J.; Silverman, M., Nucleotide sequence of the regulatory locus controlling expression of bacterial genes for bioluminescence. *NUcleic acids research* **1987,** *15* (24), 10455-10467.
155. Showalter, R. E.; Martin, M.; Silverman, M. R., Cloning and nucleotide sequence of luxR, a regulatory gene controlling bioluminescence in *Vibrio harveyi*. *Journal of Bacteriology* **1990,** *172* (6), 2946-2954.
156. Kaplan, H. B.; Greenberg, E. P., Diffusion of autoinducer is involved in regulation of the *Vibrio fischeri* luminescence system. *Journal of Bacteriology* **1985,** *163*, 1210-1214.
157. Stevens, A. M.; Dolan, K. M.; Greenberg, E. P., Synergistic binding of the Vibrio fischeri LuxR transcriptional activator domain and RNA polymerase to the lux promoter region. *Proceedings of the National Academy of Sciences of the United States of America* **1994,** *91*, 12619-12623.
158. Zhu, J.; Winans, S. C., Autoinducer binding by the quorum-sensing regulatorTraR increases affinity for target promoters in vitro and decreasesTraR turnover rates in whole *Proceedings of the National Academy of Sciences of the United States of America* **1999,** *96*, 4832-4837.
159. Manefield, M.; Turner, S. L., Quorum sensing in context: out of molecular biology and into microbial ecology. *Microbiology* **2002,** *148* (12), 3762-3764.
160. Fuqua, W. C.; Winans, S. C., A LuxR-LuxI type regulatory system activates Agrobacterium Ti plasmid conjugal transfer in the presence of a plant tumor metabolite. *Journal of Bacteriology* **1994,** *176* (10), 2796-2806.
161. Faruque, S. M.; Albert, M. J.; Mekalanos, J. J., Epidemiology, Genetics, and Ecology of Toxigenic Vibrio cholerae. *Microbiology and Molecular Biology Reviews* **1998,** *62* (4), 1301-1314.
162. Miller, M. B.; Skorupski, K.; Lenz, D. H.; Taylor, R. K.; Bassler, B. L., Parallel Quorum Sensing Systems Converge to Regulate Virulence in *Vibrio cholera*. *Cell* **2002,** *110* (3), 303-314.
163. Bassler, B. L.; Wright, M.; Silverman, M. R., Multiple signalling systems controlling expression of luminescence in *Vibrio harveyi*: sequence and function of genes encoding a second sensory pathway. *Molecular Microbiology* **1994,** *13* (2), 273-286.

164. Cámara, M.; Hardman, n.; Williams, P.; Milton, D., Quorum sensing in *Vibrio cholerae*. *Nature Genetics* **2002,** *32* (2), 217-218.
165. Shao, Y.; Bassler, B. L., Quorum regulatory small RNAs repress type VI secretion in *Vibrio cholerae*. *Molecular Microbiology* **2014,** *92* (5), 921-930.
166. Lenz, D. H.; Mok, K. C.; Lilley, B. N.; Kulkarni, R. V.; Wingreen, N. S.; Bassler, B. L., The Small RNA Chaperone Hfq and Multiple Small RNAs Control Quorum Sensing in *Vibrio harveyi* and *Vibrio cholerae*. *Cell* **2004,** *118*, 69-82.
167. Hammer, B. K.; Bassler, B. L., Quorum sensing controls biofilm formation in *Vibrio cholerae*. *Molecular Microbiology* **2003,** *50* (1), 101-114.
168. Zhu, J.; Mekalanos, J. J., Quorum Sensing-Dependent Biofilms Enhance Colonization in *Vibrio cholerae*. *Developmental Cell* **2003,** *5*, 647-656.
169. Zhu, J.; Miller, M. B.; Vance, R. E.; Dziejman, M.; Bassler, B. L.; Mekalanos, J. J., Quorum-sensing regulators control virulence gene expression in *Vibrio cholerae*. *Proceedings of the National Academy of Sciences* **2001,** *99* (5), 3129-3134.
170. Mok, K. C.; Wingreen, N. S.; Bassler, B. L., Vibrio harveyi quorum sensing: a coincidence detector for two autoinducers controls gene expression. *The EMBO Journal* **2003,** *22* (4), 870-881.
171. Passador, L.; Cook, J. M.; Gambello, M. J.; Rust, L.; Iglewski, B. H., Expression of Pseudomonas aeruginosa virulence genes requires cell-to-cell communication. *Science* **1993,** *260* (5111), 1127-1130.
172. Brint, J. M.; Ohman, D. E., Synthesis of multiple exoproducts in Pseudomonas aeruginosa is under the control of RhlR-RhlI, another set of regulators in strain PAO1 with homology to the autoinducer-responsive LuxR-LuxI family. *Journal of Bacteriology* **1995,** *177* (24), 7155-7163.
173. Seed, P. C.; Passador, L.; Iglewski, B. H., Activation of the Pseudomonas aeruginosa lasI gene by LasR and the Pseudomonas autoinducer PAI: an autoinduction regulatory hierarchy. *Journal of Bacteriology* **1995,** *177* (3), 654-659.
174. Ochsner, U. A.; Reiser, J., Autoinducer-mediated regulation of rhamnolipid biosurfactant synthesis in *Pseudomonas aeruginosa*. *Proceedings of the National Academy of Sciences of the United States of America* **1995,** *92* (14), 6424-6428.
175. Hentzer, M.; Wu, H.; Andersen, J. B.; Riedel, K.; Rasmussen, T. B.; Bagge, N.; Kumar, N.; Schembri, M. A.; Song, Z.; Kristoffersen, P.; Manefield, M.; Costerton, J. W.; Molin, S.; Eberl, L.; Steinberg, P.; Kjelleberg, S.; Høiby, N.; Givskov, M., Attenuation of Pseudomonas aeruginosa virulence by quorum sensing inhibitors. *The EMBO Journal* **2003,** *22* (15), 3803-3815.
176. Schuster, M.; Lostroh, C. P.; Ogi, T.; Greenberg, E. P., Identification, timing, and signal specificity of *Pseudomonas aeruginosa* quorum-controlled genes: a transcriptome analysis. *Journal of Bacteriology* **2003,** *185* (7), 2066-2079.
177. Zhu, J.; Oger, P. M.; Schrammeijer, B.; Hooykaas, P. J. J.; Farrand, S. K.; Winans, S. C., The Bases of Crown Gall Tumorigenesis. *Journal of Bacteriology* **2000,** *182* (14), 3885-3895.
178. Dessaux, Y.; Petit, A.; Tempe, J., Opines in Agrobacterium biology. In *In The Molecular Signals in Plant-Microbe Interaction*, Verma, D., Ed. CRC Press: Boca Raton, FL, 1992; pp 109-136.
179. Fuqua, C.; Burbea, M.; Winans, S. C., Activity of the Agrobacterium Ti plasmid conjugal transfer regulator TraR is inhibited by the product of the traM gene. *Journal of Bacteriology* **1995,** *177* (5), 1367-1373.
180. Hwang, I.; Pei-Li; Zhang, L.; Piper, K. R.; Cook, D. M.; Tate, M. E.; Farrand, S. K., TraI, a LuxI homologue, is responsible for production of conjugation factor, theTi plasmid N-acylhomoserine lactone autoinducer. *Proceedings of the National Academy of Sciences of the United States of America* **1994,** *91* (11), 4639-4643.
181. Bodman, S. B. V.; Hayman, G. T.; Farrand, S. K., Opine catabolism and conjugal transfer of the nopaline Ti plasmid pTiC58 are coordinately regulated by a single repressor. *Proceedings of the National Academy of Sciences of the United States of America* **1992,** *89*, 643-647.
182. Dong, Y.-H.; Wang, L.-H.; Xu, J.-L.; Zhang, H.-B.; Zhang, X.-F.; Zhang, L.-H., Quenching quorum-sensing-dependent bacterial infection by an N-acyl homoserine lactonase. *Nature* **2001,** *411* (6839), 813-817.

183. Leadbetter, J. R.; Greenberg, E. P., Metabolism of acyl-homoserine lactone quorum-sensing signals by Variovorax paradoxus. *Journal of Bacteriology* **2000,** *182* (24), 6921-6926.
184. Dufour, P.; Jarraud, S.; Vandenesch, F.; Greenland, T.; Novick, R. P.; Bes, M.; Etienne, J.; Lina, G., High Genetic Variability of the agr Locus in Staphylococcus Species. *Journal of Bacteriology* **2002,** *184* (4), 1180-1186.
185. Lyon, G. J.; Wright, J. S.; Muir, T. W.; Novick, R. P., Key Determinants of Receptor Activation in the agr Autoinducing Peptides of Staphylococcus aureus. *Biochemistry* **2002,** *41*, 10095-10104.
186. Lyona, G. J.; Novickb, R. P., Peptide signaling in Staphylococcus aureus and other Gram-positive bacteria. *Peptides* **2004,** *25*, 1389-1403.
187. Lin, Y.-H.; Xu, J.-L.; Hu, J.; Wang, L.-H.; Ong, S. L.; Leadbetter, J. R.; Zhang, L.-H., Acyl-homoserine lactone acylase from Ralstonia strain XJ12B represents a novel and potent class of quorum-quenching enzymes. *Molecular Microbiology* **2003,** *47* (3), 849-860.
188. Givskov, M.; NYS, R. d.; Manfield, M.; Gram, L.; Maximilien, R.; Eberl, L.; Molin, S.; Steinberg, P. D.; Kjellberg, S., Eukaryotic Interference with Homoserine Lactone-Mediated Prokaryotic Signalling. *Journal of Bacteriology* **1996,** *178* (22).
189. Manefield, M.; Rasmussen, T. B.; Henzter, M.; Andersen, J. B.; Steinberg, P.; Kjelleberg, S.; Givskov, M., Halogenated furanones inhibit quorum sensing through accelerated LuxR turnover. *Microbiology* **2002,** *148*, 1119-1127.
190. Mathesius, U.; Mulders, S.; Gao, M.; Teplitski, M.; Caetano-Anolles, G.; Rolfe, B. G.; Bauer, W. D., Extensive and specific responses of a eukaryote to bacterial quorum-sensing signals. *Proceedings of the National Academy of Sciences of the United States of America* **2003,** *100* (3), 1444-1449.
191. Chun, C. K.; Ozer, E. A.; Welsh , M. J.; Zabner, J.; Greenberg, E. P., Inactivation of a Pseudomonas aeruginosa quorum-sensing signal by human airway epithelia. *Proceedings of the National Academy of Sciences* **2003,** *101* (10), 3587-3590.
192. Nixon, B. T.; Ronson, C. W.; Ausubel, F. M., Two-component regulatory systems responsive to environmental stimuli share strongly conserved domains with the nitrogen assimilation regulatory genes ntrB and ntrC. *Proceedings of the National Academy of Sciences* **1986,** *83*, 7850-7854.
193. Ronson, C. W.; Nixon, T.; Ausubel, F. M., Conserved domains in bacterial regulatory proteins that respond to environmental stimuli. *Cell* **1987,** *49* (5), 579-581.
194. Uhl, M. A.; Miller, J. F., Integration of multiple domains in a two-component sensor protein: the Bordetella pertussis BvgAS phosphorelay. *The EMBO Journal* **1996,** *15* (5), 1028.
195. Rodrigue, A.; Quentin, Y.; Lazdunski, A.; Mejean, V.; Foglino, M., Two-component systems in Pseudomonas aeruginosa: why so many? *Trends Microbiol* **2000,** *8* (11), 498-504.
196. Freeman, J. A.; Bassler, B. L., A genetic analysis of the function of LuxO, a two-component response regulator involved in quorum sensing in *Vibrio harveyi*. *Molecular Microbiology* **1999,** *31* (2), 665-677.
197. Hess, F. J.; Bourret, R. B.; Simon, M. I., Phosphorylation assays for proteins of the two-component regulatory system controlling chemotaxis in Escherichia coli. *Methods in Enzymology* **1991,** *200*, 188-204.
198. Wei, Y.-F.; Morgan, J. E.; Matthews, H. R., Studies of histidine phosphorylation by a nuclear protein histidine kinase show that histidine-75 in histone H4 is masked in nucleosome core particles and in chromatin. *Archives of Biochemistry and Biophysics* **1989,** *268* (2), 546-550.
199. Grimshaw, C.; Huang, S.; Hanstein, C.; Strauch, M.; Burbulys, D.; Wang, L.; Hoch, J.; Whiteley, J., Synergistic kinetic interactions between components of the phosphorelay controlling sporulation in Bacillus subtilis. *Biochemistry* **1998,** *37* (5), 1365-75.
200. Tawa, P.; Stewart, R. C., Kinetics of CheA autophosphorylation and dephosphorylation reactions. *Biochemistry* **1994,** *33* (25), 7917-24.
201. Marina, A.; Mott, C.; Auyzenberg, A.; Hendrickson, W. A.; Waldburger, C. D., Structural and mutational analysis of the PhoQ histidine kinase catalytic domain. Insight into the reaction mechanism. *The Journal of Biological Chemistry* **2001,** *276* (44), 41182-41190.

202. Hultquist, D. E., The preparation and characterization of phosphorylated derivatives of histidine. *Biochimica et Biophysica Acta* **1968,** *153* (2), 329-40.
203. Hultquist, D. E.; Moyer, R. W.; Boyer, P. D., The Preparation and Characterization of 1-Phosphohistidine and 3-Phosphohistidine. *Biochemistry* **1966,** *5* (1), 322-331.
204. Attwood, P. V.; Piggott, M. J.; Zu, X. L.; Besant, P. G., Focus on phosphohistidine. *Amino Acids* **2007,** (32), 145-156.
205. Duclos, B.; Marcandier, S.; Cozzone, A. J., Chemical properties and separation of phosphoaminoacids by thin-layer chromatography and/or electrophoresis. *Methods Enzymol* **1991,** (210), 10-21.
206. Kee, J.-M.; Muir, T. W., Chasing phosphohistidine, an elusive sibling in the phosphoamino acid family. *ACS Chem Biol* **2012,** *7* (1), 44-51.
207. Carlson, H. K.; Plate, L.; Price, M. S.; Allen, J. J.; Shokat, K. M.; Marletta, M. A., Use of a semisynthetic epitope to probe histidine kinase activity and regulation. *Anal Biochem* **2010,** *397* (2), 139-43.
208. Kee, J.-M.; Oslund, R. C.; Perlman, D. H.; Muir, T. W., A pan-specific antibody for direct detection of protein histidine phosphorylation. *Nature Chemical Biology* **2013,** *9*, 416-421.
209. Bradford, M. M., A rapid and sensitive method for the quantitation of microgram quantities of protein utilizing the principle of protein-dye binding. *Analytical Biochemistry* **1976,** (72), 248-254.
210. Miller, S. I.; Kukral, A. M.; Mekalanos, J. J., A two-component regulatory system (phoP phoQ) controls *Salmonella typhimurium* virulence. *Proceedings of the National Academy of Sciences of the United States of America* **1989,** *86* (5054-5058).
211. Kasahara, M.; Nakata, A.; Shinagawa, H., Molecular Analysis of the Escherichia coli phoP-phoQ Operon. *Journal of Bacteriology* **1992,** *174* (2), 492-498.
212. Samuele, A.; Crespan, E.; Garbelli, A.; Bavagnoli, L.; Maga, G., The power of enzyme kinetics in the drug development process. *Current Pharmaceutical Biotechnology* **2013,** *14* (5), 551-560.
213. Brooks, B. D.; Brooks, A. E., Therapeutic strategies to combat antibiotic resistance. *Advanced Drug Delivery Reviews* **2014,** *78*, 14-27.
214. Wang, Z.; Cole, P. A., Catalytic Mechanisms and Regulation of Protein Kinases. *Methods in Enzymology* **2014,** *548*, 1-21.
215. Nishi, H.; Shaytan, A.; Panchenko, A. R., Physicochemical mechanisms of protein regulation by phosphorylation. *Frontiers in Genetics* **2014,** *5* (270), 1-10.
216. Wei, Y.-F.; Matthews, H. R., A filter-based protein kinase assay selective for alkali-stable protein phosphorylation and suitable for acid-labile protein phosphorylation. *Analytical Biochemistry* **1990,** *190* (2), 188-192.
217. Matthews, H. R., Protein kinases and phosphatases that act on histidine, lysine, or arginine residues in eukaryotic proteins: a possible regulator of the mitogen-activated protein kinase cascade. *pharmacology & Therapeutics* **1995,** *67* (3), 323-350.
218. El-Maghrabi, M. R.; Correia, J. J.; Heil, P. J.; Pate, T. M.; Cobb, C. E.; Pilkis, S. J., Tissue distribution, immunoreactivity, and physical properties of 6-phosphofructo-2-kinase/fructose-2,6-bisphosphatase. *Proceedings of the National Academy of Sciences* **1986,** *83* (14), 5005-5009.
219. LJ, K., Kinase activity of EnvZ, an osmoregulatory signal transducing protein of Escherichia coli. *Arch Biochem Biophys* **1997,** *346* (2), 303-11.
220. Noriega, C. E.; Schmidt, R.; Gray, M. J.; Chen, L.-L.; Stewart, V., Autophosphorylation and dephosphorylation by soluble forms of the nitrate-responsive sensors NarX and NarQ from *Escherichia coli* K-12. *J. Bacteriol* **2008,** (11), 3869-76.
221. Jiang, P.; Peliska, J. A.; Ninfa, A. J., Asymmetry in the Autophosphorylation of the Two-Component Regulatory System Transmitter Protein Nitrogen Regulator II of *Escherichia coli*. *Biochemistry* **2000,** *39*, 5057-5065.
222. FAO/WHO, *Risk assessment of Vibrio parahaemolyticus in seafood: Interpretative summary and Technical report*. 2011.

223. McCarter, L. L., The multiple identities of *Vibrio parahaemolyticus*. *Journal of Molecular Microbiology and Biotechnology* **1999,** *1* (1), 51-57.
224. McLaughlin, J. B.; DePaola, A.; Bopp, C. A.; Martinek, K. A.; Napolilli, N. P.; Allison, C. G.; Murray, S. L.; Thompson, E. C.; Bird, M. M.; Middaugh, J. P., Outbreak of Vibrio parahaemolyticus Gastroenteritis Associated with Alaskan Oysters. *The New England Journal of Medicine* **2005,** *353* (14), 1463-1470.
225. Yeung, M.; Boor, K. J., Epidemiology, Pathogenesis, and Prevention of Foodborne Vibrio parahaemolyticus Infections. *Foodborne pathogens and disease* **2004,** *1* (2), 74-88.
226. Gode-Potratz, C. J.; McCarter, L. L., Quorum Sensing and Silencing in Vibrio parahaemolyticus. *Journal of Bacteriology* **2011,** *193* (16), 4224-4237.
227. Boon, E. M.; Davis, J. H.; Tran, R.; Karow, D. S.; Huang, S. H.; Pan, D.; Miazgowicz, M. M.; Mathies, R. A.; Marletta, M. A., Nitric Oxide Binding to Prokaryotic Homologs of the Soluble Guanylate Cyclase β1 H-NOX Domain. *The Journal of Biological Chemistry* **2006,** *281* (31), 21892-21902.
228. Laub, M. T.; Biondi, E. G.; Skerker, J. M., Phosphotransfer Profiling: Systematic Mapping of Two-Component Signal Transduction Pathways and Phosphorelays. *Methods in enzymology* **2007,** *423*, 531-548.
229. Stone, J. R.; Marletta, M. A., Soluble Guanylate Cyclase from Bovine Lung: Activation with Nitric Oxide and Carbon Monoxide and Spectral Characterization of the Ferrous and Ferric States. *Biochemistry* **1994,** *33* (18), 5636-5640.
230. Kharitonov, V. G.; Sharma, V. S.; Magde, D.; Koesling, D., Kinetics of Nitric Oxide Dissociation from Five- and Six-Coordinate Nitrosyl Hemes and Heme Proteins, Including Soluble Guanylate Cyclase. *Biochemistry* **1997,** *36*, 6814-6818.
231. Kwon, O.; Georgellis, D.; Lin, E., Phosphorelay as the Sole Physiological Route of Signal Transmission by the Arc Two-Component System of Escherichia coli *Journal of Bacteriology* **2000,** *182* (13), 3858-3862.
232. Goodman, A. L.; Merighi, M.; Hyodo, M.; Ventre, I.; Filloux, A.; Lory, S., Direct interaction between sensor kinase proteins mediates acute and chronic disease phenotypes in a bacterial pathogen *Genes & Development* **2009,** *23* (2), 249-259.
233. Albanesi, D.; Martín, M.; Trajtenberg, F.; Mansilla, M. C.; Haouz, A.; Alzari, P. M.; Mendoza, D. d.; Buschiazzoa, A., Structural plasticity and catalysis regulation of a thermosensor histidine kinase *Proceedings of the National Academy of Sciences of the United States of America* **2009,** *106* (38), 16185-16190.
234. Rutherford, S. T.; Kessel, J. C. v.; Shao, Y.; Bassler, B. L., AphA and LuxR/HapR reciprocally control. *Genes & Development* **2011,** *25* (4), 397-408.
235. Zhang, Y.; Qiu, Y.; Tan, Y.; Guo, Z.; Yang, R.; Zhou, D., Transcriptional Regulation of opaR, qrr2–4 and aphA by the Master Quorum-Sensing Regulator OpaR in *Vibrio parahaemolyticus*. *PLoS One* **2012,** *7* (4).
236. Bebok, Z.; Varga, K.; Hicks, J. K.; Venglarik, C. J.; Kovacs, T.; Chen, L.; Hardiman, K. M.; Collawn, J. F.; Sorscher, E. J.; Matalon, S., Reactive Oxygen Nitrogen Species Decrease Cystic Fibrosis Transmembrane Conductance Regulator Expression and cAMP-mediated Cl^- Secretion in Airway Epithelia. *The Journal of Biological Chemistry* **2002,** *277* (45), 43041-43049.